

REVIEW

Open Access



The response of the hydrological cycle to temperature changes in recent and distant climatic history

Shailendra Pratap*  and Yannis Markonis

Abstract

The relationship between the hydrological cycle and the temperature is rather complex and of great importance to human socioeconomic activities. The prevailing theory suggests that as temperature increases the hydrological cycle is intensified. Practically, this means more and heavier precipitation. However, the exact magnitude of hydrological cycle response and its spatio-temporal characteristics is still under investigation. Looking back in Earth's hydroclimatic history, it is easy to find some periods where global temperature was substantially different than present. Here, we examine some of these periods to present the current knowledge about past hydrological cycle variability (specifically precipitation), and its relationship to temperature. The periods under investigation are the Mid-Miocene Climate Optimum, the Eemian Interglacial Stage, the Last Glacial Maximum, the Heinrich and Dansgaard–Oeschger Events, the Bølling–Allerød, the Younger Dryas, the 8.2 ka event, the Medieval Climate Anomaly, and the Little Ice Age. We report that the hypothesis that a warmer climate is a wetter climate could be an oversimplification, because the response of water cycle appears to be spatio-temporally heterogeneous.

Keywords: Global water cycle, Paleoclimate, Hydrological cycle, Water cycle intensification, Hydroclimatic variability

1 Introduction

Looking back in Earth's hydroclimatic history, there have been substantial shifts in the hydrological cycle (Ljungqvist et al. 2016). In the past few million years, many rapid climate transitions have occurred, with time scales ranging from decades to centuries (Corrick et al. 2020). For example, during Holocene, i.e. the last 18–20 thousand years (ka) before present (BP), the paleoclimatic records show considerable fluctuations in both the seasonal and spatial distribution of precipitation (Badgley et al. 2020). During the late glacial (18–16.5 ka), sea surface temperature (SST) was about 5–10 °C colder than the recent Holocene (11.5–9 ka) over both the North Pacific and the North Atlantic (Praetorius et al. 2020). For the same period, the global averaged precipitation

was about 10–14% lower than today, with the maximum reduction over the Northern Hemisphere (NH) due to reduced convective activity (Gates 1976; Kwiciecien et al. 2009; Sun et al. 2019). As the Last Glacial ended and the climate became warmer, there was a shift to wetter conditions as well. From 13 to 12 ka BP, the monsoon circulation was intensified, resulting to an increase in precipitation by about 200–300 mm at lower latitudes (Knox and Wright 1983; Maher 2008; Pausata et al. 2020). Stronger monsoons were also observed between 8 to 3 ka BP, coupling the widespread warming (Chawchai et al. 2021). The most affected region was East Asia (Rao et al. 2016), where precipitation was over 30% higher than today from 7.8 to 5.3 ka BP (Yang et al. 2016). All these changes occurred in various spatiotemporal scales, and therefore, it is still challenging to estimate the hydrological cycle variability and quantify it on global, continental, and regional scales.

*Correspondence: pratap@fzp.czu.cz

Faculty of Environmental Sciences, Czech University of Life Sciences Prague, Kamýcká 129, Praha – Suchbátka 165 00, Czech Republic

Besides natural variability, anthropogenic forcing (GHG emissions and land-use changes) is also regarded as one of the possible drivers of abrupt changes of the hydrological cycle (Allan et al. 2014). Global warming is expected to intensify the global hydrologic cycle, and increase the frequencies of extremes like heavy rainfall, flood, and drought conditions (Huntington 2010). The term intensification of the hydrological cycle is used to describe an acceleration in the rates of atmospheric water vapor content, precipitation, evaporation, and evapotranspiration (ET) (Trenberth 1998). There is a solid theoretical basis that relates atmospheric warming and the intensification of hydrological cycle. The basis for this relationship is the Clausius–Clapeyron relation, which suggests the exponential response of specific humidity to temperature increase (Huntington 2006). The Clausius–Clapeyron formulation implies the slope of this relationship has to remain below the 6.5% per Kelvin as the evaporation is energy limited (Norris et al. 2019). However, precipitation is also energy limited, because the atmosphere should be able to radiate away the latent heat produced during precipitation events (O’Gorman 2012). This makes the estimation of the precipitation response under energy constrain conditions a complex task.

Due to this complexity, General Circulation Models (GCMs) are being extensively used in the estimation of the intensification hydrological cycle (Watterson et al. 1997). The GCMs still show strong variance in their results, although there is general agreement that there is a detectable increase in global mean precipitation, also evident in observational records (Markonis et al. 2019). For example, Allen and Ingram (2002) reported that the precipitation will increase by approximately 3.4% per Kelvin degree, while Wentz et al. (2007) report a slower rate, between 1 and 3% per Kelvin. Another study using 20 coupled ocean–land–atmosphere models shows that precipitation, runoff, and evaporation will globally increase by 5.2%, 7.3%, and 5.2%, respectively, responding to a mean surface air temperature increase of 2.3 °C by 2050 (Wetherald and Manabe 2002). Durack et al. (2012) present a 4% increase in precipitation in response to 0.5 °C warming. As we see, the precise quantification of the relationship between temperature and hydrological cycle remains unresolved. A plausible alternative and complementary approach to the GCMs is the study of the past states of hydrological cycle through paleoclimatic reconstructions. By investigating the past hydroclimatic variability range, we can shed more light to the underlying physical mechanisms and/or constrain the climate model simulations (Seftigen et al. 2017).

This study aims to map the current knowledge about hydrological cycle variability, and its relationship to temperature. Since it is extremely difficult to assess all the

processes related to the global hydrological cycle, we focus our review to precipitation and temperature (as a proxy for evaporation), which can be used indirectly to describe the global water balance Vargas Godoy et al. (2021). We have selected past periods with significant hydroclimatic fluctuations, that span from centuries to million years. The lengthiest of them is Mid-Miocene Climate Optimum (MMCO; 17–14.5 million years BP), when global temperature was 3–8 °C higher than pre-industrial levels. Such a warmer climate can help us determine future changes of water cycle to extremely high temperature conditions. Alternatively, warmer periods such as the Eemian Interglacial Stage (temperature 1.3 °C higher than today) can provide insight in the near future changes due to global warming. On the other hand, the study of ice age climates can help us determine the hydrological cycle response to colder regimes (e.g. Last Glacial Maximum when global temperature was 4.3 °C lower than today). The rapid transitions between cold and warm conditions are also of interest, and here, we will explore the hydrological cycle shifts during the Heinrich and Dansgaard–Oeschger Events. Finally, the study of Holocene allows us to examine time scales closer to the one of the recent temperature increase. We investigate the hydroclimatic conditions for Bølling–Allerød, Younger Dryas, the 8.2 ka event, the Medieval Climate Anomaly, and the Little Ice Age. Assessing the state of hydrological cycle during all these periods can offer an alternative pathway for anticipating the hydroclimatic changes that are yet to come both in the near and distant future (Meehl et al. 2007).

Please note that the pre-industrial values of temperature or precipitation corresponds to the period 1850–1900. On the other hand, there are studies that compare the climatic conditions with today. In this case, we assume today as the reference time when the corresponding study was published (industrial era). We use the same assumption for the studies without any explicit reference to a comparison period.

2 Climatic regimes of the distant past

2.1 MMCO

The MMCO (14 million years BP) is a rather long period of significantly warmer conditions compared to present (Böhme et al. 2007). What makes it particularly interesting is the evidence of enhanced fluctuations in the carbon cycle (Holbourn et al. 2014). Proxy records of alkenones (Zhang et al. 2013), paleosols (Breecker and Retallack 2014), stomata (Grein et al. 2013), and marine boron isotopes (Greenop et al. 2014) show that during the MMCO event, atmospheric CO_2 was less than 450 ppm, which is not far from the current CO_2 levels and within the range of near future CO_2 projections (Steinthorsdottir et al.

2020). However, there are also studies that report lower CO_2 concentrations, equal to or less than today (Zhang et al. 2013), implying that CO_2 might not be the main climatic driver (Pearson and Palmer 2000). Nevertheless, MMCO presents an excellent opportunity to investigate the functioning of the hydrological cycle in a warmer climate.

Air temperature reconstructions and model simulations suggest that during the MMCO, the annual mean global temperature was between 3 and 8 °C more than the pre-industrial levels (You et al. 2009; Pound et al. 2012; Steinhorsdottir et al. 2020). This is in good agreement with temperature proxies of deep-ocean water, which reveal a 5–6 °C warmer temperature as of today (Haq 1973; Miller et al. 1991; Zachos et al. 2008). The regions with higher temperatures are located mostly at mid to high latitudes (Böhme et al. 2007; Bruch et al. 2007; You 2010). Alongside with the warmer conditions, the MMCO also exhibited a rather humid climate (Zachos et al. 2001). This is also supported by model simulations, which show widespread increases in mean annual precipitation across northern and central Africa, North America, northern Eurasia, and Greenland (Kennett 1994; Fox and Koch 2004; Retallack 2007; Henrot et al. 2010; Herold et al. 2011).

The prevailing wet conditions are also confirmed by regional studies. Wet conditions of the MMCO have also been reported for Europe, where there was an increase in average annual precipitation of about 830–1350 mm (Böhme et al. 2007; Methner et al. 2020; Kuhlmann and Kempf 2002; Schlunegger et al. 1996). In addition, the isotope estimations at the Pannonian basin (Central Europe) suggest higher summer precipitation during the Late Miocene (about 10 million years BP) (Harzhauser et al. 2007). Pollen and leaf proxies from the Nenancoal field (Alaska Range, Alaska) imply a particular warmer period from about 18 to 14 million years BP (Leopold and Denton 1987). Pollen investigation at the Tian Shan (China) and sediment analysis at northeastward of Tibetan Plateau (China) show a wet and warm stage (Sun and Zhang 2008; Song et al. 2018). Stable isotope sclerochronology over northern South America (Guajira Peninsula, Colombia) indicates wet conditions with enhanced seasonality in regions that today have semiarid conditions due to a northerly shift of the Inter Tropical Convergence Zone (ITCZ) (Scholz et al. 2020). Finally, warm and wet climate dominated at Antarctica and the some regions of Southern Hemisphere (SH) high latitudes (You 2010; Feakins et al. 2012).

We have to note, though, that there is also evidence for increased aridity over Africa (Retallack 1992; Levin et al. 2006; Eronen et al. 2012; Morales-García et al. 2020), Australia (Stein and Robert 1985; Byrne et al. 2008; Wu

et al. 2018), South America (Pascual and Jaureguizar 1990), and some regions of North America (Wolfe 1985; Chamberlain et al. 2014) and Asia (Jiang and Ding 2010; Liu et al. 2009). In the latter, there was an expansion of the arid region from the western to the eastern coast of China, whereas the humid areas were limited to the northern and southern parts (Steininger 1999; Wan et al. 2007; Cliff et al. 2014). The physical mechanism that regulated the aridification over Asia, and the widespread mid-latitude arid region of the NH remains enigmatic (Hou et al. 2014). Analysis of bulk $\delta^{13}C$, over the central-eastern Idaho (Railroad Canyon section, USA), suggests an average mean annual precipitation of about 190 mm (ranges from 10 to 510 mm/year) during the MMCO that is almost equivalent to today's values (about 236 mm/year) (Harris et al. 2020). In addition, a paleosols analysis over the northern Pakistan (Zaleha 1997) suggests middle Miocene monsoon was similar to today (Allen and Armstrong 2012).

In Table 1, all the analysed studies are presented by region, hemisphere, latitudinal zone, and time period. In order to highlight the spatiotemporal variability of the hydroclimatic conditions, some studies appear to more than one rows, e.g. You (2010). In this manner, we can see that even in a much warmer world, there is no uniform shift of hydrological cycle; some regions became wetter, some became drier, and some appear to be similar to today. Still, the comparative examination of temperature and precipitation reveals that warmer conditions favor more an increase in precipitation than drier climate conditions in an approximately 2:1 ratio (Fig. 1).

2.2 The Eemian Interglacial Stage

The Eemian Interglacial Stage, also known as the Marine Isotope Stage (MIS) 5e, is a period that lasted 15 to 17 thousand years at approximately 130 ka BP (Abarbanel and Lall 1996). Commonly referred as the Last Interglacial, it is the period that preceded the last glacial stage, with stable climatic conditions similarly to Holocene. Initially, the Eemian was thought to be quite warmer than interglacial. Andersen et al. (2004) reported that the temperature was 5 °C higher as to today, according to an oxygen isotope reconstruction. However, more recent studies suggested that global average surface temperature was up to 1.3 °C warmer than the pre-industrial levels (Fischer et al. 2018), reaching a 2 °C maximum in the middle of the period (Snyder 2016). The global average temperature over land was 1.7 °C warmer than the pre-industrial levels, while the oceans were 0.8 °C warmer (Otto-Bliesner et al. 2013). The temperature differences were quite heterogeneous over land. The mid and high northern latitudes experienced considerably warmer temperatures, ranging between 2 and 5 °C (Turney and

Table 1 Temperature and precipitation conditions during the MMCO

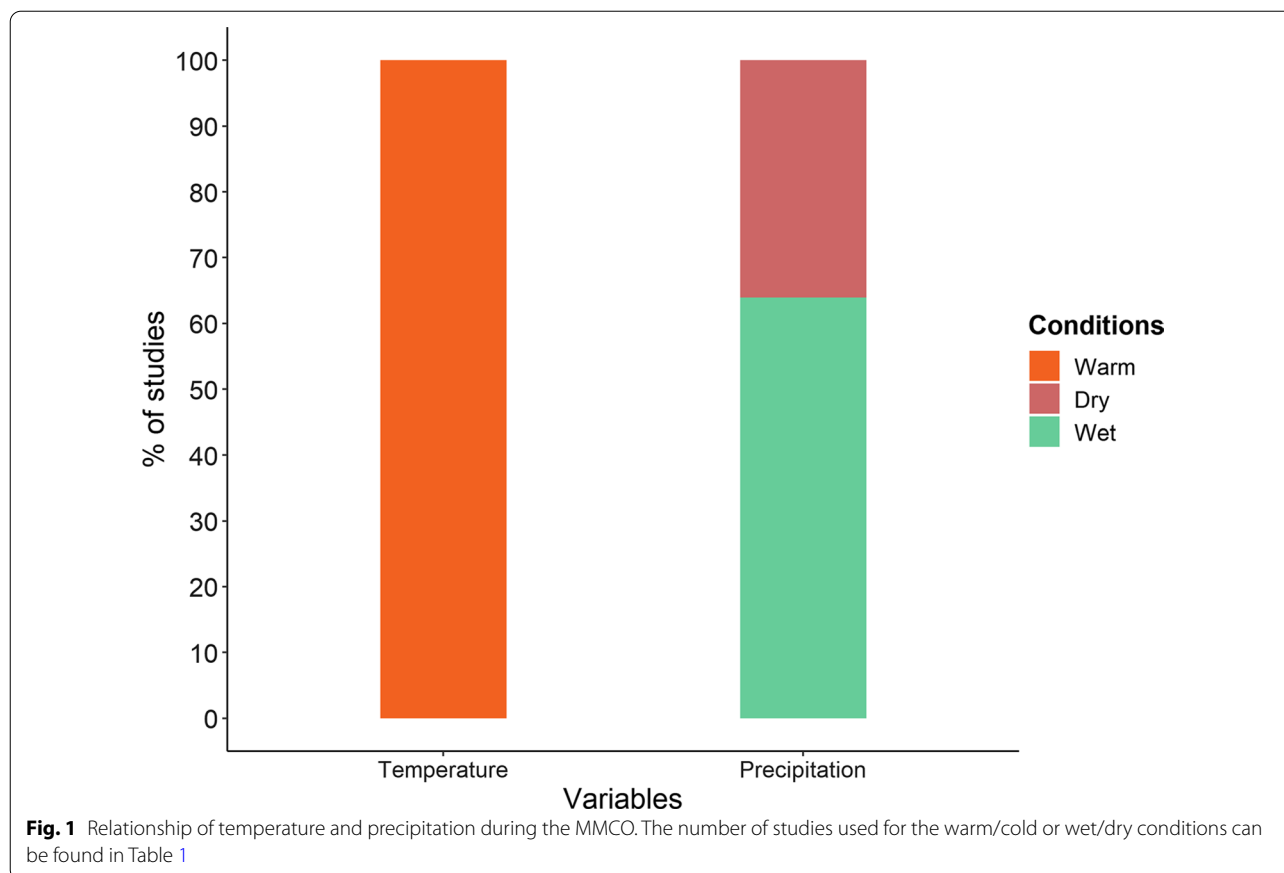
Study site	Hemisphere	Zone	Period	T	P	Citation(s)
Global	NH/SH	0	17–14.5	Warm	0	You et al. (2009) Pound et al. (2012) Steinthorsdottir et al. (2020)
N. Hemisphere	NH	M-L	17–14.5	Warm	Dry	Böhme et al. (2007); Bruch et al. (2007); You (2010) Zachos et al. (2001)
N. Hemisphere	NH	H-L	17–14.5	Warm	Dry	Böhme et al. (2007) Bruch et al. (2007), You (2010), Zachos et al. (2001)
Deep Ocean	NH	H-L	17–14.5	Warm	0	Haq (1973), Miller et al. (1991) Zachos et al. (2008)
S. Hemisphere	SH	H-L	17–14.5	Warm	Wet	You (2010), Feakins et al. (2012)
Asia	NH	M-L	17–14.5	0	Dry	Jiang and Ding (2010) Liu et al. (2009)
Africa	NH	L-L	17–14.5	0	Dry	Retallack (1992) Levin et al. (2006) Eronen et al. (2012) Morales-García et al. (2020)
Antarctica	SH	H-L	17–14.5	Warm	Wet	You (2010); Feakins et al. (2012)
S. America	SH	L-L	17–14.5	0	Dry	Pascual and Jaureguizar (1990)
N. America	NH	M-L	20–14.5	Warm	Wet	Kennett (1994); Retallack (2007) Fox and Koch (2004); Henrot et al. (2010) Herold et al. (2011)
N. America	NH	M-L	17–14.5	0	Dry	Wolfe (1985) Chamberlain et al. (2014)
Europe	NH	M-L	17–14.5	0	Wet	Böhme et al. (2007); Methner et al. (2020) Kuhlemann and Kempf (2002) Schlunegger et al. (1996)
Australia	SH	M-L	17–14.5	0	Dry	Stein and Robert (1985) Byrne et al. (2008) Wu et al. (2018)
N. Eurasia	NH	H-L	21–14.5	Warm	Wet	Kennett (1994); Retallack (2007) Fox and Koch (2004); Henrot et al. (2010) Herold et al. (2011)
Central Africa	NH	L-L	19–14.5	Warm	Wet	Kennett (1994); Retallack (2007) Fox and Koch (2004); Henrot et al. (2010) Herold et al. (2011)
N. Africa	NH	M-L	18–14.5	Warm	Wet	Kennett (1994); Retallack (2007) Fox and Koch (2004); Henrot et al. (2010) Herold et al. (2011)
Northern S. America	SH	L-L	17–14.5	0	Wet	Scholz et al. (2020)
China	NH	M-L	17–14.5	Warm	Wet	Sun and Zhang (2008) Song et al. (2018) Steininger (1999) Wan et al. (2007) Clift et al. (2014)
Greenland	NH	H-L	21–14.5	Warm	Wet	Kennett (1994); Retallack (2007) Fox and Koch (2004); Henrot et al. (2010) Herold et al. (2011)
E. Idaho, USA	NH	M-L	17–14.5	0	Dry	Harris et al. (2020)
N. Pakistan	NH	M-L	17–14.5	0	Dry	Allen and Armstrong (2012)
Alaska Range, Alaska	NH	H-L	18–14	Warm	0	Leopold and Denton (1987)

NH Northern Hemisphere, SH Southern Hemisphere, H-L High-latitudes, M-L Mid-latitudes, L-L Low-latitudes. Period units are in million years BP and average age uncertainty is ± 1 million years

Jones 2010), which are comparable to some global warming projections (Change 2014). Similarly to the MMCO, the Eemian is also an excellent analogue for analysing the state of hydrological cycle in warmer conditions (Adams et al. 1999).

Most of the available paleoclimatic records show that the Last Interglacial was wetter than Holocene. This is also supported by model simulations, demonstrating an

intensified hydrological cycle (Weaver and Hughes 1994; Pedersen et al. 2017; Johnston et al. 2018; Zhang et al. 2021b). Enhanced precipitation is observed mainly at the NH in paleoclimatic records over the low latitudes (Williams et al. 2020), boreal mid-latitude regions (Members 2006), and the Arctic (Kim et al. 2010). In addition, the ice melt pulses from Greenland have been suggested to influence the enhanced climate variability across the



Mediterranean (Tzedakis et al. 2018). During that time, when insolation was at its peak over the NH (Nehme et al. 2015), wet intervals were observed over Southern Europe (Brauer et al. 2007), and specifically, over the Eastern Mediterranean (Bar-Matthews 2014; Bar-Matthews et al. 2019). Continental North America was also wetter and warmer compared to today (Anderson et al. 2014). However, there were, also, some fluctuations to dry intervals (Curry and Baker 2000), which are further observed in the high values of carbon isotope ($\delta^{13}C_{29}$ and $\delta^{13}C_{31}$) (Suh et al. 2020).

Furthermore, there is an increase in NH summer monsoons (Wang et al. 2008). Both the proxy and model approaches explicitly suggest higher monsoon activity over North African and Asia (Prell and Kutzbach 1987; Scussolini et al. 2019). Terrestrial proxy records suggest wetter and warmer climate over the Sahara Arabian desert area compared to the present (Rosenberg et al. 2013; Petit-Maire et al. 2010). This is further confirmed by both the oxygen isotopes on speleothems at Soreq Cave (Israel) and climate models, showing increased regional rainfall during the Last Interglacial, attributed to wetter winters and increased summer monsoons (Orland et al. 2019). In addition, speleothems and fossil corals

reconstructions in the reef terraces also indicate a wetter Eemian interglacial alongside the Gulf of Aqaba at Arabian Peninsula (Yehudai et al. 2017). Similar speleothem findings as well confirm a wetter climate over Southern Arabia (Vaks et al. 2006).

On the other hand, there are also regions that experienced enhanced aridity. The evaluation of the Eemian climate across Europe using pollen reconstructions presents a different picture to the one described above. Colder and dryer conditions prevailed in the southern regions and conditions that are similar to today in the higher latitudes (Brewer et al. 2008). Sediment records from Maar lake (Germany) show a late Eemian cold and arid event that lasted 468 years (Sirocko et al. 2005). Weakening of the southern summer monsoon has been reported in the modeling and some proxy records (Montoya et al. 2000). Supporting evidence can be found in the speleothems of Western Australia, which indicate arid conditions (Zhao et al. 2001). Drier conditions also appeared in Argentina as detected in loess (paleosols) records (Tofalo et al. 2011), and Bolivia, where sediment records from Lake Titicaca suggest warmer and more arid conditions during the Eemian period (Fritz et al. 2007). This seems to be a recurring pattern during warm interstadials and

interglacials, when the southeastern regions of Australia show comparatively arid conditions (Ayliffe et al. 1998). In general, both proxy records and model simulations suggest weakened monsoonal precipitation over the SH compared to the pre-industrial times (Nikolova et al. 2013).

Similarly to the MMCO, during the MIS-5e, there was a substantial warm-and-wet pattern which was far from homogeneous. The majority of the studies on temperature shows warmer climate, i.e. about 85%, while the rest reveal cold conditions (Fig. 2 and Table 2). In precipitation records, the difference is slightly milder with about 75% of the studies suggesting wet conditions and about 25% a drier climate.

2.3 The Last Glacial Maximum

The Last Glacial Maximum (LGM) corresponds to the period during the last Glacial Stage that the ice sheets extended to their maximum length reaching their highest mass. It occurred between 30 and 15 ka (Prentice et al. 1992), although more recent estimates place it between 26.5 and 19 ka BP (Clark et al. 2009). During the LGM, the climate conditions at NH high latitudes were much colder and drier than today (Bigelow et al.

2003; Otto-Bliesner et al. 2006; Yokoyama et al. 2000). The global average temperature is estimated at 3–6 °C lower than the modern values (Bush and Philander 1999; Schmittner et al. 2011), while locally, e.g. at Greenland Summit, reached approximately 15–20 °C colder than the present levels (Johnsen et al. 1995; Cuffey et al. 1995; Miller et al. 2010). Even the tropics were substantially colder, ranging between 2 and 3.5 °C below present temperatures (Barker et al. 2005; Annan and Hargreaves 2013). This has also been confirmed by model results, which also estimate the difference around 2.5 °C across the equatorial regions (Crowley 2000; Ballantyne et al. 2005). Similarly to the Eemian the main driver for the temperature decline is the incoming insolation (Bush and Philander 1999; Clark et al. 2009).

The decline in temperature is also confirmed by decrease in the SST over multiple oceans. The Multi-proxy Approach for the Reconstruction of the Glacial Ocean surface (MARGO) project suggests that there was an annual tropical SST cooling of 1.7(±1) °C during the LGM. Similarly, the eastern and western equatorial Pacific, northwestern Pacific subarctic gyre, and northwestern tropical Pacific regions also show that the SST was lower (0.9–3.6 °C) than the present (Kucera et al.

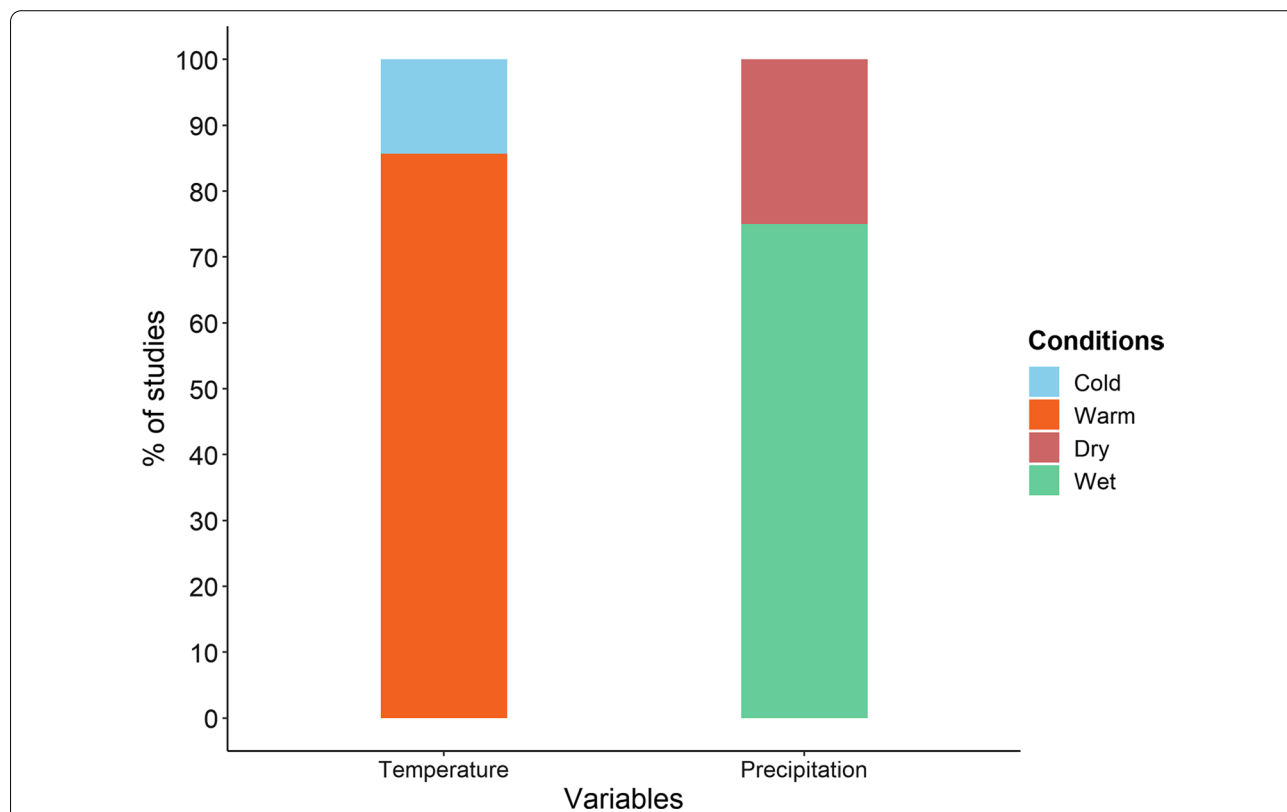


Fig. 2 Relationship of temperature and precipitation during the Eemian Interglacial Stage. The number of studies used for the warm/cold or wet/dry conditions can be found in Table 2

Table 2 Temperature and precipitation conditions during the Eemian Interglacial Stage

Study site	Hemisphere	Zone	Period	T	P	Citation(s)
Global	NH/SH	0	130–116	Warm	0	Fischer et al. (2018) Snyder (2016) Otto-Bliesner et al. (2013)
Global	NH/SH	0	130–116	0	Wet	Weaver and Hughes (1994) Pedersen et al. (2017) Johnston et al. (2018) Zhang et al. (2021b)
N. Hemisphere	NH	0	130–116	Warm	0	Andersen et al. (2004)
N. Hemisphere	NH	0	130–116	0	Wet	Wang et al. (2008) Williams et al. (2020) Members (2006) Kim et al. (2010)
N. Hemisphere	NH	M-L	130–116	Warm	0	Turney and Jones (2010)
N. Hemisphere	NH	H-L	130–116	Warm	0	Turney and Jones (2010)
Asia	NH	M-L	130–116	0	Wet	Prell and Kutzbach (1987) Scussolini et al. (2019)
N. America	NH	M-L	130–116	Warm	Wet	Anderson et al. (2014)
Europe	NH	M-L	130–116	Cold	Dry	Brewer et al. (2008)
Australia	SH	M-L	130–116	0	Dry	Ayliffe et al. (1998)
N. Africa	NH	M-L	130–116	0	Wet	Prell and Kutzbach (1987) Scussolini et al. (2019)
S. Europe	NH	M-L	130–116	0	Wet	Brauer et al. (2007)
W. Australia	SH	M-L	130–116	0	Dry	Zhao et al. (2001)
Arabian desert	NH	M-L	130–116	Warm	Wet	Rosenberg et al. 2013 Petit-Maire et al. (2010)
Greenland	NH	H-L	130–116	Warm	0	Tzedakis et al. (2018)
E. Mediterranean	NH	M-L	130–116	0	Wet	Bar-Matthews (2014) Bar-Matthews et al. (2019)
Arabian Pen	NH	M-L	130–116	0	Wet	Yehudai et al. (2017)
Germany	NH	M-L	130–116	Cold	Dry	Sirocko et al. (2005)
Bolivia	SH	L-L	130–116	Warm	Dry	Fritz et al. (2007)
Argentina	SH	M-L	130–116	0	Dry	Tofalo et al. (2011)
Argentina	SH	M-L	130–116	0	Dry	Nikolova et al. (2013)
S. Arabian Pen	NH	M-L	130–116	0	Wet	Vaks et al. (2006)
Soreq Cave, Israel	NH	M-L	130–116	0	Wet	Orland et al. (2019)

NH Northern Hemisphere, SH Southern Hemisphere, H-L High-latitudes, M-L Mid-latitudes, L-L Low-latitudes. Period units are in ka BP and average age uncertainty is ± 5 ka

2005). The lower SST resulted in increased upwelling of colder water across the continental margin and, finally, a cooler climate, especially over the NH (Rosell-Mel'è et al. 2004). There is also limited evidence about the SST decline in finer scales. For example, the Mediterranean Sea shows that the SST was about a 1 °C lower than the present, particularly in the eastern part (Hayes et al. 2005). On the other hand, not all the studies agree on a lower SST during the LGM. The SST derived from the central tropical Pacific and northern subtropics were similar to the modern levels of the SST (Lee et al. 2001), while a few regions have experienced a higher SST, such as the Northwest Pacific margin, southern parts of Iceland–Faroe Ridge, Iberian margin, north–south-west African boundary currents, and Japan Sea (Waelbroeck

et al. 2009). Still the majority of the SST records advocate for cold conditions, which are expected to affect the hydroclimate of the nearby landmasses (Seager et al. 2007).

Most of the proxy records suggest that during the LGM the global hydrological cycle was weaker compared to today (Cragin et al. 1977; Yung et al. 1996; Steffensen 1997; Li and Zhang 2020). Dry conditions were typical over both hemispheres and model simulations show that the decline in global temperature is linked to a decline in atmospheric water vapor concentration. Otto-Bliesner et al. (2006) estimated that precipitable water was 18% less than today resulting to an annual average precipitation of about 2.49 mm per day. The weakening the global hydrological cycle is due to a reduction of about 10% in

both evaporation and precipitation (Bush and Philander 1998; Gasse 2000). The simulations also suggested a surplus of precipitation over evaporation that has lowered the net amount of water vapor in the atmosphere (Bush and Philander 1999; Rojas et al. 2009).

Proxy records and model simulations (CCSM3) report a weakened summer monsoon for both tropical as well as northern Africa (Prentice et al. 2000). Moreover, analysis of lake sediments from the Pretoria Saltpan (South Africa) suggests a negative shift in the monsoonal precipitation with total precipitation approximately 15 to 20% less than today (Patridge et al. 1997; Simon et al. 2015). The drier conditions were also confirmed by diatom estimates from the same site (Metcalf 1999; Gasse and Van Campo 2001). The lake records from the east and southwest Amazonia also suggest lower precipitation levels than the present (Absy et al. 1991; Sifeddine et al. 2001). Similar changes are reported for high latitudes. Lake sediment records over southern east Siberia (Lake Baikal) show a drop of about 11% in annual precipitation and about 80% drop in summer precipitation, compared to the present climate (Osipov and Khlystov 2010). Similarly, the yearly precipitation over the Greenland Summit has been found up to three times less than the present values (Cuffey and Clow 1997; Johnsen et al. 2001).

In Europe, where regional climate modeling suggests that the annual average air temperature was about 6–9 °C lower than the present, while the precipitation was quite lower, especially over the northern regions (Strandberg et al. 2011). Interestingly, the decline was linked to a change in the atmospheric circulation pattern that determines the precipitation regime and strength. Currently, the precipitation pattern over central Europe is controlled by a westerly to northwesterly circulation system. During the LGM, the atmospheric moisture reached central Europe through south-westerly advection (Becker et al. 2016). This was also supported by the oxygen isotope analysis on speleothems of the Sieben Hengste cave (Bernese Alps), which report southwesterly moisture advection (during 26.5–23.5 ka) (Luetscher et al. 2015). The change in atmospheric circulation resulted to an increase in precipitation over southern Europe (Kuhlemann et al. 2008). In the eastern and central Mediterranean, there has been evidence for an increase in mountain glaciers at several locations, as well as an increased rate of winter precipitation (Strandberg et al. 2011). The Mediterranean is not the only region that wetter conditions appeared, as there is evidence of similar fluctuations over the extra-tropics (Clark and Mix 2002). Similar findings were found in the assessment on lake levels over East Africa, even though palaeovegetation analysis point to a dry climate (Barker and Gasse 2003). However, these changes are spatially limited and

do not significantly alter the global signal of decline in precipitation.

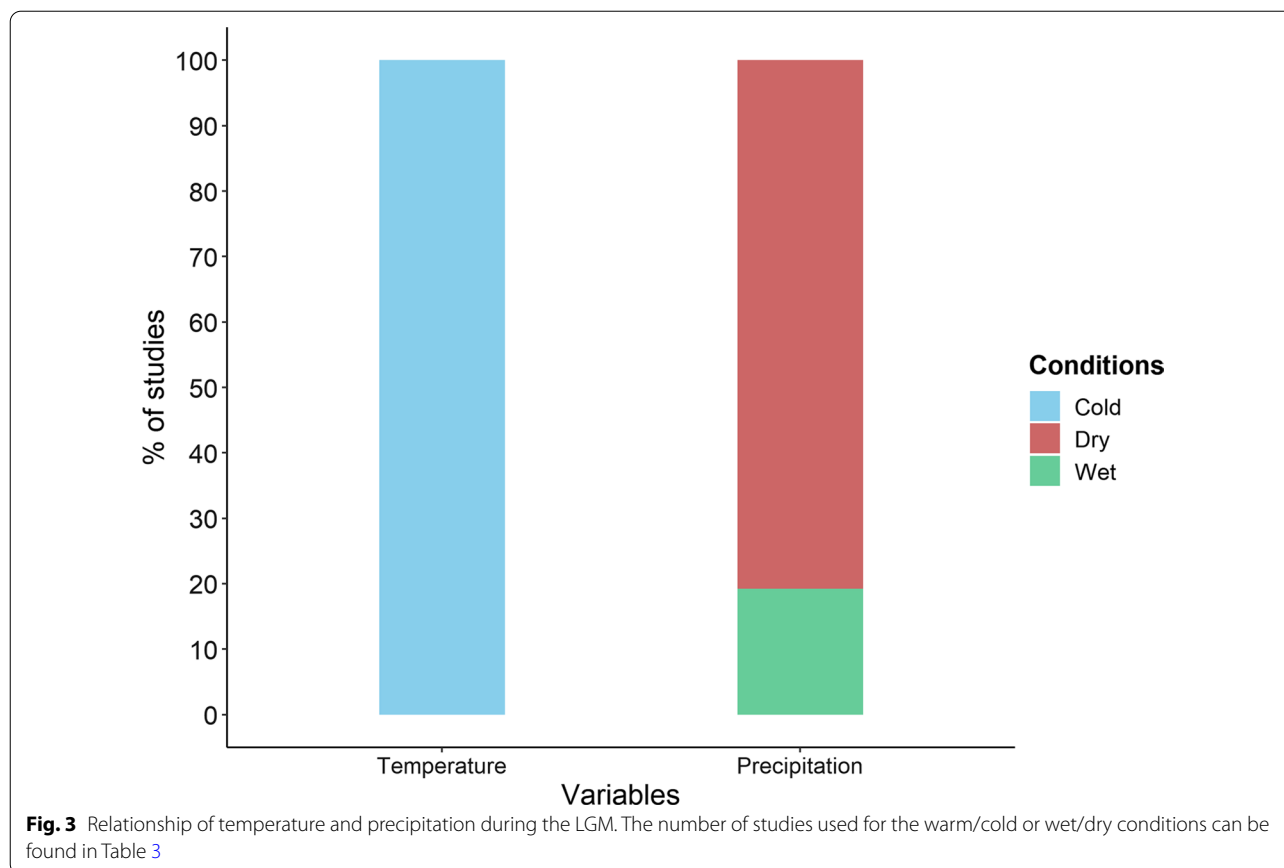
Contrary to the warm conditions of the MMCO and the Eemian Interglacial Stage, the cold conditions that prevailed in the LGM are mostly associated with drier climate. However, again the climatic conditions may differ spatially. For instance, in Fig. 3 and Table 3, we can see that about 20% of precipitation records correspond to regions with wet climate during this doubtlessly cold period. Another plausible explanation, besides spatially heterogeneity, could lie to the climatic proxy nature and the processes involved, which might falsely interpret solid precipitation or glacial extension as a wet regime. In any case, the global signal advocates for a weakening in water cycle strength (Li and Zhang 2020).

3 The abrupt climatic events of the last glacial

3.1 Dansgaard–Oeschger and Heinrich events

During the last glacial period, Earth's climate has gone through some abrupt changes over the North Atlantic region (Dansgaard et al. 1993). Proxy records suggest more than 24 cooling and warming events, termed as the Dansgaard–Oeschger (D–O) events (Rasmussen et al. 2016). During the D–O events, most of the NH is influenced by abrupt warming, which is then succeeded by a more gradual cooling (Martrat et al. 2004). Ice core records collected from Greenland suggest a rapid increase in atmospheric temperature ranging between 10 and 16 °C that occurred within a few decades (Johnsen et al. 1989; Lang et al. 1999; Budsky et al. 2019). In addition, there is evidence that warmer climate conditions were coupled with higher precipitation (Genty et al. 2003). The factors driving the D–O events are under vigorous debate, ranging from ocean–atmosphere or sea ice–atmosphere interactions (Broecker et al. 1990; Li and Born 2019) to cyclic Greenland ice sheet calving (Van Kreveld et al. 2000) and Earth's orbital forcing (Van Geel et al. 1999). Widespread signs of D–O events in the Nordic seas and North Atlantic have been found to be associated with the Atlantic Meridional Overturning Circulation (AMOC) instability, influenced by the variability in convection rate (Rasmussen et al. 2016). However, there are also D–O events that did not only influence the North Atlantic, but had a large-scale, or even global, impact to the climatic system. The fingerprint of D–O events can be found in deep-sea records, where it can be seen on planktonic and benthic records across the globe (Shackleton et al. 2000), or the Vostok ice core record at Antarctica (Jouzel et al. 1987). This is probably due to the relationship between the D–O events and the intensity of the AMOC (Santos et al. 2020).

The D–O events are also evident over the Mediterranean region, where there was an increase in precipitation



over the Iberian Peninsula (Nebout et al. 2002; Budsky et al. 2019) and Italy (Alley and Clark 1999). In addition, the D–O events are observed in the oxygen isotope record of the Soreq cave (Israel), where low $\delta^{18}\text{O}$ and high $\delta^{13}\text{C}$ values suggest wet conditions (Bar-Matthews et al. 2000). An increase in precipitation is also reported for Great Basin (Nevada; United States), where there is an increase in the lake levels, derive by the analysis of $\delta^{18}\text{O}$ proxy records (Benson et al. 1998). Some D–O events can also be linked with climatic fluctuations across the Indian Ocean (Altabet et al. 2002), such as events D–O events 7 and 8, which occurred at approximately 34–41 ka BP (Beck et al. 2001). The $\delta^{18}\text{O}$ estimates in the stalagmites collected from northern Vietnam, Indian, and Chinese caves show strengthening in the Indian and Asian summer monsoons (Dung et al. 2020; Cheng et al. 2016; Kathayat et al. 2016). Additionally, the D–O event 12 (45 ka BP (Genty et al. 2003)) was linked to the increased intensity of the Asian southwest monsoon during about 50–40 ka (Anderson and Prell 1993). Similar findings have been reported for other regions over Asia (Wang et al. 2001), while there is evidence that the D–O events can also be detected at South America (Peterson et al. 2000).

Between the D–O events, there are also some abrupt transitions to rather cold periods. They were named after Hartmut Heinrich, who investigated the characteristics of six intervals from 70 to 14 ka BP that occurred between the D–O events and appear to be the coldest events of the glacial (Heinrich 1988). The Heinrich events affected most of the Eurasia and North America, resulting to drier and colder conditions (Genty et al. 2003; Benson et al. 1996; Asmerom et al. 2010). Although the drivers of the Heinrich events are still not fully understood, there is general agreement that they are related to changes in the oceanic circulation over the North Atlantic (Thomas et al. 1995) and in the ice sheets over NH (Broecker 2000). They are mainly linked with the release of large volume of freshwater through iceberg melting (Boers 2018). These large-scale cold freshwater pulses caused further changes all over the global climatic system.

A 5 to 8 °C cooling has been observed over the Mediterranean surface water (Rohling et al. 1998), and significant aridity has been observed over the southwestern USA (Wagner et al. 2010). The influence of some Heinrich events extends to the tropics, where enhanced aridity has been reported (Leuschner and Sirocko 2000). Other Heinrich events are correlated with arid and cold

Table 3 Temperature and precipitation conditions during the LGM

Study site	Hemisphere	Zone	Period	T	P	Citation(s)
Global	NH/SH	0	30–15	Cold	0	Bush and Philander (1999) Schmittner et al. (2011)
Global	NH/SH	0	30–15	0	Dry	Cragin et al. (1977) Yung et al. (1996) Steffensen (1997) Li and Zhang (2020) Bush and Philander (1998) Gasse (2000)
N. Hemisphere	NH	0	30–15	Cold	Dry	Bigelow et al. (2003) Otto-Bliesner et al. (2006) Yokoyama et al. (2000)
Tropics	NH/SH	L-L	30–15	Cold	0	Barker et al. (2005) Annan and Hargreaves (2013) Crowley (2000) Ballantyne et al. (2005)
Tropics	NH/SH	L-L	30–15	0	Dry	Prentice et al. (2000)
Europe	NH	M-L	30–15	Cold	0	Strandberg et al. (2011)
Extra-tropics	NH	L-L	30–15	0	Wet	Clark and Mix (2002)
E. Africa	NH	L-L	30–15	0	Wet	Barker and Gasse (2003)
N. Africa	NH	M-L	30–15	0	Dry	Prentice et al. (2000)
S. Africa	SH	L-L	30–15	0	Dry	Patridge et al. (1997) Simon et al. (2015)
N. Europe	NH	M-L	30–15	0	Dry	Strandberg et al. (2011)
S. Europe	NH	M-L	30–15	0	Wet	Strandberg et al. (2011); Kuhlemann et al. (2008)
Mediterranean	NH	M-L	30–15	0	Wet	Clark and Mix (2002)
SE. Siberia	NH	M-L	30–15	0	Dry	Osipov and Khlystov (2010)
E. & SW. Amazonia	SH	L-L	30–15	0	Dry	Absy et al. (1991) Sifeddine et al. (2001)
Greenland	NH	H-L	30–15	Cold	0	Johnsen et al. (1995) Cuffey et al. (1995) Miller et al. (2010)
Greenland	NH	H-L	30–15	0	Dry	Cuffey and Clow (1997) Johnsen et al. (2001)

NH Northern Hemisphere, SH Southern Hemisphere, H-L High-latitudes, M-L Mid-latitudes, L-L Low-latitudes. Period units are in ka BP and average age uncertainty is ± 5 ka

climate at central China and even to Antarctica (Thompson 1991). Finally, they can also be detected over the Indian Ocean (Bay of Bengal), linked to increased variability in the summer monsoon and drier conditions all over India (Colin et al. 1998; Wang et al. 2001). Similarly to the LGM or other glacial stages, there is strong evidence that the decline in atmospheric/oceanic temperature results to the weakening or deceleration of the hydrological cycle and consequently to drier conditions (Mangerud et al. 2003; Grimm et al. 2006).

However, fluctuations to warm and wet conditions have also been reported. Warmer SST has prevailed over Southern California (Hendy and Kennett 2000), while low isotopic values suggest an extremely wet climate across the western USA between 40–30 ka 28.5–26.5 ka, and around 13 ka (Benson et al. 1996). In addition, the $\delta^{18}\text{O}$ records from the Owens Lake, Great Basin (western United States) present overflow

conditions, which were caused by either high precipitation or enhanced ice melting (Gale 1914; Oster et al. 2014). The substantial growth in central Andean glaciers is an indication of increased precipitation across tropical South America during the Heinrich events 1 and 2 (Wang et al. 2004) and across northeast Brazil for Heinrich events 1 to 5 (Smith and Rodbell 2010).

The studies on the Last Glacial abrupt climatic transitions are divided in warm (D–O) and cold (Heinrich) events. All D–O events are associated with wet conditions, while the hydroclimatic shift for Heinrich events is not so clear (Fig. 4 and Table 4). The cold transitions appear to result to both dry and wet conditions, with the dry conditions appearing more often (about a third of the studies). Thus, the hydrological cycle response to Heinrich events appears more heterogeneous compared to the D–O events. Still the relatively low number of studies may affect these findings.

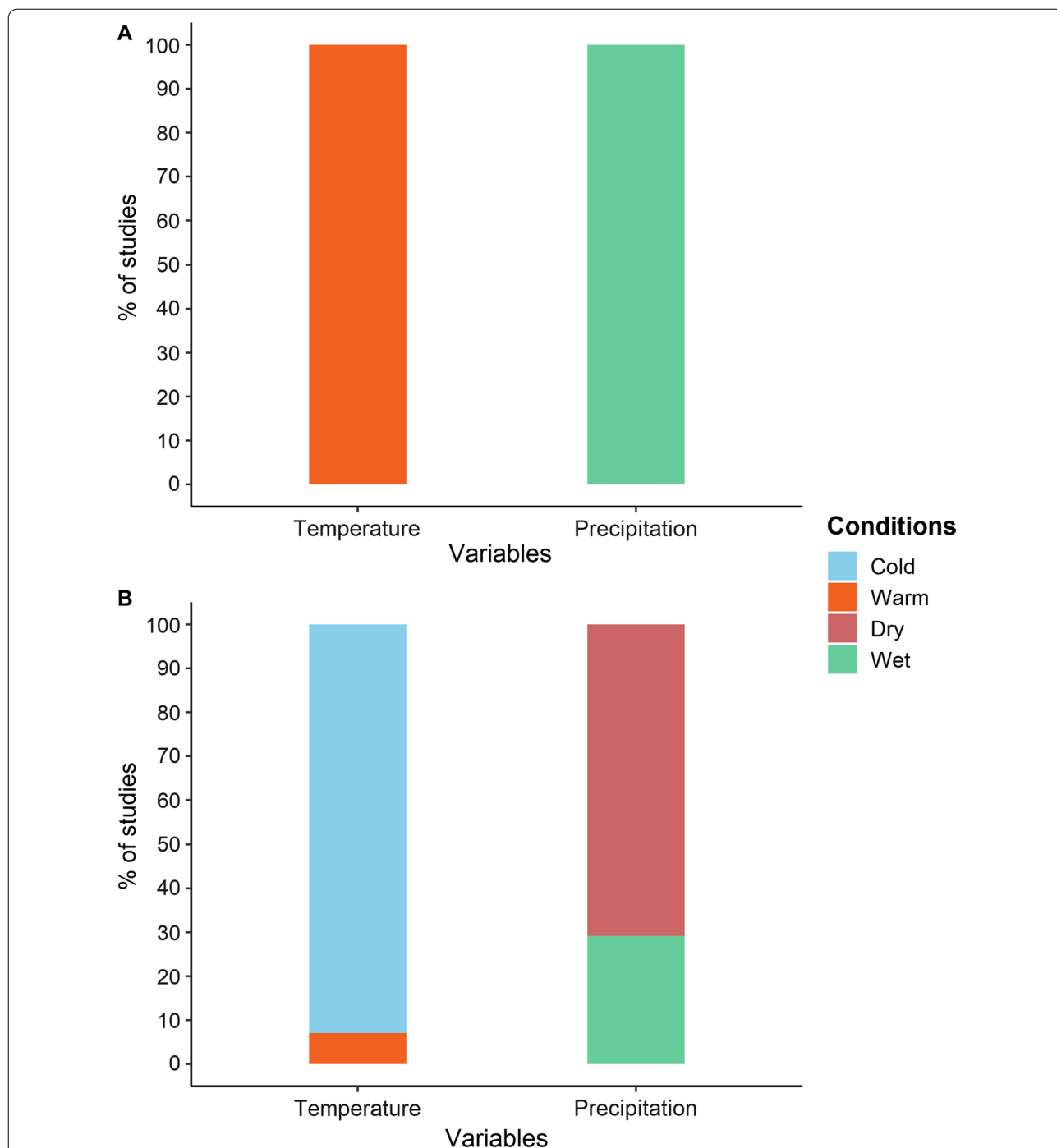


Fig. 4 Relationship of temperature and precipitation during the Last Glacial. **A** D–O events, **B** Heinrich events. The number of studies used for the warm/cold or wet/dry conditions can be found in Table 4

3.2 Bølling–Allerød interstadial

During the final stages of the last glacial period, an abrupt warm and moist period that occurred between 14.8 and 12.85 ka BP (On et al. 2018). In some regions, the period is divided into the Bølling oscillation, with a peak closer

to 14.5 ka BP and duration around 1400 years, and the Allerød oscillation, with a peak around 13 ka BP and a duration of 700 years (Seierstad et al. 2005). According to the $\delta^{18}\text{O}$ proxies of the GRIP ice core, the Bølling climate was 1 °C colder than today, while Allerød was 5–12 °C

Table 4 Temperature and precipitation conditions during the Last Glacial

Study site	Hemisphere	Zone	Event	Period	T	P	Citation(s)
Global	NH/SH	0	Heinrich	18–16.5	0	Dry	Gates (1976) Kwiecien et al. (2009) Sun et al. (2019)
N. Hemisphere	NH	0	D–O	80–12	Warm	0	Martrat et al. (2004)
Tropics	NH/SH	0	Heinrich	70–14	0	Dry	Leuschner and Sirocko (2000)
Eurasia	NH	M-L	Heinrich	70–14	Cold	Dry	Genty et al. (2003) Benson et al. (1996) Asmerom et al. (2010)
Asia	NH	M-L	D–O	80–12	0	Wet	Dung et al. (2020) Cheng et al. (2016) Kathayat et al. (2016)
Asia	NH	M-L	D–O	50–40	0	Wet	Wang et al. (2001)
N. America	NH	M-L	Heinrich	70–14	Cold	Dry	Genty et al. (2003) Benson et al. (1996) Asmerom et al. (2010)
S. America	SH	L-L	D–O	50–40	0	Wet	Peterson et al. (2000)
Antarctica	SH	H-L	Heinrich	70–14	Cold	Dry	Thompson (1991)
Tropical S. America	SH	M-L	Heinrich	15 and 22	0	Wet	Wang et al. (2004)
SW. Asia	NH	M-L	D–O	50–40	0	Wet	Anderson and Prell (1993)
W. Europe	NH	M-L	D–O	80–12	Warm	Wet	Genty et al. (2003)
N. Europe	NH	M-L	Heinrich	43–26	Cold	Dry	Mangerud et al. (2003) Grimm et al. (2006)
Mediterranean	NH	M-L	Heinrich	70–14	Cold	0	Rohling et al. (1998)
India	NH	M-L	Heinrich	70–14	Cold	Dry	Colin et al. (1998) Wang et al. (2001)
Central China	NH	M-L	Heinrich	70–14	Cold	Dry	Thompson (1991)
Iberian Peninsula	NH	M-L	D–O	80–12	0	Wet	Nebout et al. (2002) Budsky et al. (2019)
Greenland	NH	H-L	D–O	80–12	Warm	0	Johnsen et al. (1989) Lang et al. (1999) Budsky et al. (2019)
Italy	NH	M-L	D–O	80–12	0	Wet	Alley and Clark (1999)
Israel	NH	M-L	D–O	80–12	0	Wet	Bar-Matthews et al. (2000)
NE. Brazil	SH	L-L	Heinrich	40–15	0	Wet	Smith and Rodbell (2010)
SW. US	NH	M-L	Heinrich	70–14	0	Dry	Wagner et al. (2010)
W. US	NH	M-L	Heinrich	40–30	0	Wet	Benson et al. (1996) Gale (1914) Oster et al. (2014)
W. US	NH	M-L	Heinrich	28.5–26.5	0	Wet	Benson et al. (1996) Gale (1914) Oster et al. (2014)
Florida, US	NH	M-L	Heinrich	70–14	Warm	Wet	Grimm et al. (2006)
Great Basin (Nevada, US)	NH	M-L	D–O	80–12	0	Wet	Benson et al. (1998)

NH Northern Hemisphere, SH Southern Hemisphere, H-L High-latitudes, M-L Mid-latitudes, L-L Low-latitudes. Period units are in ka BP and average age uncertainty for this period is ± 10 ka

colder (Johnsen et al. 1995). The lake sediments from the Lago di Origlio at Southern Swiss Alps suggest that during the Bølling–Allerød interstadial the temperature increased about 2.5 to 3.2 °C (Samartin et al. 2012). Sediment analyses over the Aegean Sea and Lake Maliq show an increased average annual temperature of about 10 °C in the onset of the Bølling–Allerød interstadial, which remained rather stable consequently (Bordon et al. 2009; Kotthoff et al. 2011). Still, its onset is considered amongst

the most dramatic deglaciation events over the NH, possibly linked with the revival of the AMOC (Thiagarajan et al. 2014).

The changes in Atlantic oceanic circulation intensified the hydrological cycle over various regions across the globe. One of the regions that were significantly affected is the Mediterranean. Sediment analysis from Lake Prespa (Greece) revealed enhanced humid conditions (Aufgebauer et al. 2012). Additionally, this increased

humid conditions were observed at Lake Maliq (Bordon et al. 2009), Eastern Mediterranean (Bar-Matthews et al. 1999), and also Lago Grande di Monticchio (Italy) (Allen et al. 1999). At the same time, there was a widespread increase in both tropical and monsoon precipitation. Significant increases are reported for equatorial Africa (Putnam and Broecker 2017; Tierney and deMenocal 2013), western Himalayas, Nepal and India (Sinha et al. 2005; Zech et al. 2014), and Northwest China (Zhou et al. 2001). Similar fluctuations in precipitation were observed over Southern and Central America. Wet and warm conditions have been identified in lake sediments of Laguna de Los Anteosojos (Venezuela) (Stansell et al. 2010), Pet'en Itz'a (Guatemala) (Hodell et al. 2008), La Yeguada and El Valle (Panama) (Bush et al. 1992) and Caribbean (Hughen et al. 1996).

All the evidence suggest that the multi-centennial increase in temperature was accompanied by an increase in precipitation too. In Fig. 5 and Table 5, we can see that more than 90% of temperature records are confirming warm conditions and about 85% of precipitation records for wet conditions. Again, this abrupt transition suffers from a low number of studies, especially at larger spatial scales (global, hemispheric, and continental).

3.3 Younger Dryas

The Bølling–Allerød interstadial was followed by another cool phase, the Younger Dryas event (from 13 to 11.7 ka BP). An abrupt decline in temperature disrupted the general warming trend that was driven by the increasing solar insolation (Dansgaard et al. 1989). Similarly to LGM and Heinrich events, the drop in temperature was accompanied by generally dry conditions (Hodell et al. 2008; Mayewski et al. 1993; Mayewski and Bender 1995). The Younger Dryas was mainly observed over the North Atlantic region (Fairbanks 1990), but is also evident in paleoclimatic records from all over the globe. However, the shift in the global climate was not homogeneous; contrary to the colder conditions of the high latitudes, the tropics were characterized by comparatively warmer conditions (Gagan et al. 2000). The temperature reconstructions of the Younger Dryas show a decline in temperature around 15 °C over central Greenland (Johnsen et al. 1995), and a drop between 6 and 9 °C in the Norwegian Sea (Karpuz and Jansen 1992). There is no doubt that Europe was substantially influenced by the Younger Dryas event (Brauer et al. 2008; Rach et al. 2014). A 4 to 6 °C decrease over western Europe has been reported, reaching 6 to 7 °C over Poland (Go'slar et al. 1995). There

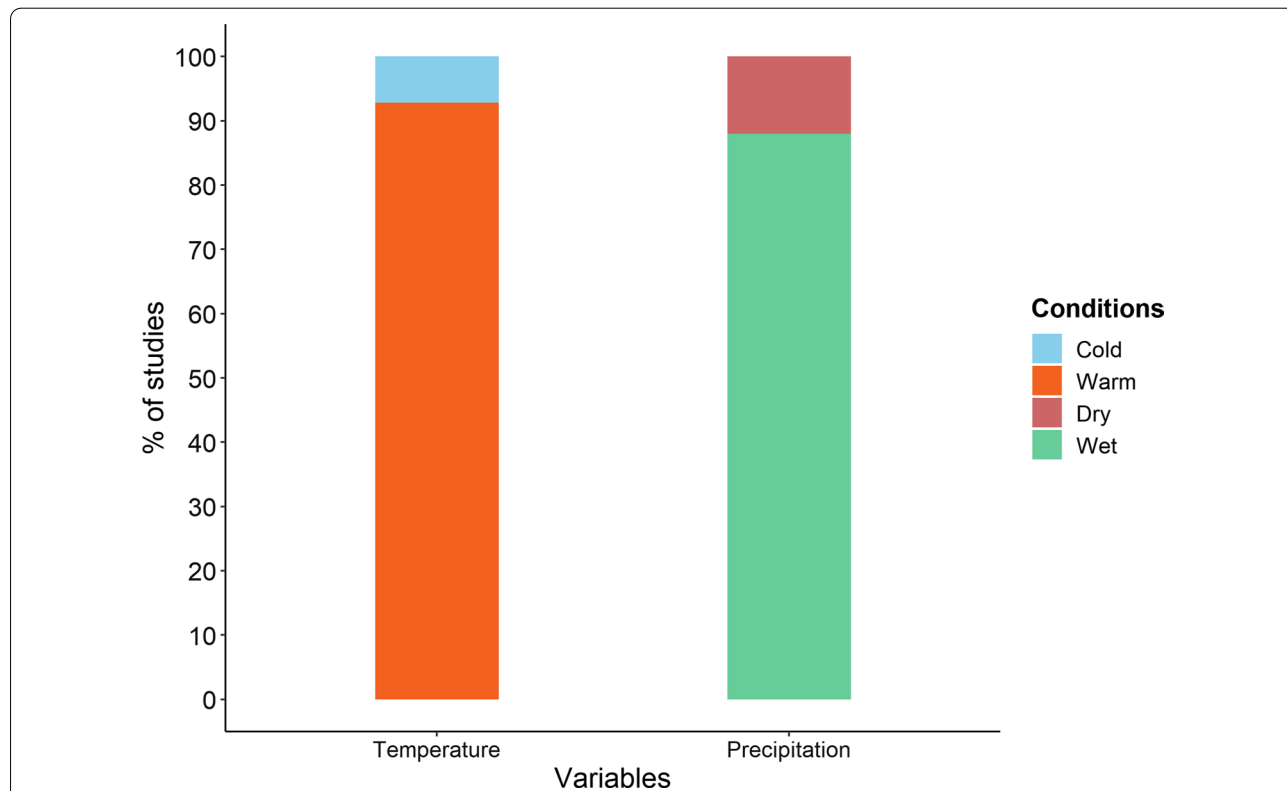


Fig. 5 Relationship of temperature and precipitation during the Bølling–Allerød interstadial. The number of studies used for the warm/cold or wet/dry conditions can be found in Table 5

Table 5 Temperature and precipitation conditions during the Bølling–Allerød interstadial

Study site	Hemisphere	Zone	Period	<i>T</i>	<i>P</i>	Citation(s)
N. Hemisphere	NH	L-L	13–12	0	Wet	Knox and Wright (1983) Maher (2008) Pausata et al. (2020)
S. & C. America	NH	M-L	14.8–12.85	Warm	Wet	Stansell et al. (2010) Hodell et al. (2008) Bush et al. (1992) Hughen et al. (1996)
Equatorial Africa	NH	M-L	14.8–12.85	0	Wet	Putnam and Broecker (2017) Tierney and deMenocal (2013)
Arctic	NH	H-L	14.5	Cold	0	Johnsen et al. (1995)
E. Mediterranean	NH	M-L	14.8–12.85	0	Dry	Bar-Matthews et al. (1999)
Greece	NH	M-L	14.8–12.85	0	Dry	Aufgebauer et al. (2012)
Italy	NH	M-L	14.8–12.85	0	Dry	Allen et al. (1999)
W. USA	NH	M-L	13	0	Wet	Benson et al. (1996) Gale (1914) Oster et al. (2014)
Aegean Sea	NH	M-L	14.8–12.85	Warm	0	Bordon et al. (2009) Kotthoff et al. (2011)
S. Swiss Alps	NH	M-L	14.8–12.85	Warm	0	Samartin et al. (2012)
W. Himalayas (Nepal & India)	NH	M-L	14.8–12.85	0	Wet	Sinha et al. (2005) Zech et al. (2014) Zhou et al. (2001)
Lake Maliq, Albania	NH	M-L	14.8–12.85	Warm	0	Bordon et al. (2009) Kotthoff et al. (2011)

NH Northern Hemisphere, SH Southern Hemisphere, H-L High-latitudes, M-L Mid-latitudes, L-L Low-latitudes. Period units are in ka BP and average age uncertainty is ± 1 ka

is also evidence of re-extension of the North European ice sheet (Aufgebauer et al. 2012). Consequently, this process led to the southerly flow of dry and cold northern air masses towards the Mediterranean area (Bordon et al. 2009), which led to colder temperatures in the Aegean Sea (Kotthoff et al. 2011). On the other hand, a pollen record from east Beringia revealed a more constrained drop in temperature, estimated at 1.5 °C (Fritz et al. 2012), which is in agreement with evidence that several coastal areas near western Novaya Zemlya (Russia) were ice-free (Serebryanny et al. 1998).

In terms of hydroclimate, various regions of the NH have experienced drier conditions during the Younger Dryas (Dahl and Nesje 1992; Fawcett et al. 1997; Hughen et al. 2000; Starkel 1991; Velichko et al. 2002). However, there are many regions that did not maintain a stable cold and dry regime, but instead the cold climate was coupled by centennial oscillations between dry and wet phases (Wang et al. 2018). For instance, the increase in the hydrogen isotope values at about 12 ka BP and 12.2 ka BP suggesting wetter and warmer phases over western Europe (Rach et al. 2014). This is also evident in Central Europe, where paleoclimatic records (Magny 2001) and certain periglacial characteristics (Kaiser and Clausen 2005) suggest wet conditions during the Younger Dryas (Weber et al. 2011), especially during winter (Isarin and Bohncke 1999). Other evidence of precipitation

comparative to the present has been recorded in Poland (Proсна River, about 30% higher) (Rotnicki 1991), Netherlands (Bos et al. 2006), and Scotland highlands (Lukas and Bradwell 2010). A multi-proxy reconstruction from central Poland for the Younger Dryas reports two phases (Pawlowski et al. 2015). The first (12.5–12 ka BP) was marked by a decrease in precipitation and temperatures during winter, but a rise in summer precipitation. The second (12–11.5 ka BP) shows increased winter and summer temperature with increased annual precipitation. In the southern Europe, pollen records from Mediterranean show increased precipitation during the whole deglaciation phase (18–10 ka), without any influence by Younger Dryas (Paterne et al. 1999).

A zonal gradient in precipitation response appears in North America. Drier conditions dominate the northern parts of the continent (Carlson 2013; Dorale et al. 2010), transitioning to considerably wetter conditions as we move southwards (Grimm et al. 2006; Voelker et al. 2015). There, the precipitation levels have been estimated at about 15% higher values than today, probably due to increased southern atmospheric moisture flow (Renssen et al. 2018). Wetter phases over central and southern North America are further supported by various proxy evidence in plant-macrofossil and palynology studies over Florida, and speleothems from New Mexico (Polyak et al. 2004) and Arizona (Wagner et al. 2010). Climate

model simulations also present a warmer climate with increased precipitation in the central regions of North America during the Younger Dryas when compared to the Bølling–Allerød period (Renssen 2020).

In the SH, there are conflicting results. Some studies provide evidence for enhanced precipitation and conditions similar to the Heinrich Events (Arz et al. 1998). For instance, the analysis lake sediments from Lake Titicaca (Bolivia, Peru) demonstrates the overflowing of the lake and thus higher precipitation between 13 and 11.5 ka BP (Baker et al. 2001). On the other hand, the lake sediment records at the lake Laguna de Los Anteosojos (Venezuela) present a transition to an intense cold and dry regime during the Younger Dryas (Stansell et al. 2010). This is further supported by a significant drop in the Amazon River discharge that is probably a result of reduced monsoon precipitation over the lowland tropical South America (Maslin and Burns 2000). Moreover, arid conditions are reported across the northern tropical Andes and wetter conditions over the southern tropical Andes (Stansell et al. 2010).

With 80% of the studies revealing a transition to cold conditions, there is little doubt about the temperature conditions of the Younger Dryas (Fig. 6). The same

cannot be said about the hydroclimatic regime, where studies remain split almost in the half. About 60% of the records suggest wet conditions, while the remaining 40% present a drier climate. The majority of the studies at larger spatial scales (global and N. Hemisphere) point to dry conditions, while wet conditions are more frequent in the finer scales.

4 Climatic fluctuations in the Holocene

4.1 The 8.2 ka event

The '8.2 ka cold event' is another abrupt climatic event that was experienced across the entire globe originating from the North Atlantic region (Alley and Ágústsdóttir 2005). As the name implies, it occurred around 8.2 ka BP and lasted for 160.5 ± 5.5 years, with the coldest period spanning 69 ± 2 years (Thomas et al. 2007). Other estimates suggest a duration between 150 and 200 years (Von Grafenstein et al. 1998; Snowball et al. 2002). The available proxy records show an abrupt cooling up to 6 ± 2 °C (Allen et al. 2007; Alley et al. 1997; Dansgaard et al. 1993), resulting to a global decrease by 0.9–1.8 °C (Heikkilä and Seppä 2010). Greenland is one of the regions with the most intense drops, about 3 to 8 °C (Alley et al. 1997; Von Grafenstein et al. 1998), as well as, enhanced windy and

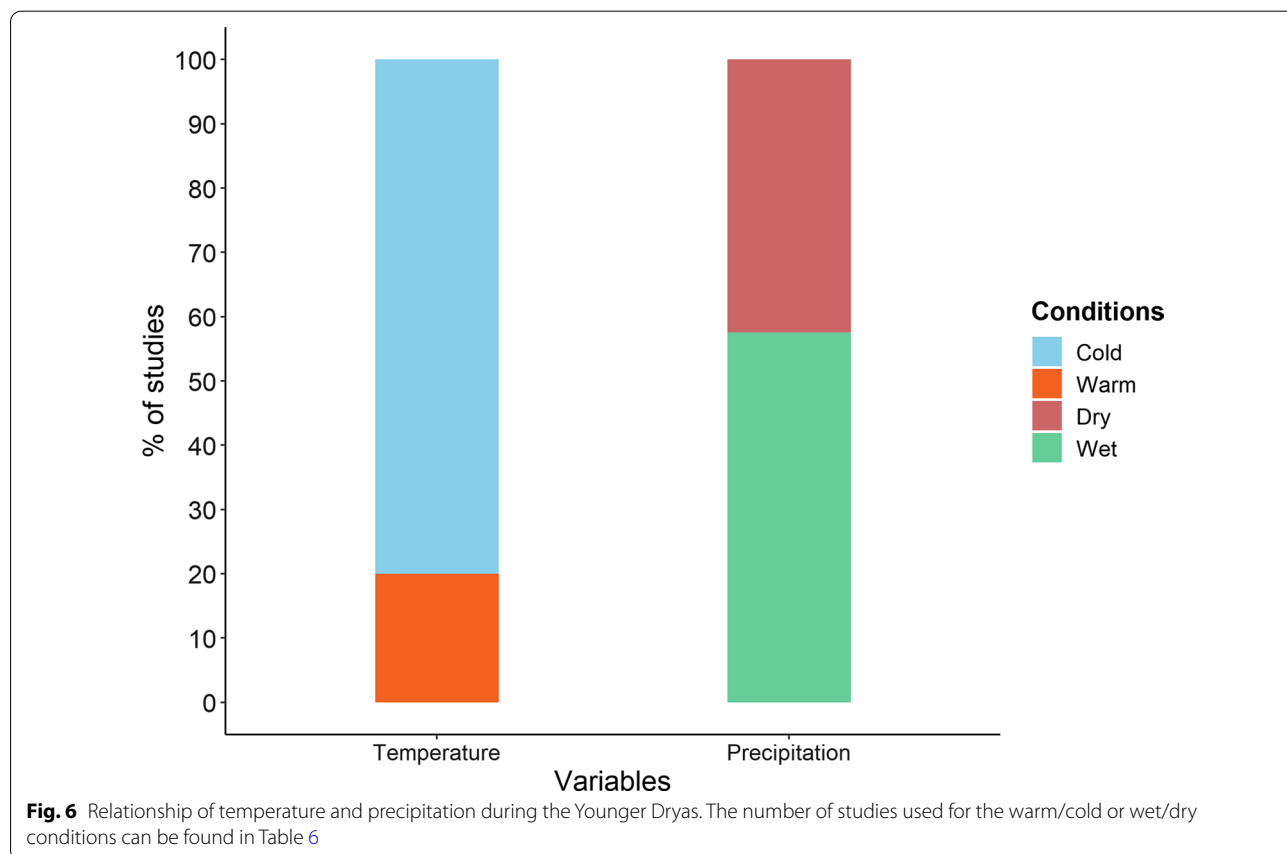


Table 6 Temperature and precipitation conditions during the Younger Dryas

Study site	Hemisphere	Zone	Period	T	P	Citation(s)
Global	NH/SH	0	13–11.7	Cold	Dry	Hodell et al. (2008) Mayewski et al. (1993) Mayewski and Bender (1995) Fairbanks (1990)
N. Hemisphere	NH	H-L	13–11.7	Cold	0	Gagan et al. (2000)
N. Hemisphere	NH	0	13–11.7	0	Dry	Dahl and Nesje (1992) Fawcett et al. (1997) Hughen et al. (2000), Starkel (1991) Velichko et al. (2002)
Tropics	NH/SH	L-L	13–11.7	Warm	0	Gagan et al. (2000)
Norwegian Sea	NH	H-L	13–11.7	Cold	0	Karpuz and Jansen (1992)
N. America (Northern part)	NH	M-L	13–11.7	0	Dry	Carlson (2013) Dorale et al. (2010)
N. America (Southern part)	NH	M-L	13–11.7	0	Wet	Grimm et al. (2006) Voelker et al. (2015) Renssen et al. (2001)
Central & Southern N. America	NH	M-L	13–11.7	0	Wet	Polyak et al. (2004) Wagner et al. (2010)
N. America (Central)	NH	M-L	13–11.7	Warm	Wet	Renssen (2020)
W. Europe	NH	M-L	13–11.7	Cold	0	Go'slar et al. (1995)
W. Europe	NH	M-L	12–12.2	Warm	Wet	Rach et al. (2014)
Central Europe	NH	M-L	13–11.7	0	Wet	Magny (2001) Kaiser and Clausen (2005) Weber et al. (2011) Isarin and Bohncke (1999)
S. Europe	NH	M-L	18–10	0	Wet	Paterne et al. (1999)
N. Tropical Andes	SH	M-L	13–11.7	0	Dry	Stansell et al. (2010)
S. Tropical Andes	SH	M-L	13–11.7	0	Wet	Stansell et al. (2010)
Tropical S. America	SH	L-L	13–11.7	0	Dry	Maslin and Burns (2000)
Bolivia & Peru	SH	L-L	13–11.7	0	Wet	Baker et al. (2001)
Poland	NH	M-L	13–11.7	Cold	0	Go'slar et al. (1995)
Poland	NH	M-L	13–11.7	0	Wet	Rotnicki (1991)
Netherlands	NH	M-L	13–11.7	0	Wet	Bos et al. (2006)
Venezuela	NH	L-L	13–11.7	Cold	Dry	Stansell et al. (2010)
E. Beringia	NH	M-L	13–11.7	Cold	0	Fritz et al. (2012)
N. Scotland	NH	M-L	13–11.7	0	Wet	Lukas and Bradwell (2010)
Aegean Sea	NH	M-L	13–11.7	Cold	0	Kotthoff et al. (2011)
Central Greenland	NH	H-L	13–11.7	Cold	0	Johnsen et al. (1995)

NH: Northern Hemisphere, SH: Southern Hemisphere, H-L: High-latitudes, M-L: Mid-latitudes, L-L: Low-latitudes. Period units are in ka BP and average age uncertainty is ± 0.5 ka

dry conditions over most parts of the NH (Törnqvist et al. 2004) at a time when the climatic conditions were similar as of today (Alley et al. 1997).

The areas with the most rapid transition were widespread across the entire Baltic Sea basin (Borzenkova et al. 2015), the western Europe (Davis et al. 2003), and the regions affected by the NAO, in particular (Seppä et al. 2008). The latter experienced a decline between 1.5 and 3 °C, as both land and marine records suggest (Klitgaard-Kristensen et al. 1998; Bond et al. 1997; Von Grafenstein et al. 1998). The above results are in good agreement with model simulations. The models present cooling around 2 to 5 °C over Greenland (Gasse 2000),

2.5 °C at the lake Annecy (France) (Magny et al. 2003), 1 to 2 °C over northwestern Europe (Renssen et al. 2001), as well as approximately 2 °C over Germany and the North Sea (Klitgaard-Kristensen et al. 1998).

Some model simulations also suggest a 30% drop in precipitation (Gasse 2000). This is in good terms with the dry conditions which have been generally observed over the NH (Clarke et al. 2004; Alley et al. 1997), particularly in the wintertime (Alley and Ágústsdóttir 2005). In Europe, the transition to dryer conditions was observed to latitudes over 50°N, as well as a significant part of the Mediterranean, including Spain, Northern Africa, and Italy (Magny and Bégeot 2004). On the other hand,

during the 8.2 event, a worldwide snowfall increase was observed (Borzenkova et al. 2015). This could explain the lake-level rises in many European palaeoclimate records, related to higher runoff (Magny 1992). The lake-level rise becomes more evident over the central Alps (Switzerland, France, and northern Italy) (Magny and B'egeot 2004).

All the evidence suggest that the 8.2 event was characterized by colder and drier climate conditions (Fig. 7), with only two studies presenting wet conditions over the Alps (Table 7). Even though there is good agreement between the records at both coarse and fine spatial scales, we cannot rule out though a small-sample bias in this conclusion due to the limited number of studies describing the precipitation of this cold period.

4.2 Medieval climate anomaly

The Medieval Climate Anomaly (MCA), also known as Medieval Warm Period, is the most recent period of abrupt warming, with onset around 800–1000 CE and termination at 1300–1400 CE (Hughes and Diaz 1994). It affected mostly Europe and parts of North America, which mainly experienced warmer than average conditions (Lamb 1965). The centennial-scale patterns of

spatiotemporal temperature reconstructions suggest widespread warm and arid conditions over the NH with a similar geographic extent and magnitude as in the twentieth century mean (Ljungqvist et al. 2016). Between 1200 and 1300 CE, the temperature was similar to the present over northwestern Europe (Guiot 1992). In addition, a temperature reconstruction across the Alps suggests that in the twelfth century the temperature was 0.3 °C higher than today (Trachsel et al. 2012). In North America, there is conflicting evidence about the increase magnitude. Viau et al. (2012) demonstrated that there was a 0.5 degree increase, which resulted to cooler than the present conditions, whereas Woodhouse et al. (2010) report temperatures of about 1 °C higher than today. There is also evidence of high temperatures over China (Yang et al. 2002), South Atlantic (Jones and Mann 2004), and Northern Pacific (Mann et al. 2009). Even though the extent of temperature increases during MCA remains under investigation, there is general agreement that there has been a clear signal of the increase at least in the NH.

The hydroclimatic response, though, was not so homogeneous. Substantial precipitation deficiencies were observed in northern Europe (Cook et al. 2015) and East Africa (Verschuren et al. 2000). In addition, model and

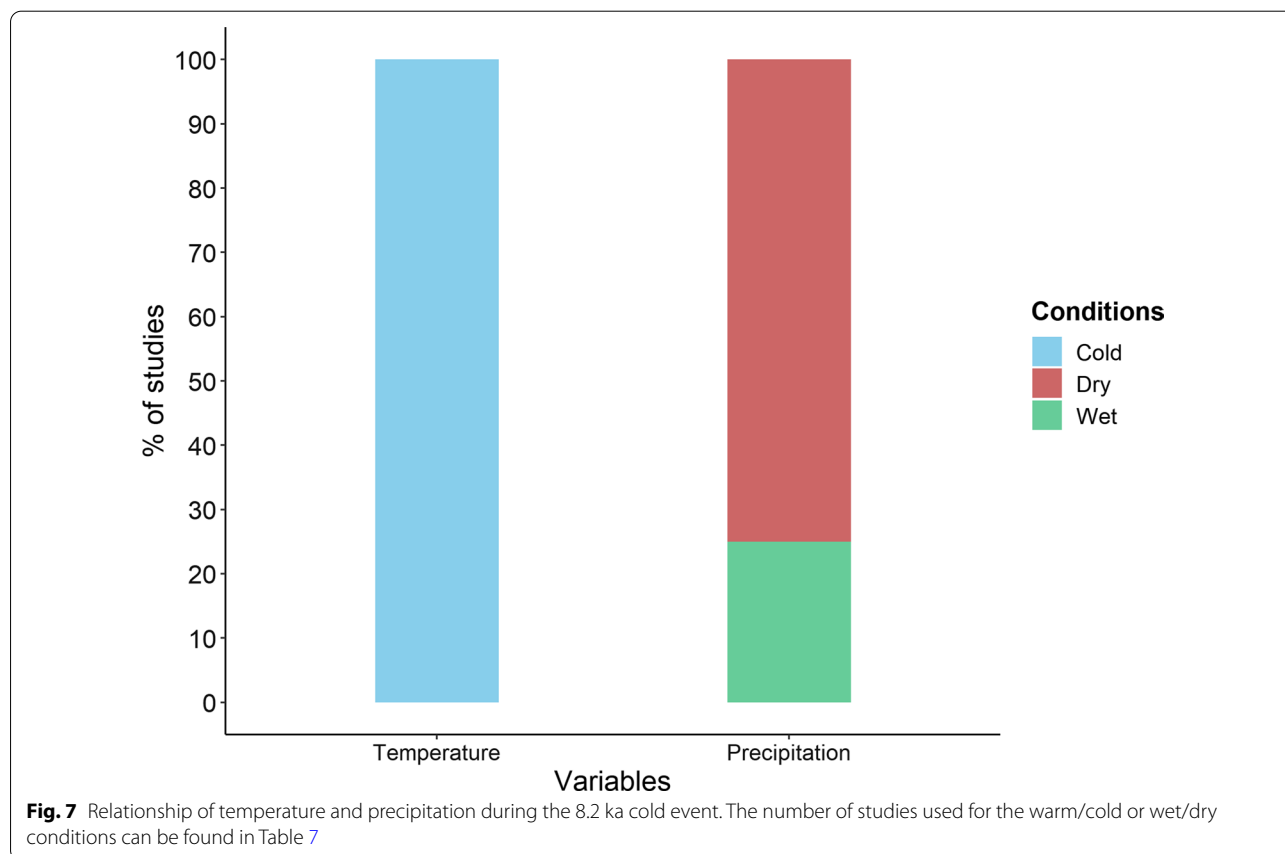


Table 7 Temperature and precipitation conditions during the 8.2 event

Study site	Hemisphere	Zone	Time	T	P	Citation(s)
Global	NH/SH	0	8.2	Cold	0	Alley and Ágústsdóttir (2005) Thomas et al. (2007) Heikkilä and Seppä (2010)
N. Hemisphere	NH	0	8.2	Cold	Dry	T'ornqvist et al. (2004) Clarke et al. (2004) Alley et al. (1997)
North Sea	NH	M-L	8.2	Cold	0	Klitgaard-Kristensen et al. (1998)
N. Africa	NH	M-L	8.2	Cold	Dry	Magny and B'egeot (2004)
NW. Europe	NH	M-L	8.2	Cold	0	Renssen et al. (2001)
Greenland	NH	H-L	8.2	Cold	0	Alley et al. (1997) Von Grafenstein et al. (1998) Gasse (2000)
Germany	NH	M-L	8.2	Cold	0	Klitgaard-Kristensen et al. (1998)
France	NH	M-L	8.2	Cold	0	Magny et al. (2003)
Spain	NH	M-L	8.2	Cold	Dry	Magny and B'egeot (2004)
Italy	NH	M-L	8.2	Cold	Dry	Magny and B'egeot (2004)
Central Alps	NH	M-L	8.2	0	Wet	Magny (1992); Magny and B'egeot (2004)

NH Northern Hemisphere, SH Southern Hemisphere, H-L High-latitudes, M-L Mid-latitudes. Period units are in ka BP

paleoclimatic records show that western North America experienced persistent and extensive aridity from 900 to 1300 CE (Woodhouse et al. 2010). On the other hand, anomalously lower $\delta^{18}\text{C}$ values in bristlecone pine from the White Mountains, California, highlight a wet period from 1080 to 1129 CE (Hughes and Diaz 1994). Similarly, Mauquoy et al. (2004) also suggested the times from 1030 to 1100 CE was a wet period for western North America, while there is also evidence of higher lake levels, or freshwater availability, over the Arizona monsoon-influenced area from 700 to 1350 CE (Hughes and Diaz 1994). However, the occurrence of increased aridity over most of the areas of western North America was also evident in tree-ring records between 650 and 1050 CE (Parish et al. 2020) and from 900 to 1300 CE (Cook et al. 2007).

In Asia, dry climatic conditions prevailed, mainly linked with atmospheric circulation (Chen et al. 2015). This in good terms with the proxy analysis over southern China indicates comparatively weak monsoonal precipitation over most of the regions (Chen et al. 2015) and the periods of extensive aridity from 1140 to 1220 and 1420 to 1490 (Li et al. 1987). On the contrary, pollen estimates from Maili pond at northeast China reveal wet conditions (from 950 to 1290 CE), suggesting an increase in the East Asian summer monsoon (EASM) during this period (Ren 1998). Additionally, the decades between 1230–1250 CE, and 1380–1410 CE show intensification of the South-Asian monsoon resulting to wet conditions (Li et al. 1987). Most of the proxy records suggest precipitation decrease over the EASM region after the termination of MCA around 1300 CE (Lan et al. 2020).

South America also experienced a highly variable climate during MCA. Perhaps this is due to a humidity

dipole between the southern and northern Amazon Basin (Marengo 2004). This humidity dipole could suggest an enhanced land–ocean temperature gradient or north–south migration of the ITCZ, driven by seasonal variation in the distribution of insolation (Wright et al. 2017). Consequently, the wetter phase over the northeast area was synchronous with the drier phase over Southern Amazonia (Thompson et al. 2013). For instance, a marine sediment core at Peru (12°S) shows intense aridity between 800 to 1250 CE (Rein et al. 2004), while a titanium (Ti) record from the Cariaco Basin (Venezuela) indicates wetter conditions between 950 to 1450 CE (Haug et al. 2001). Additionally, the assessment of lake sediment oxygen isotopes ($\delta^{18}\text{O}$) at the Central Peruvian Andes presents higher values from 900 to 1100 CE, implying a weakened South American Summer Monsoon and a prolonged period of aridity (Bird et al. 2011). On the other hand, wet conditions prevailed in Central America, as indicated by the lower values of oxygen isotope in sediments from Nicaragua from 950 to 1250 CE (Stansell et al. 2013).

Another feature of MCA is the emergence of simultaneous mega-droughts in various regions of the globe (Stager et al. 2005). The main region affected of these multi-decadal droughts can be found at North America (Cook et al. 2014). There, two prolonged drought events with an approximately 90 years time span have been recorded over North America. The first event occurred between 1197 and 1289 CE, while the second event occurred between 1486 and 1581 CE (Parish et al. 2020). Other shorter events have been also detected, presenting higher severity, though, such as the mega-drought from 1140 to 1162 CE or the one between 1150 to 1159 CE (Cook et al. 2007). In Europe, the multi-decadal

reconstruction over the Sierra Nevada (Spain) highlights four multi-decadal droughts that prevailed during the MCA (800–859 CE, 1020–1070 CE, 1197–1217 CE, and 1249–1365 CE) (Graumlich 1993).

The main hypothesis about the driver of the enhanced hydroclimatic variability of MCA is the positive state of NAO, which persisted at centennial time scale (Trouet et al. 2009). The result was a northeastward shift of the cyclonic storm tracks, and consequently the transport of atmospheric moisture to higher latitudes (Solomon et al. 2007). The spatial hydroclimatic variability is also evident in finer scales. A typical case is highlighted over the Iberian Peninsula. There, a climate reconstruction shows warmer and humid conditions across the northwest regions, while the rest of the peninsula shows warm and arid conditions (Moreno et al. 2012). Similar patterns can be seen in tree-ring records over Morocco, where some unusually frequent wet years occurred from 1250 to 1300 CE (Till et al. 1990).

During the MCA, all the studies analyzed clearly suggest a warmer climate (Fig. 8 and Table 8). However, contrary to the other warm periods presented in this study, the multi-centennial warming was coupled with dry conditions. About two thirds of the records indicate a

transition to a dry climate, which might be seen as contradiction to the prevailing theory of water cycle intensification and will be discussed in detail below.

4.3 Little Ice Age

The Little Ice Age (LIA) is the most recent shift to colder conditions. It lasted from 1350–1450 CE to 1900 CE (Mayewski and Bender 1995), and the global temperature was 0.5 to 1.5 °C lower than the twentieth century average (Crowley and North 1991; Graumlich 1993; Mann et al. 1998; Christiansen and Ljungqvist 2012; Schneider et al. 2015). Trachsel et al. (2012) have reported that during fourteenth, late sixteenth, and seventeenth century, the global temperature was a 1 °C lower than the twentieth century average. The NH experienced the most substantial decrease (about 0.9 °C lower) from 1570 to 1730 CE (Bradley and Jonest 1993), whereas in Europe LIA peaked in 1650–1750 CE (Bond et al. 2001). In SH, paleoclimatic oceanic records show an average cooling of 1.6 °C (± 1.4) compared to the last 150 years (Rhodes et al. 2012). Ice core analysis near the Ross Sea (Antarctica) shows colder conditions of 2 °C in surface temperature, as well as lower SST over the Southern Ocean coupled by enhanced sea ice extent during the LIA (Bertler et al. 2011). In general,

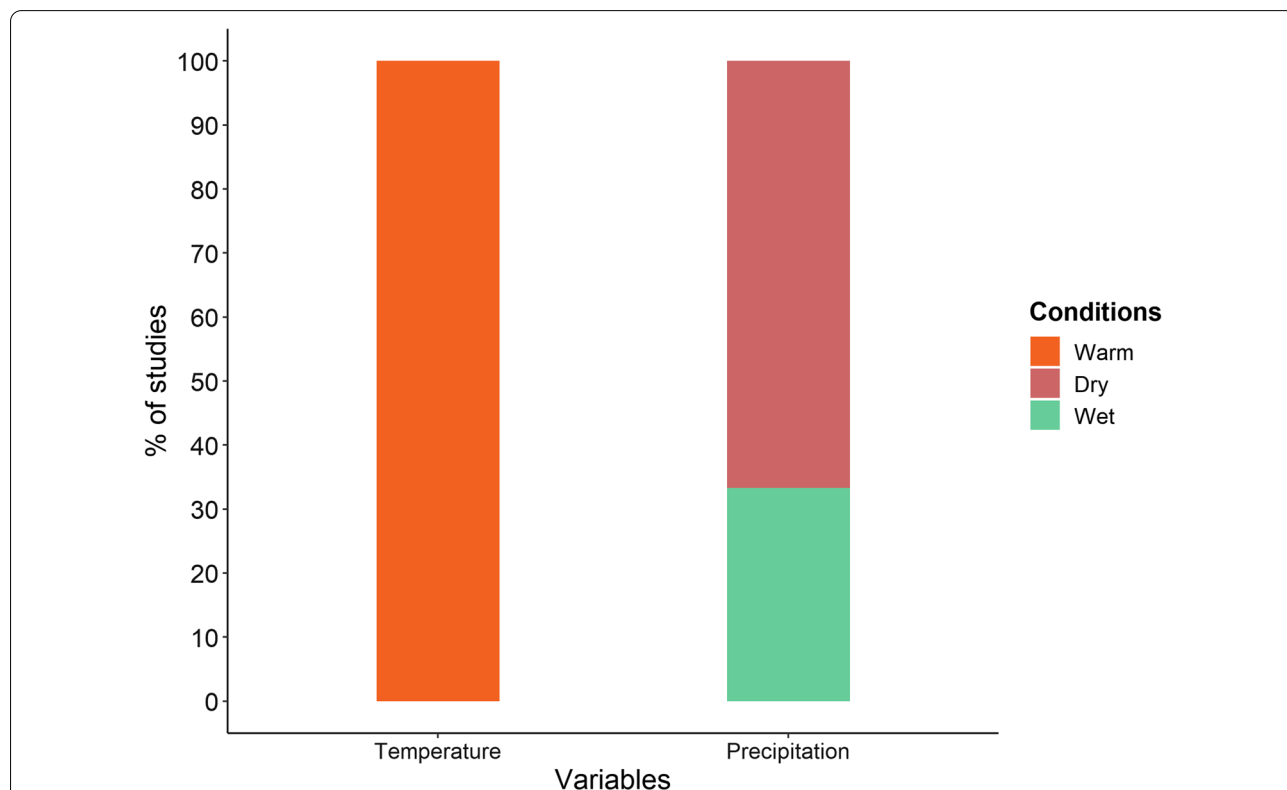


Fig. 8 Relationship of temperature and precipitation during the MCA. The number of studies used for the warm/cold or wet/dry conditions can be found in Table 8

Table 8 Temperature and precipitation conditions during the MCA

Study site	Hemisphere	Zone	Time	T	P	Citation(s)
N. Hemisphere	NH	0	800–1400	Warm	Dry	Ljungqvist et al. (2016)
Asia	NH	M-L	900–1300	0	Dry	Chen et al. (2015)
N. America	NH	M-L	1197–1289 And 1486–1581	0	Dry	Cook et al. (2014) Parish et al. (2020)
N. America	NH	M-L	1140–1162	0	Dry	Cook et al. (2007)
N. America	NH	M-L	800–1400	Warm	0	Woodhouse et al. (2010)
N. America	NH	M-L	800–1400	Warm	0	Lamb (1965)
Europe	NH	M-L	800–1400	Warm	0	Lamb (1965)
N. Europe	NH	M-L	800–1400	0	Dry	Cook et al. (2015)
S. Asia	NH	M-L	1230–1250 and 1380–1410	0	Wet	Li et al. (1987)
E. Asia	NH	M-L	1300	0	Dry	Lan et al. (2020)
NW. Europe	NH	M-L	1200–1300	Warm	0	Guiot (1992)
S. America (NE area)	SH	L-L	800–1400	0	Wet	Thompson et al. (2013)
Western N. America	NH	M-L	900–1300	Warm	Dry	Woodhouse et al. (2010)
Western N. America	NH	M-L	1030–1100	0	Wet	Mauquoy et al. (2004)
Western N. America	NH	M-L	650–1050	0	Dry	Parish et al. (2020)
Western N. America	NH	M-L	900–1300	0	Dry	Cook et al. (2007)
E. Africa	NH	M-L	800–1400	0	Dry	Verschuren et al. (2000)
S. Atlantic	SH	M-L	800–1400	Warm	0	Jones and Mann (2004)
N. Pacific	NH	M-L	800–1400	Warm	0	Mann et al. (2009)
China	NH	M-L	800–1400	Warm	0	Yang et al. (2002)
S. China	NH	M-L	800–1400	0	Dry	Chen et al. (2015)
S. China	NH	M-L	1140–1220 and 1420–1490	0	Dry	Li et al. (1987)
NE. China	NH	M-L	950–1290	0	Wet	Ren (1998)
Southern Amazonia	SH	L-L	800–1400	0	Dry	Thompson et al. (2013)
Peru	SH	L-L	800–1250	0	Dry	Rein et al. (2004)
Morocco	NH	M-L	1250–1300	0	Wet	Till et al. (1990)
Central America	NH	M-L	950–1250	0	Wet	Stansell et al. (2013)
Spain (Sierra Nevada)	NH	M-L	800–859, 1020–1070, 1197–1217, And 1249–1365	0	Dry	Graumlich (1993)
Venezuela	NH	L-L	950–1450	0	Wet	Haug et al. (2001)
Arizona, USA	NH	M-L	700–1350	0	Wet	Hughes and Diaz (1994)
California, USA	NH	M-L	1080–1129	0	Wet	Hughes and Diaz (1994)
Iberian Peninsula	NH	M-L	800–1400	Warm	Dry	Moreno et al. (2012)
Central Peruvian Andes	SH	L-L	900–1100	0	Dry	Bird et al. (2011)
Alps	NH	M-L	twelfth century	Warm	0	Trachsel et al. (2012)

NH Northern Hemisphere, SH Southern Hemisphere, H-L High-latitudes, M-L Mid-latitudes, L-L Low-latitudes. Period units are in AD and average age uncertainty for the MCA is ± 100 years

the lowest temperatures were observed in the period of 1680 to 1730 CE, for both Hemispheres (Stuiver et al. 1995).

The LIA has been compared to the abrupt changes that occurred in the last glacial stage (Bond et al. 1999), such as the D–O events (Broecker 2000). However, even though LIA affected the whole globe, this did not happen

simultaneously. Most local or regional paleoclimatic reconstructions show unusually cold phases from 1580 to 1880 CE, interrupted by decades of warmer conditions (Ahmed et al. 2013). Similarly to MCA, the main hypothesis for the spatio-temporal variability lies in the changes of atmospheric circulation (Zhang et al. 2021a). Compared to the current patterns of atmospheric circulation,

LIA experienced stronger meridional transport (Lamb 2013). This was observed over the North Atlantic and polar South Pacific at the beginning of the LIA, evident in ice cores from central Greenland, Siple Dome, and West Antarctica (Kreutz et al. 1997). The colder and drier conditions that prevailed were a result of the enhanced atmospheric circulation, as reported in numerous paleoclimatic records in the NH and the Equator (Thompson et al. 1995; O'Brien et al. 1995). Additionally, numerical model experiments have identified sea ice-ocean-atmosphere (Zhong et al. 2011) and volcanic feedbacks (Miller et al. 2012) as a factor that triggered the LIA cooling over the North Atlantic and Europe.

The drop of temperature was coupled to wet conditions over the most of the European territory (Luoto and Nevalainen 2018; Brönnimann et al. 2019). Both the speleothem record from Scotland (Proctor et al. 2000) and a reconstruction from England-Wales (Lamb 1965) are notably similar, showing a 10% decrease in the precipitation (for September to June) from the late thirteenth to the mid fourteenth century, and a constant drop from the mid of sixteenth to late eighteenth century. Precipitation reconstructions from southern Moravia (Czech Republic) show that the highest precipitation occurred between 1670 and 1710 CE, succeeding a period with low precipitation (Brázdil et al. 2002). Proxy estimates of seasonal precipitation over Europe exhibit increased winter (DJF) precipitation during the beginning of the eighteenth century (Pauling et al. 2006), which is attributed to a significant increase in winter temperatures (Nesje et al. 2008). This is in good agreement with the abrupt increase in floods reported from 1760 to 1800 CE over various locations (Blöschl et al. 2020). Other similar periods are 1560–1580 and 1840–1870, when the climate conditions were abruptly shifted to a warmer phase (Glaser et al. 2010) and consequently increasing precipitation and/or snowmelt (Brázdil et al. 1999). This is particularly true for the end of the LIA, when there has been a monotonic increase towards more humid conditions (Cook et al. 2015; Markonis et al. 2018).

Over the North American continent, there is evidence of strong spatiotemporal heterogeneity in the observed changes. In general, wetter conditions were observed in the central regions compared to the present, while drier conditions prevailed over both the West and East Coast (Ladd et al. 2018). In most of the wet periods, precipitation increased during the winter (Parish et al. 2020), lasted for a couple of decades and were succeeded by long dry intervals (Meko 1992). For instance, a precipitation reconstruction at Banff, Alberta (Canada) shows higher precipitation from 1515 to 1550 CE, 1585 to 1610 CE, 1660 to 1680 CE, and during the 1880s, while 1950 to 1970s exhibit both enhanced precipitation and decreased

summer temperatures (Luckman 2000). On the other hand, the spatio-temporal drought and precipitation records over North America suggest a widespread limitation in moisture availability during the late sixteenth century while relative abundance during the early seventeenth century (Cook et al. 1997; Bradley et al. 2003; Matthews and Briffa 2005).

Various changes are reported in the rest of the world, related to the fluctuations of atmospheric circulation. Sediment records from the northeastern Arabian Sea show a weakening of Indian summer monsoon from 1450 to 1750 CE and consequently a shift to drier conditions (Agnihotri et al. 2002). Northern China also faced a moderately weak monsoon (Chen et al. 2015). The lakelevels and diatom estimates over Africa (Street-Perrott and Perrott 1990), and dust records in an equatorial ice core (Thompson et al. 1995) also display increased aridity. The paleoclimate records from the Argentina show during about 1800 and 1930 as the wet period (Mauquoy et al. 2004). However, the isotope (increased values) evidence from Central America suggests the persistence of drier conditions during most of the LIA (Stansell et al. 2013). Additionally, the tree-ring analysis from southern South America indicates cold-dry/drought phase between 1280 and 1450, 1550 and 1670, and 1780 to 1830 CE; while the warm-wet/high-rainfall phases from 1220 to 1280, 1450 to 1550, 1720 to 1780, and 1830 to 1905 CE (Villalba 1994).

Increased precipitation was also observed in various regions across the world. Low concentration of microparticles in ice core records from the Antarctic Peninsula indicates likely higher precipitation and intense cyclonic activity (Rogers 1983). The enhanced meridional circulation has been expected to influence the mid and low latitude circulation, resulting to a shift of the westerlies belt and increased precipitation over the Patagonia and California around 1400 CE (Stine 1994). Additionally, the arid central Asia region is showing relatively wet conditions, and pluvial conditions prevailed over southern China (Chen et al. 2015). The wet conditions were often succeeded by arid conditions, resulting to 18 extreme flood and 16 drought events during the LIA in China (Zheng et al. 2006). Similarly, sediment geochemistry from a subalpine lake at northern Taiwan indicated four pluvials (1660 CE, 1730, 1820, and about 1920) (Wang et al. 2013; Zhao et al. 2018). In South America, the oxygen isotope ($\delta^{18}\text{O}$) estimates of a speleothem record at northeastern Peru report enhanced variability in precipitation, with annual precipitation being 10% higher than today from fifteenth to eighteenth century (Reuter et al. 2009). This is in good agreement with the results of an oxygen isotopes ($\delta^{18}\text{O}$) analysis at the Central Peruvian Andes lake, showing a

prolonged regionally synchronous intensification in the South American Summer Monsoon (Bird et al. 2011). Similar conclusions were drawn in the study of Polissar et al. (2006) about the growth of glaciers at the high elevations over the Venezuelan Andes, which can be interpreted as evidence of higher precipitation.

The analysis of the corresponding literature advocates that LIA is not homogeneous event in space and time. There are approximately 25% of studies that reveal some region and/or period of warm conditions (Fig. 9). This is due to the availability of higher resolution reconstructions, which can detect shorter warmer periods within the prevailing cold conditions, such as for example the 1560–1580 and 1840–1870 warm intervals over Europe (Brázdil et al. 1999; Glaser et al. 2010). In addition, there are numerous locations with cold and wet conditions, resulting to a sum of 60% of studies presenting a wet LIA, and 40% of records suggesting otherwise. Similarly to MCA, this is a reversed relationship between temperature and precipitation compared to the other periods studied. A possible explanation for this outcome could lie to the fact that the majority of the studies come from Europe, amplifying the wet signal (Table 9).

5 Insights from the past

Although our literature review study focuses in providing the empirical evidence of past hydroclimatic changes, in this last Section we will briefly discuss some plausible explanations for our findings. Perhaps the most striking result is that even during the highest temperature deviations amongst the ones we examined, the hydrological cycle fluctuated within a reasonable range. No extreme cases of global long-term aridity or humidity have been imprinted in the paleoclimatic records. On the contrary, most climatic shifts present substantial spatial heterogeneity regardless of their time scale. Of course, different physical mechanisms will drive hydroclimatic variability in different spatio-temporal scales. Due to the large uncertainties involved and the scarcity of the data records, it is rather questionable if the exact processes could be described, though. What could be more pragmatic is to distinguish the impact of the thermodynamic and dynamic component.

Higher temperatures appear more strongly related to wet conditions than lower temperatures to dry (Table 10). Out of the five warm periods studied, four present a distinct warm-and-wet signal and only during the MCA the dry conditions prevailed. On the other hand, only two

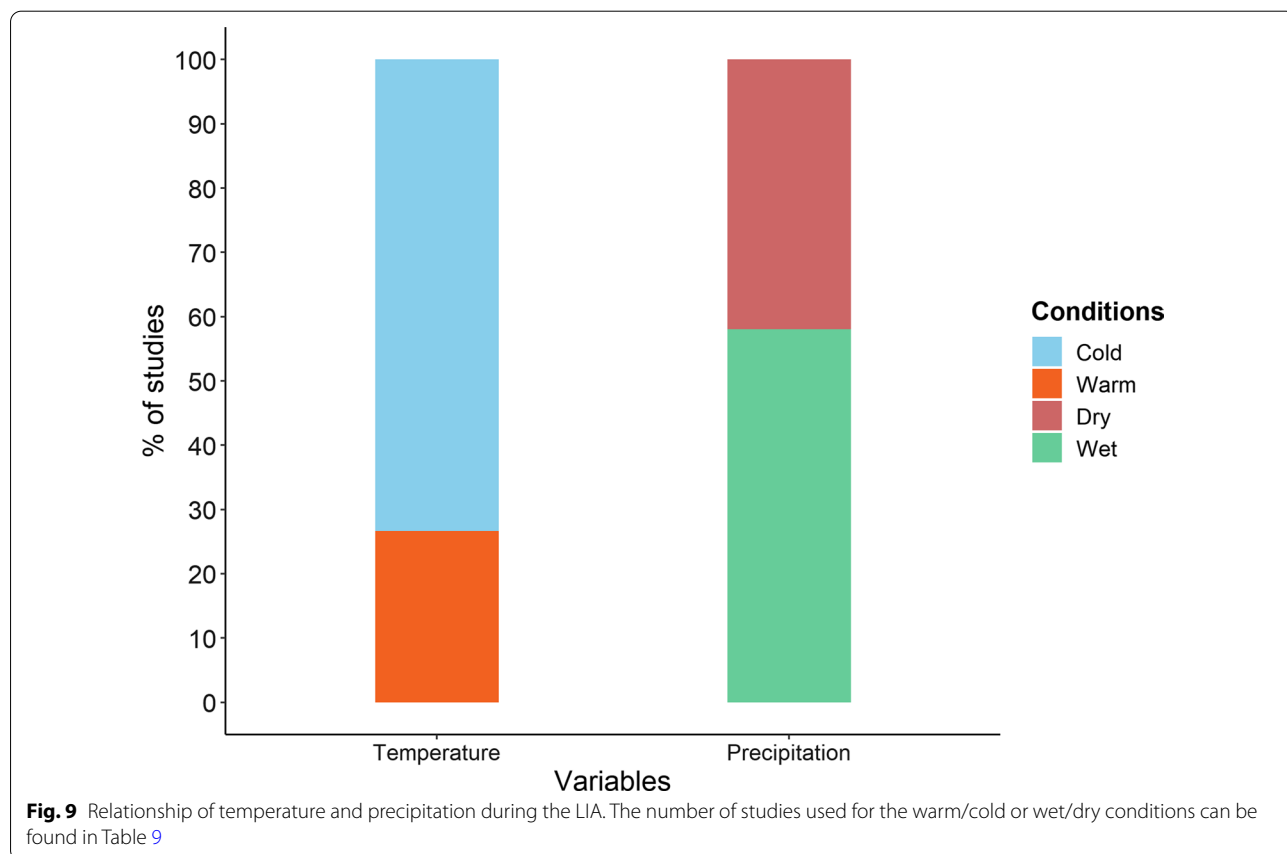


Table 9 Temperature and precipitation conditions during the LIA

Study site	Hemisphere	Zone	Time	T	P	Citation(s)
Global	NH/SH	0	1350–1900 CE	Cold	0	Crowley and North (1991) Graumlich (1993) Mann et al. (1998) Christiansen and Ljungqvist (2012) Schneider et al. (2015)
Global	NH/SH	0	14th, Late sixteenth and seventeenth century	Cold	0	Trachsel et al. (2012)
N. Hemisphere	NH	0	1570–1730 CE	Cold	0	Bradley and Jonest (1993)
S. Hemisphere	SH	0	1350–1900 CE	Cold	0	Rhodes et al. (2012)
Africa	NH	L-L	1350–1900 CE	0	Dry	Street-Perrott and Perrott (1990)
Antarctica	SH	H-L	1350–1900 CE	Cold	0	Bertler et al. (2011)
Europe	NH	M-L	1650–1750 CE	Warm	0	Bond et al. (2001)
Europe	NH	M-L	Early eighteenth century	0	Wet	Pauling et al. (2006)
Europe	NH	M-L	Early eighteenth century	Warm	0	Nesje et al. (2008)
Europe	NH	M-L	1760–1800 CE	0	Wet	Blöschl et al. (2020)
Europe	NH	M-L	1560–1580 CE	Warm	Wet	Glaser et al. (2010) Br'azdil et al. (1999)
Europe	NH	M-L	1840–1870 CE	Warm	Wet	Glaser et al. (2010) Br'azdil et al. (1999)
N. America	NH	M-L	Late 16 th and Early seventeenth century	0	Dry	Cook et al. (1997) Bradley et al. (2003) Matthews and Briffa (2005)
Central Asia	NH	M-L	1350–1900 CE	0	Wet	Chen et al. (2015)
Central America	NH	M-L	1350–1900 CE	0	Dry	Stansell et al. (2013)
N. America (Central regions)	NH	M-L	1350–1900 CE	0	Wet	Ladd et al. (2018)
N. America (W & E Coast)	NH	M-L	1350–1900 CE	0	Dry	Ladd et al. (2018)
Southern S. America	SH	M-L	1280–1450 CE, 1550–1670 CE, and 1780–1830 CE	Cold	Dry	Villalba (1994)
Southern S. America	SH	M-L	1220–1280 CE, 1450–1550 CE, 1720–1780 CE, and 1830–1905 CE	Warm	Wet	Villalba (1994)
Antarctic Pen	SH	H-L	1350–1900 CE	0	Wet	Rogers (1983)
Arabian Sea	NH	L-L	1450–1750 CE	0	Dry	Agnihotri et al. (2002)
Argentina	SH	M-L	1800 and 1930	0	Wet	Mauquoy et al. (2004)
Canada	NH	M-L	1515–1550 CE, 1585–1610 CE, 1660–1680 CE, and 1880s	0	Wet	Luckman (2000)
Czech Republic	NH	M-L	1670–1710 CE	0	Wet	Br'azdil et al. (2002)
Venezuelan Andes	NH	L-L	1400–1700 CE	0	Wet	Polissar et al. (2006)
Scotland	NH	M-L	Late 13 th to mid fourteenth century	0	Wet	Proctor et al. (2000)
Peru	SH	L-L	1400–1700 CE	0	Wet	Reuter et al. (2009) Bird et al. (2011)
California, USA	NH	M-L	1400 CE	0	Wet	Stine (1994)
Wales, UK	NH	M-L	Late 13th mid fourteenth century	0	Wet	Lamb (1965)
England	NH	M-L	Late 13th mid fourteenth century	0	Wet	Lamb (1965)
Patagonia	NH	M-L	1400 CE	0	Wet	Stine (1994)
N. China	NH	M-L	1450–1750 CE	0	Dry	Chen et al. (2015)
N. Taiwan	NH	M-L	1660, 1730, and 1820 CE	0	Wet	Wang et al. (2013) Zhao et al. (2018)

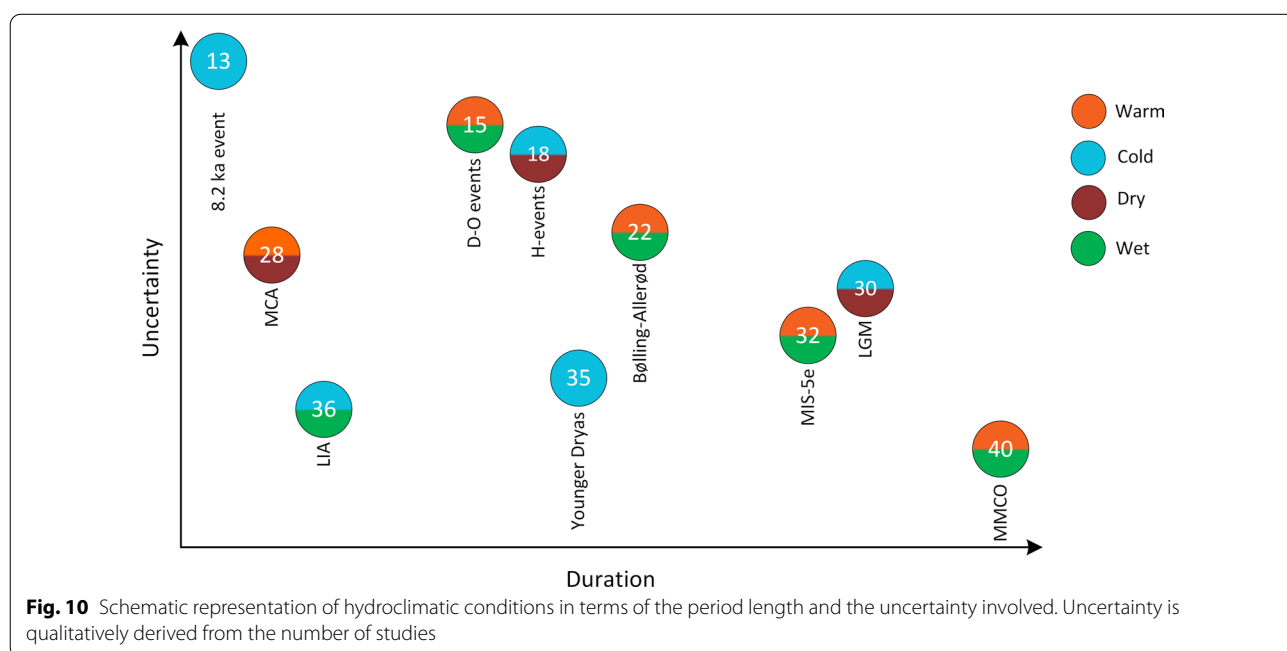
NH Northern Hemisphere, SH Southern Hemisphere, H-L High-latitudes, M-L Mid-latitudes, L-L Low-latitudes and average age uncertainty for the LIA is ± 50 years

Table 10 Number of studies per period and conditions. The *Hydroclimate* column describes the most common condition. Average duration is estimated in thousand years

Period	Duration (ky)	Studies	Warm	Cold	Dry	Wet	Hydroclimate
MMCO	2500	40	49	0	22	39	Warm and wet
MIS-5e	14	32	12	2	7	21	Warm and wet
LGM	15	30	0	13	20	5	Cold and dry
D–O events	0.8	15	5	0	0	12	Warm and wet
H-events	1	18	1	13	17	10	Cold and dry
Bølling–Allerød	2	22	7	1	3	15	Warm and wet
Younger Dryas	1.3	35	3	12	14	17	Cold
The 8.2 ka event	0.16	13	0	16	6	6	Cold
MCA	0.4	28	11	0	24	10	Warm and dry
LIA	0.5	36	9	15	16	25	Cold and wet

out of five cold periods show a cold-and-dry regime, one exhibits cold-and-wet conditions (Little Ice Age) and two remain inconclusive (Younger Dryas and 8.2 k event). It is easy to note that the periods that diverge from the Clausius-Clapeyron thermodynamic response are the shorter ones (Fig. 10). Longer periods with duration comparable to Holocene, such as the Eemian Interglacial Stage and the Last Glacial Maximum follow the warm-and-wet and cold-and-dry paradigms. A similar pattern manifests in the spatial domain. Global or hemispheric studies are more tightly linked to the thermodynamic response, while as spatial scale becomes finer the heterogeneity increases highlighting the impact of the changes in atmospheric and oceanic circulation (Gasse 2000; Li et al. 2012).

Thus, it is reasonable to claim that the atmospheric/oceanic circulation (dynamic component) appears to have a more dominant role in the regional fluctuations of the hydrological cycle, than the total atmospheric moisture content (thermodynamic component). This is particularly true for the abrupt climatic events. Even though the exact physical mechanisms of their genesis remain under investigation, there is a general agreement that most of the past abrupt climatic transitions are related to changes in the oceanic circulation. Still, it is a concern whether these abrupt climate changes arisen from internal climate system processes or be the consequence of a stimulated response to a progressive external forcing (Clement et al. 2001). In the case of longer climatic regimes, warmer/colder oceans develop different circulation patterns, which in turn affect the



atmosphere system resulting to different modes of atmospheric circulation (Wright et al. 1992).

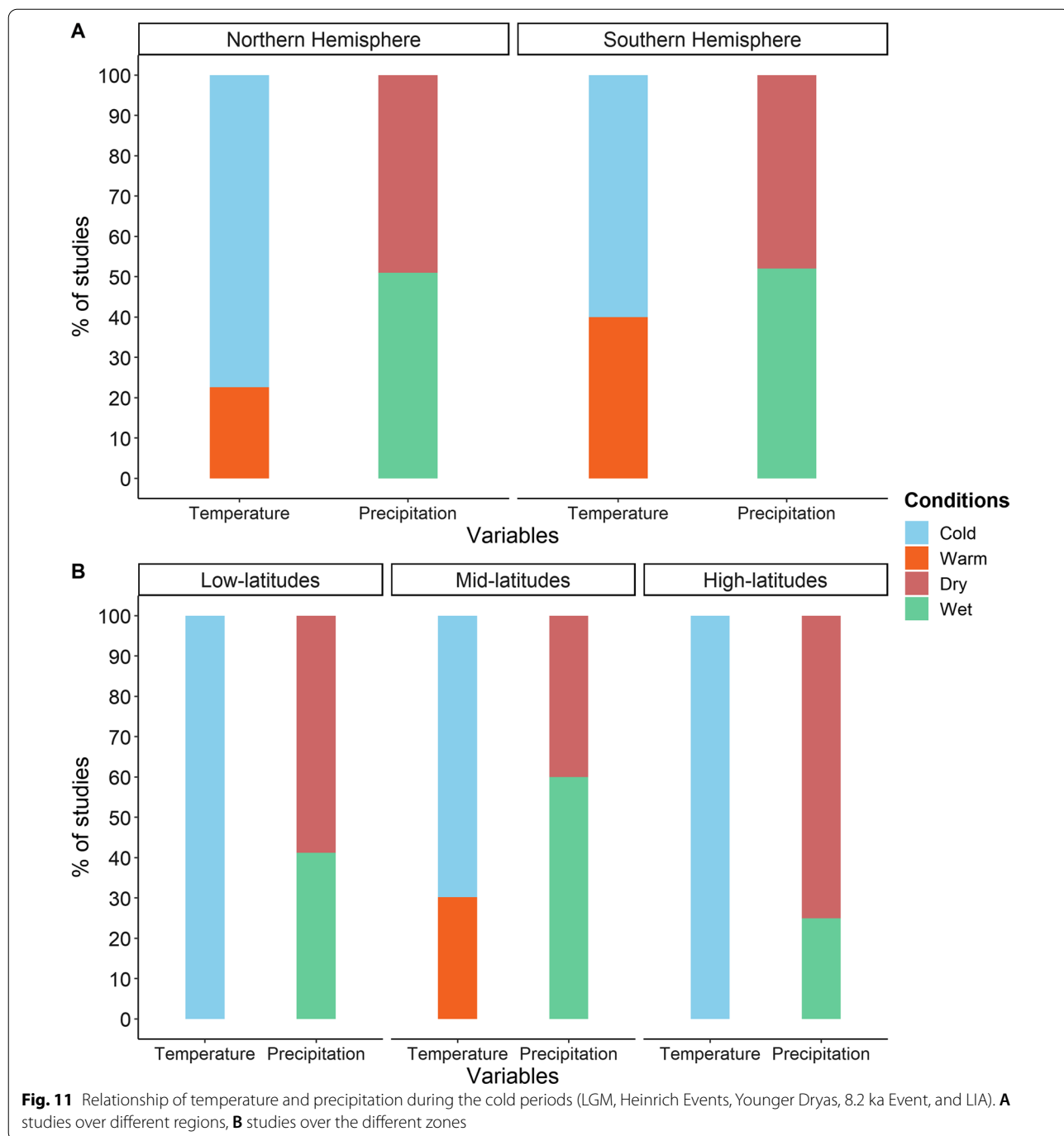
The majority of the abrupt events studied here were mainly associated with the Atlantic longterm variability and AMOC in specific. The AMOC is not a circulation pattern appearing only in Holocene. Its existence has been confirmed both for the Eemian Interglacial Stage and the D–O intervals (Corrick et al. 2020). The decline of AMOC strength has also been linked to Heinrich events, Younger Dryas, the 8.2 ka event, and phases of cold conditions in general (Ellison et al. 2006; Renssen et al. 2018). It's weakening is related to freshwater pulses caused by the melting of Arctic ice and high latitude glaciers (Li et al. 2012). The AMOC variability can affect the Westerlies, and, thus the atmospheric moisture amount that is transferred over land. When weak, it has been linked to decline in precipitation from western Europe to continental Asia (Mackay et al. 2013), as well as monsoon activity (Gupta et al. 2003). The latter is likely due to the links between the weakening of AMOC and the southward shift of Inter Tropical Convergence Zone (ITCZ). As the AMOC weakens, the temperature gradient between tropical and North Atlantic becomes more intense and drives ITCZ to the south (Mohtadi et al. 2014).

Overall, the southward shift of the ITCZ has been related to the colder conditions across the northern tropics such as Heinrich events (Leduc et al. 2007), Younger Dryas (Peterson and Haug 2006), and the weak monsoon during MIS-5e (McGowan et al. 2020). In addition, the latitudinal variations of the ITCZ have been identified to affect summer-monsoon variations in tropical and Asian regions during the D–O and Heinrich events (Ivanochko et al. 2005). On the contrary, the northward shift of the ITCZ has been reported to intensify the Asian summer monsoon (Peterson et al. 2000; Wang et al. 2001), which is also related to warmer conditions (Stansell et al. 2010; Schneider et al. 2020). There is some evidence of this behaviour also during mid-Miocene; the enhanced precipitation observed across northern Colombia was likely due to the northward shift of ITCZ (Scholz et al. 2020). Most importantly, as ITCZ shifts the regions that are no longer under its effect will become drier, with an opposite outcome to the ones that no longer affected. This is a straightforward example of why wetter and drier conditions can co-exist when there is some atmospheric reorganization. As ITCZ and the monsoon systems involve a large fraction of global precipitation, further research is increasingly important to further understand the relationship between oceanic circulation and ITCZ/monsoon in past climates.

It is interesting that even though there is substantial evidence of the connection between ITCZ and temperature in the paleoclimatic reconstructions, this was not the case for atmospheric moisture divergence zones as well. Nowadays, the dominant hypothesis suggests that global warming makes the regions with atmospheric divergence to become drier and the regions with atmospheric convergence to become wetter, termed as 'dry gets drier, wet gets wetter' (Held and Soden 2006). However, our results are not in favor of this hypothesis, which have also been recently debated by some empirical studies of observational (Greve et al. 2014) and paleoclimatic records (Burls and Fedorov 2017). On the other hand, we notice that in many periods, the prevailing hydroclimatic regime, e.g. warm and wet, appears in 65–80% of the studies. This could imply that the convergence/divergence did become stronger in the past warmer periods, but at the same time a substantial reorganization of the atmospheric circulation patterns occurred. Plainly speaking the intensification did occur, but it might have affected different regions.

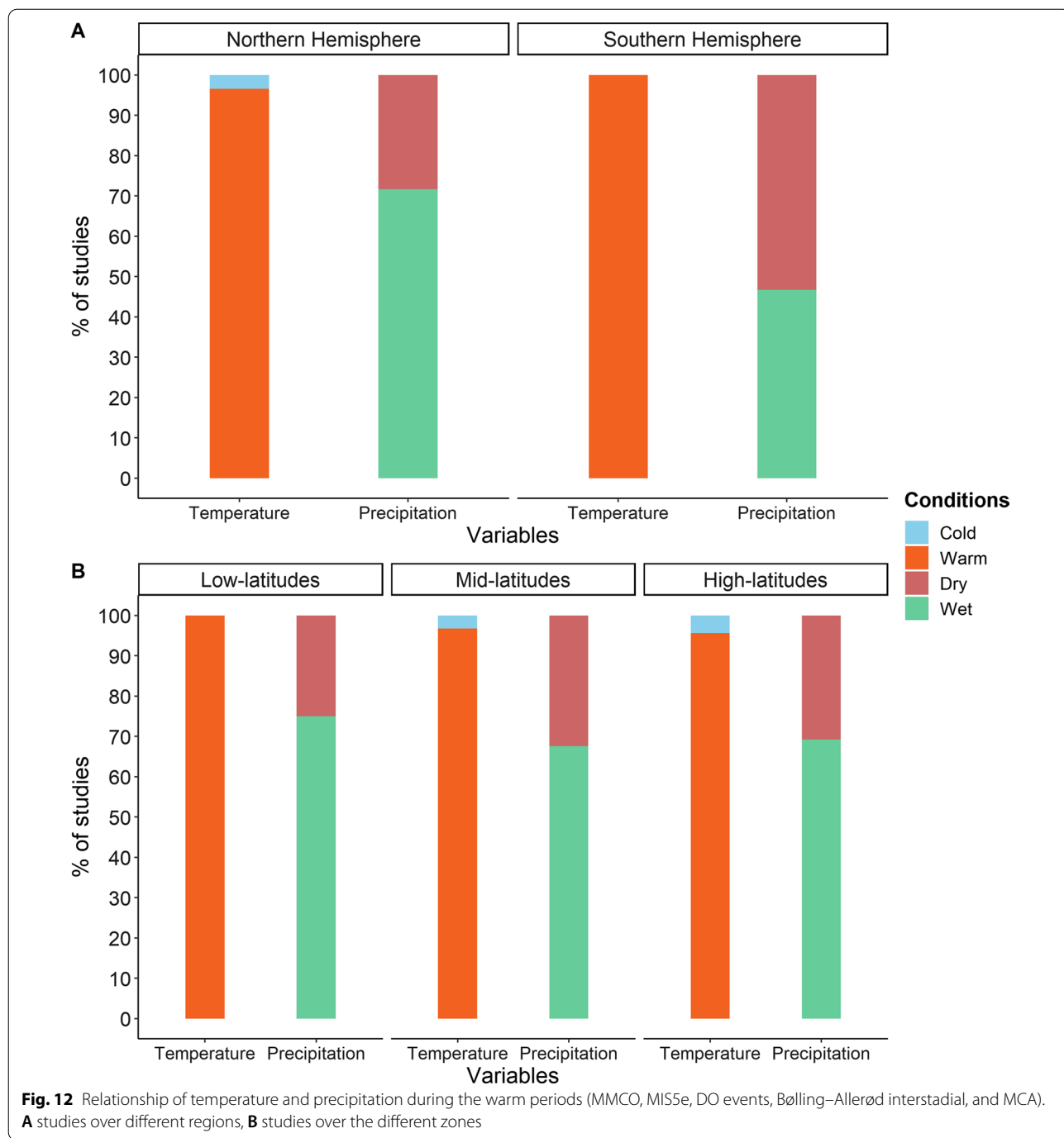
To further investigate the spatial heterogeneity of the temperature/precipitation relationship, we also examined the hemispheric and latitudinal distribution of the records during cold and warm periods. No significant changes are observed between the hemispheric distribution of studies during cold periods (Fig. 11A). In the zonal domain, there is a divergence between mid and high latitudes, with the former exhibiting a tendency to cold-and-wet conditions and the latter cold-and-dry (Fig. 11B). In addition, approximately one-third of the studies document warm climates over mid latitudes, with a higher occurrence in SH. Even though the uneven number of studies per hemisphere and latitudinal zone makes the interpretation of the results ambiguous, it provides some insight of the enhanced heterogeneity, especially when compared with the warm periods. The warm periods appear quite more homogeneous in terms of temperature for both hemispheres (Fig. 12A). The NH appears to favor warm-and-wet conditions in a 2:1 ratio, which drops to approximately 1:1 for SH. The distribution appears quite similar for all three latitudinal zones, also close to 2:1 (Fig. 12B). Again, the bias of the low number of studies in SH should be taken into account. Nevertheless, the hemispheric and latitudinal distribution of the records advocate for an asymmetric response of precipitation to temperature increase and decrease. It should be noted though that due to the limited number of records (especially precipitation), it is difficult to adequately describe the spatial features of the water cycle's response.

A plausible approach to overcome the reconstruction scarcity barrier can be found in earth system modeling. Indeed, evidence of abrupt or mild atmospheric



reorganization has been presented for some of the climatic periods discussed in our review. For instance, model simulations show that during the MCA was associated with a substantial expansion of the NH Hadley circulation (Graham et al. 2011). This change the atmospheric circulation patterns could explain the drying over the mid-latitudes and the shifts in the monsoon patterns across Africa and South Asia. Other

reorganization patterns have been suggested for the termination of the last deglaciation (Wassenburg et al. 2016) or the LGM (Justino et al. 2005). Even though this evidence is far from conclusive, the hypothesis of a circulation-modulated water cycle intensification is a promising direction to reconcile the 'dry gets drier, wet gets wetter' paradigm with the observed changes.



Unfortunately, earth system modelling comes with certain limitations as well. The consistency between model output and proxy data shows agreement over larger scales, but there are crucial discrepancies in the regional scales (Heiri et al. 2014). This is a known issue in model performance related to the challenges in reproducing precipitation properties at finer/regional scales (Flato et al. 2014). However, some uncertainties still remain in

larger scales, due to inconsistencies in the simulation of atmospheric circulation (Allan et al. 2020) and its modes such as ENSO (Bellenger et al. 2014) or NAO (Zappa and Shepherd 2017; Deser et al. 2017). Inevitably, the AMOC is also poorly represented (Zhang et al. 2019), which might be related by a common bias in the model’s parameterization regarding AMOC stability (Liu et al. 2017). On the other hand, the past millennium scale records

reveal no evidence of internally originated multidecadal oscillation. These multidecadal Atlantic Multi-decadal Oscillation-like oscillations have contradicted as the manifestation of high-amplitude explosive volcanism episodes (Mann et al. 2021). With all these open challenges in earth system modelling, the need for more high-resolution paleoclimatic reconstructions is increasing.

More paleoclimatic reconstructions would further improve our understanding the interaction between temperature and water cycle. The evidence presented here suggest that the hypothesis that a warmer climate is a wetter climate could be an oversimplification even for centennial scales. On the contrary, precipitation response appear to be spatio-temporally heterogeneous, with certain differences among periods. This should be taken into account when assessing the future intensification of the global water cycle. Even if not regionally precise, the precipitation response heterogeneity should be evident in model simulations or our theoretical constructs of the global water cycle functioning. This qualitative metric could help improve the model performance, and in turn shed more light on the influence of atmospheric and oceanic circulation. The remaining challenge, though, is to quantify the spatial variability of precipitation response in a robust manner. As the number of paleoclimatic reconstructions increases, we will soon be able to have a more coherent picture of specific warm or cold periods, and increase the likelihood to address it.

6 Conclusions

Most climate projections report that the hydrological cycle will intensify when the climate will get warmer. As a result, the hydrological cycle sensitivity is a major concern for the coming decades. In this study, we reviewed the relationship between the hydroclimate and temperature in the recent and distant past. We confirmed that, in general, most paleoclimate records suggest that the hydrological cycle intensified in a warmer climate. Correspondingly, the hydrological cycle weakened during the colder periods. However, the spatial distribution of hydroclimatic changes was not homogeneous around the world.

This lack of homogeneity makes paradigms such as “a warmer climate is a wetter climate” or “dry gets drier, wet gets wetter” appearing as oversimplifications. The evidence presented in this study agrees to the hypothesis that climate changes at global scale are thermodynamic-driven, while regional climate changes are more related to variations in ocean-atmospheric circulation. However, due to its enhanced spatiotemporal distribution, hydroclimate variability is difficult to be quantified on a regional, continental, and global scale. In this context, large-scale paleo-hydroclimatic shifts, especially during

the warm periods, need further investigation as they could provide new insights into the present and future hydroclimatic changes.

Acknowledgements

The authors would like to thank the two anonymous reviewers for their constructive remarks that helped to improve the manuscript. This work was carried out within the project “Investigation of Terrestrial Hydrological Cycle Acceleration (ITHACA)” funded by the Czech Science Foundation (Grant 22-33266M). SP was supported by the Internal Grant Agency of the Faculty of Environmental Sciences, Czech University of Life Sciences Prague (Grant 2020B0039).

Author contributions

SP and YM conceived the idea and designed the study. SP carried out the literature research, analyzed the data, and prepared the manuscript with support from YM. Both authors discussed the results and approved the final manuscript.

Funding

This study was financially supported by the Czech Science Foundation (Grant 22-33266M) and the Internal Grant Agency of the Faculty of Environmental Sciences, Czech University of Life Sciences Prague (Grant 2020B0039).

Availability of data and materials

The datasets used for this study are obtained from NOAA's National Centers for Environmental Information webdata portal, available at <https://www.ncei.noaa.gov/products/paleoclimatology>. Another source for paleoclimate data is Past Global Changes (PAGES) databases, available at <https://www.pastglobalchanges.org/science/data/databases>.

Declarations

Competing interests

The authors declare that they have no competing interest.

Received: 6 December 2021 Accepted: 16 May 2022

Published online: 31 May 2022

References

- Abarbanel HD, Lall U (1996) Nonlinear dynamics of the Great Salt Lake: system identification and prediction. *Clim Dyn* 12(4):287–297
- Absy M, Cleef A, Fournier M, Martin L, Servant M, Sifeddine A, Ferreira da Silva M, Soubiès F, Suguio K, Turcq B et al (1991) Mise en évidence de quatre phases d'ouverture de la forêt dense dans le Sud-Est de l'Amazonie au cours des 60 000 dernières années : première comparaison avec d'autres régions tropicales. *Comptes Rendus De L'académie Des Sciences. Série 2. Mécanique, Physique, Chimie, Astronomie* 312(6):673–678
- Adams J, Maslin M, Thomas E (1999) Sudden climate transitions during the quaternary. *Prog Phys Geogr* 23(1):1–36
- Agnihotri R, Dutta K, Bhushan R, Somayajulu B (2002) Evidence for solar forcing on the indian monsoon during the last millennium. *Earth Planet Sci Lett* 198(34):521–527
- Ahmed M, Anchukaitis KJ, Asrat A, Borgaonkar HP, Braidia M, Buckley BM, Büntgen U, Chase BM, Christie DA, Cook ER et al (2013) Continental-scale temperature variability during the past two millennia. *Nat Geosci* 6(5):339–346
- Allan R, Barlow M, Byrne MP, Cherchi A, Douville H, Fowler HJ, Gan TY, Pendergrass AG, Rosenfeld D, Swann AL et al (2020) Advances in understanding large-scale responses of the water cycle to climate change. *Annals of the New York Academy of Sciences*
- Allan RP, Liu C, Zahn M, Lavers DA, Koukouvgias E, Bodas-Salcedo A (2014) Physically consistent responses of the global atmospheric hydrological cycle in models and observations. *Surv Geophys* 35(3):533–552
- Allen JR, Brandt U, Brauer A, Hubberten H-W, Huntley B, Keller J, Kraml M, Mackensen A, Mingram J, Negendank JF et al (1999) Rapid

- environmental changes in southern Europe during the last glacial period. *Nature* 400(6746):740–743
- Allen JR, Long AJ, Ottley CJ, Pearson DG, Huntley B (2007) Holocene climate variability in northernmost Europe. *Quatern Sci Rev* 26(9–10):1432–1453
- Allen MB, Armstrong HA (2012) Reconciling the intertropical convergence zone, himalayan/tibetan tectonics, and the onset of the Asian monsoon system. *J Asian Earth Sci* 44:36–47
- Allen MR, Ingram WJ (2002) Constraints on future changes in climate and the hydrologic cycle. *Nature* 419(6903):228–232
- Alley RB, Ágústssdóttir AM (2005) The 8k event: cause and consequences of a major Holocene abrupt climate change. *Quatern Sci Rev* 24(10–11):1123–1149
- Alley RB, Clark PU (1999) The deglaciation of the northern hemisphere: a global perspective. *Annu Rev Earth Planet Sci* 27(1):149–182
- Alley RB, Mayewski PA, Sowers T, Stuiver M, Taylor KC, Clark PU (1997) Holocene climatic instability: a prominent, widespread event 8200 yr ago. *Geology* 25(6):483–486
- Altabet MA, Higgsinon MJ, Murray DW (2002) The effect of millennial-scale changes in Arabian Sea denitrification on atmospheric CO₂. *Nature* 415(6868):159–162
- Andersen KK, Azuma N, Barnola J-M, Bigler M, Biscaye P, Caillon N, Chappellaz J, Clausen HB, Dahl-Jensen D, Fischer H et al (2004) High-resolution record of the northern hemisphere climate extending into the last interglacial period. *Nature* 431:147–151
- Anderson DM, Prell WL (1993) A 300 kyr record of upwelling off oman during the late quaternary: evidence of the Asian southwest monsoon. *Paleoceanography* 8(2):193–208
- Anderson RS, Jiménez-Moreno G, Ager T, Porinchu DF (2014) High-elevation paleoenvironmental change during mis 6–4 in the central rock-ies of colorado as determined from pollen analysis. *Quatern Res* 82(3):542–552
- Annan J, Hargreaves JC (2013) A new global reconstruction of temperature changes at the last glacial maximum. *Clim past* 9(1):367–376
- Arz HW, Pätzold J, Wefer G (1998) Correlated millennial-scale changes in surface hydrography and terrigenous sediment yield inferred from last-glacial marine deposits off northeastern brazil. *Quatern Res* 50(2):157–166
- Asmerom Y, Polyak VJ, Burns SJ (2010) Variable winter moisture in the southwestern United States linked to rapid glacial climate shifts. *Nat Geosci* 3(2):114–117
- Aufgebauer A, Panagiotopoulos K, Wagner B, Schaezbitz F, Viehberg FA, Vogel H, Zanchetta G, Sulpizio R, Leng MJ, Damaschke M (2012) Climate and environmental change in the Balkans over the last 17 ka recorded in sediments from lake prespa (Albania/Fyr of Macedonia/Greece). *Quatern Int* 274:122–135
- Ayliffe LK, Marianelli PC, Moriarty KC, Wells RT, McCulloch MT, Mortimer GE, Hellstrom JC (1998) 500 ka precipitation record from southeastern Australia: evidence for interglacial relative aridity. *Geology* 26(2):147–150
- Badgley JA, Steig EJ, Hakim GJ, Fudge TJ (2020) Greenland temperature and precipitation over the last 20 000 years using data assimilation. *Clim past* 16(4):1325–1346
- Baker PA, Seltzer GO, Fritz SC, Dunbar RB, Grove MJ, Tapia PM, Cross SL, Rowe HD, Broda JP (2001) The history of South American tropical precipitation for the past 25,000 years. *Science* 291(5504):640–643
- Ballantyne A, Lavine M, Crowley T, Liu J, Baker P (2005) Meta-analysis of tropical surface temperatures during the last glacial maximum. *Geophys Res Lett* 32(5)
- Bar-Matthews M (2014). History of water in the Middle East and North Africa. In: Reference module in earth systems and environmental sciences, treatise on geochemistry, 2nd edn, pp 109–128
- Bar-Matthews M, Ayalon A, Kaufman A (2000) Timing and hydrological conditions of sapropel events in the Eastern Mediterranean, as evident from speleothems, Soreq Cave, Israel. *Chem Geol* 169(1–2):145–156
- Bar-Matthews M, Ayalon A, Kaufman A, Wasserburg GJ (1999) The eastern mediterranean paleoclimate as a reflection of regional events: Soreq cave, Israel. *Earth Planet Sci Lett* 166(1–2):85–95
- Bar-Matthews M, Keinan J, Ayalon A (2019) Hydro-climate research of the late quaternary of the eastern mediterranean-levant region based on speleothems research—a review. *Quatern Sci Rev* 221:105872
- Barker P, Gasse F (2003) New evidence for a reduced water balance in east Africa during the last glacial maximum: implication for model-data comparison. *Quatern Sci Rev* 22(8–9):823–837
- Barker S, Cacho I, Benway H, Tachikawa K (2005) Planktonic foraminiferal Mg/Ca as a proxy for past oceanic temperatures: a methodological overview and data compilation for the last glacial maximum. *Quatern Sci Rev* 24(7–9):821–834
- Beck JW, Richards DA, Lawrence R, Silverman BW, Smart PL, Donahue DJ, HererraOsterheld S, Burr GS, Calsoyas L, Timothy A et al (2001) Extremely large variations of atmospheric 14c concentration during the last glacial period. *Science* 292(5526):2453–2458
- Becker P, Seguinot J, Jouvét G, Funk M (2016) Last glacial maximum precipitation pattern in the alps inferred from glacier modelling. *Geogr Helv* 71(3):173–187
- Bellenger H, Guilyardi E, Leloup J, Lengaigne M, Vialard J (2014) Enso representation in climate models: From cmip3 to cmip5. *Clim Dyn* 42(7–8):1999–2018
- Benson LV, Burdett JW, Kashgarian M, Lund SP, Phillips FM, Rye RO (1996) Climatic and hydrologic oscillations in the Owens lake basin and adjacent Sierra Nevada, California. *Science* 274(5288):746–749
- Benson LV, Lund SP, Burdett JW, Kashgarian M, Rose TP, Smoot JP, Schwartz M (1998) Correlation of late-Pleistocene lake-level oscillations in Mono Lake, California, with North Atlantic climate events. *Quatern Res* 49(1):1–10
- Bertler N, Mayewski P, Carter L (2011) Cold conditions in antarctica during the little ice age—implications for abrupt climate change mechanisms. *Earth Planet Sci Lett* 308(1–2):41–51
- Bigelow NH, Brubaker LB, Edwards ME, Harrison SP, Prentice IC, Anderson PM, Andreev AA, Bartlein PJ, Christensen TR, Cramer W et al (2003) Climate change and arctic ecosystems: 1. Vegetation changes north of 55° n between the last glacial maximum, mid-Holocene, and present. *J Geophys Res Atmos* 108(D19)
- Bird BW, Abbott MB, Vuille M, Rodbell DT, Stansell ND, Rosenmeier MF (2011) A 2,300-year-long annually resolved record of the South American summer monsoon from the peruvian andes. *Proc Natl Acad Sci* 108(21):8583–8588
- Blöschl G, Kiss A, Viglione A, Barriendos M, Böhm O, Brázdil R, Coeur D, Demarée G, Llasat MC, Macdonald N et al (2020) Current European flood-rich period exceptional compared with past 500 years. *Nature* 583(7817):560–566
- Boers N (2018) Early-warning signals for Dansgaard–Oeschger events in a high-resolution ice core record. *Nat Commun* 9(1):1–8
- Böhme M, Bruch AA, Selmeier A (2007) The reconstruction of early and Middle Miocene climate and vegetation in southern Germany as determined from the fossil wood flora. *Palaeogeogr Palaeoclimatol Palaeoecol* 253(1–2):91–114
- Bond G, Kromer B, Beer J, Muscheler R, Evans MN, Showers W, Hoffmann S, Loti-Bond R, Hajdas I, Bonani G (2001) Persistent solar influence on north Atlantic climate during the Holocene. *Science* 294(5549):2130–2136
- Bond G, Showers W, Cheseby M, Lotti R, Almasi P, DeMenocal P, Priore P, Cullen H, Hajdas I, Bonani G (1997) A pervasive millennial-scale cycle in north Atlantic Holocene and glacial climates. *Science* 278(5341):1257–1266
- Bond GC, Showers W, Elliot M, Evans M, Lotti R, Hajdas I, Bonani G, Johnson S (1999) The North Atlantic's 1–2 kyr climate rhythm: relation to heinrich events, Dansgaard/Oeschger cycles and the Little Ice Age. *Geophys Monogr Am Geophys Union* 112:35–58
- Bordon A, Peyron O, Lézine A-M, Brewer S, Fouache E (2009) Pollen-inferred lateglacial and Holocene climate in Southern Balkans (Lake Maliq). *Quatern Int* 200(12):19–30
- Borzenkova I, Zorita E, Borisova O, Kalniņa L, Kisieliënė D, Koff T, Kuznetsov D, Lemdahl G, Sapelko T, Stančikaitė M et al (2015) Climate change during the Holocene (past 12,000 years). In: The BACC II Author Team (ed) Second assessment of climate change for the Baltic Sea basin. Springer, Cham, pp 25–49
- Bos JA, Bohncke SJ, Janssen CR (2006) Lake-level fluctuations and small-scale vegetation patterns during the late glacial in The Netherlands. *J Paleolimnol* 35(2):211–238
- Bradley RS, Briffa KR, Cole J, Hughes MK, Osborn TJ (2003) The climate of the last millennium. In: Alvenson KD, Pedersen TF, Bradley RS (eds) *Paleoclimate, global change and the future*. Springer, Cham, pp 105–141

- Bradley RS, Jonest PD (1993) 'Little Ice Age' summer temperature variations: their nature and relevance to recent global warming trends. *The Holocene* 3(4):367–376
- Brauer A, Allen JR, Mingram J, Dulski P, Wulf S, Huntley B (2007) Evidence for last interglacial chronology and environmental change from Southern Europe. *Proc Natl Acad Sci* 104(2):450–455
- Brauer A, Haug GH, Dulski P, Sigman DM, Negendank JF (2008) An abrupt wind shift in Western Europe at the onset of the Younger Dryas cold period. *Nat Geosci* 1(8):520–523
- Brázdil R, Glaser R, Pfister C, Dobrovolný P, Antoine J-M, Barriendos M, Camuffo D, Deutsch M, Enzi S, Guidoboni E et al (1999) Flood events of selected European rivers in the sixteenth century. *Clim Change* 43(1):239–285
- Brázdil R, Stepánková P, Kyncl T, Kyncl J (2002) Fir tree-ring reconstruction of march/july precipitation in Southern Moravia (Czech Republic), 1376–1996. *Clim Res* 20(3):223–239
- Breecker D, Retallack G (2014) Refining the pedogenic carbonate atmospheric CO₂ proxy and application to Miocene CO₂. *Palaeogeogr Palaeoclimatol Palaeoecol* 406:1–8
- Brewer S, Guiot J, Sánchez-Goñi MF, Klotz S (2008) The climate in Europe during the Eemian: a multi-method approach using pollen data. *Quatern Sci Rev* 27(2526):2303–2315
- Broecker WS (2000) Abrupt climate change: causal constraints provided by the paleoclimate record. *Earth Sci Rev* 51(1–4):137–154
- Broecker WS, Bond G, Klas M, Bonani G, Wolff W (1990) A salt oscillator in the glacial Atlantic? 1. The concept. *Paleoceanography* 5(4):469–477
- Brönnimann S, Franke J, Nussbaumer SU, Zumbühl HJ, Steiner D, Trachsel M, Hegerl GC, Schurer A, Worni M, Malik A et al (2019) Last phase of the Little Ice Age forced by volcanic eruptions. *Nat Geosci* 12(8):650–656
- Bruch AA, Uhl D, Mosbrugger V (2007) Miocene climate in Europe—patterns and evolution: a first synthesis of neoclimate
- Budsky A, Wassenburg JA, Mertz-Kraus R, Spötl C, Jochum KP, Gibert L, Scholz D (2019) Western mediterranean climate response to Dansgaard/Oeschger events: new insights from speleothem records. *Geophys Res Lett* 46(15):9042–9053
- Burls NJ, Fedorov AV (2017) Wetter subtropics in a warmer world: contrasting past and future hydrological cycles. *Proc Natl Acad Sci* 114(49):12888–12893
- Bush AB, Philander SGH (1998) The role of ocean-atmosphere interactions in tropical cooling during the last glacial maximum. *Science* 279(5355):1341–1344
- Bush AB, Philander SGH (1999) The climate of the last glacial maximum: results from a coupled atmosphere-ocean general circulation model. *J Geophys Res Atmos* 104(D20):24509–24525
- Bush MB, Piperno DR, Colinvaux PA, De Oliveira PE, Krissek LA, Miller MC, Rowe WE (1992) A 14 300-yr paleoecological profile of a lowland tropical lake in panama. *Ecol Monogr* 62(2):251–275
- Byrne M, Yeates D, Joseph L, Kearney M, Bowler J, Williams M, Cooper S, Donnellan S, Keogh J, Leys R et al (2008) Birth of a biome: insights into the assembly and maintenance of the Australian arid zone biota. *Mol Ecol* 17(20):4398
- Carlson AE (2013) Paleoclimate—the Younger Dryas climate event. In: Reference module in earth systems and environmental sciences, encyclopedia of Quaternary science, 2nd edn, pp 126–134
- Chamberlain CP, Winnick MJ, Mix HT, Chamberlain SD, Maher K (2014) The impact of neogene grassland expansion and aridification on the isotopic composition of continental precipitation. *Glob Biogeochem Cycles* 28(9):992–1004
- Intergovernmental Panel on Climate Change (2014) Climate change 2013: the physical science basis: Working Group I contribution to the Fifth assessment report of the Intergovernmental Panel on Climate Change. Cambridge University Press, Cambridge
- Chawchai S, Tan L, Löwemark L, Wang H-C, Yu T-L, Chung Y-C, Mii H-S, Liu G, Blauw M, Gong S-Y et al (2021) Hydroclimate variability of central Indo-Pacific region during the Holocene. *Quatern Sci Rev* 253:106779
- Chen J, Chen F, Feng S, Huang W, Liu J, Zhou A (2015) Hydroclimatic changes in China and surroundings during the medieval climate anomaly and little ice age: spatial patterns and possible mechanisms. *Quatern Sci Rev* 107:98–111
- Cheng H, Edwards RL, Sinha A, Spötl C, Yi L, Chen S, Kelly M, Kathayat G, Wang X, Li X et al (2016) The Asian monsoon over the past 640,000 years and ice age terminations. *Nature* 534(7609):640–646
- Christiansen B, Ljungqvist FC (2012) The extra-tropical northern hemisphere temperature in the last two millennia: reconstructions of low-frequency variability. *Clim past* 8(2):765–786
- Clark PU, Dyke AS, Shakun JD, Carlson AE, Clark J, Wohlfarth B, Mitrovica JX, Hostetler SW, McCabe AM (2009) The Last Glacial Maximum. *Science* 325(5941):710–714
- Clark PU, Mix AC (2002) Ice sheets and sea level of the last glacial maximum. *Quatern Sci Rev* 21(1–3):1–7
- Clarke GK, Leverington DW, Teller JT, Dyke AS (2004) Paleohydraulics of the last outburst flood from glacial lake agassiz and the 8200bp cold event. *Quatern Sci Rev* 23(3–4):389–407
- Clement AC, Cane MA, Seager R (2001) An orbitally driven tropical source for abrupt climate change. *J Clim* 14(11):2369–2375
- Clift PD, Wan S, Blusztajn J (2014) Reconstructing chemical weathering, physical erosion and monsoon intensity since 25 Ma in the northern South China Sea: a review of competing proxies. *Earth Sci Rev* 130:86–102
- Colin C, Kissel C, Blamart D, Turpin L (1998) Magnetic properties of sediments in the Bay of Bengal and the Andaman Sea: impact of rapid north Atlantic Ocean climatic events on the strength of the Indian monsoon. *Earth Planet Sci Lett* 160(3–4):623–635
- Cook BI, Smerdon JE, Seager R, Cook ER (2014) Pan-continental droughts in north America over the last millennium. *J Clim* 27(1):383–397
- Cook ER, Meko DM, Stockton CW (1997) A new assessment of possible solar and lunar forcing of the bidecadal drought rhythm in the Western United States. *J Clim* 10(6):1343–1356
- Cook ER, Seager R, Cane MA, Stahle DW (2007) North American drought: reconstructions, causes, and consequences. *Earth Sci Rev* 81(1–2):93–134
- Cook ER, Seager R, Kushnir Y, Briffa KR, Büntgen U, Frank D, Krusic PJ, Tegel W, van der Schrier G, Andreu-Hayles L et al (2015) Old world megadroughts and pluvials during the common era. *Science Adv* 1(10):e1500561
- Corrick EC, Drysdale RN, Hellstrom JC, Capron E, Rasmussen SO, Zhang X, Fleitmann D, Couchoud I, Wolff E (2020) Synchronous timing of abrupt climate changes during the last glacial period. *Science* 369(6506):963–969
- Cragin J, Herron M, Langway C Jr, Klouda G (1977) Interhemispheric comparison of changes in the composition of atmospheric precipitation during the late Cenozoic era. In: Dunbar MJ (ed) Polar oceans. Arctic Institute of North America, Calgary, pp 617–631
- Crowley T (2000) Climap ssts re-visited. *Clim Dyn* 16(4):241–255
- Crowley TJ, North GR (1991) Paleoclimatology. Oxford University Press, New York
- Cuffey KM, Clow GD (1997) Temperature, accumulation, and ice sheet elevation in central Greenland through the last deglacial transition. *J Geophys Res Oceans* 102(C12):26383–26396
- Cuffey KM, Clow GD, Alley RB, Stuiver M, Waddington ED, Saltus RW (1995) Large arctic temperature change at the Wisconsin-Holocene glacial transition. *Science* 270(5235):455–458
- Curry BB, Baker RG (2000) Paleohydrology, vegetation, and climate since the late Illinois episode (130 ka) in south-central Illinois. *Palaeogeogr Palaeoclimatol Palaeoecol* 155(1–2):59–81
- Dahl SO, Nesje A (1992) Paleoclimatic implications based on equilibrium-line altitude depressions of reconstructed younger Dryas and Holocene cirque glaciers in inner nordfjord, western Norway. *Palaeogeogr Palaeoclimatol Palaeoecol* 94(1–4):87–97
- Dansgaard W, Johnsen SJ, Clausen HB, Dahl-Jensen D, Gundestrup N, Hammer C, Hvidberg C, Steffensen J, Sveinbjörnsdóttir A, Jouzel J et al (1993) Evidence for general instability of past climate from a 250-kyr ice-core record. *Nature* 364(6434):218–220
- Dansgaard W, White J, Johnsen S (1989) The abrupt termination of the Younger Dryas climate event. *Nature* 339(6225):532–534
- Davis BA, Brewer S, Stevenson AC, Guiot J (2003) The temperature of Europe during the Holocene reconstructed from pollen data. *Quatern Sci Rev* 22(15–17):1701–1716
- Deser C, Hurrell JW, Phillips AS (2017) The role of the north Atlantic oscillation in European climate projections. *Clim Dyn* 49(9–10):3141–3157
- Dorale J, Wozniak L, Bettis E III, Carpenter S, Mandel R, Hajic E, Lopinot N, Ray J (2010) Isotopic evidence for Younger Dryas aridity in the north American midcontinent. *Geology* 38(6):519–522
- Dung NC, Chen Y-G, Chiang H-W, Shen C-C, Wang X, Lam DD, Yuan S, Lone MA, Yu T-L, Lin Y et al (2020) A decadal-resolution stalagmite record of

- strong Asian summer monsoon from northwestern Vietnam over the Dansgaard–Oeschger events 2–4. *J Asian Earth Sci* 3:100027
- Durack PJ, Wijffels SE, Matear RJ (2012) Ocean salinities reveal strong global water cycle intensification during 1950 to 2000. *Science* 336(6080):455–458
- Ellison CR, Chapman MR, Hall IR (2006) Surface and deep ocean interactions during the cold climate event 8200 years ago. *Science* 312(5782):1929–1932
- Eronen JT, Fortelius M, Micheels A, Portmann F, Puolamäki K, Janis CM (2012) Neogene aridification of the northern hemisphere. *Geology* 40(9):823–826
- Fairbanks RG (1990) The age and origin of the “Younger Dryas climate event” in Greenland ice cores. *Paleoceanography* 5(6):937–948
- Fawcett PJ, Ágústsdóttir AM, Alley RB, Shuman CA (1997) The Younger Dryas’ termination and north atlantic deep water formation: insights from climate model simulations and Greenland ice cores. *Paleoceanography* 12(1):23–38
- Feakins SJ, Warny S, Lee J-E (2012) Hydrologic cycling over Antarctica during the Middle Miocene warming. *Nat Geosci* 5(8):557–560
- Fischer H, Meissner K, Mix A, Abram N, Austermann J, Brovkin V, Capron E, Colombaroli D, Daniou A, Dyez K et al (2018) Palaeoclimate constraints on a world with postindustrial warming of 2 degrees and beyond. *Nat Geosci* 11:615
- Flato G, Marotzke J, Abiodun B, Braconnot P, Chou SC, Collins W, Cox P, Driouech F, Emori S, Eyring V et al (2014) Evaluation of climate models. In: *Climate change 2013: the physical science basis. Contribution of Working Group I to the Fifth Assessment Report of the Intergovernmental Panel on Climate Change*. Cambridge University Press, pp 741–866
- Fox DL, Koch PL (2004) Carbon and oxygen isotopic variability in neogene paleosol carbonates: constraints on the evolution of the c4-grasslands of the Great Plains, USA. *Palaeogeogr Palaeoclimatol Palaeoecol* 207(3–4):305–329
- Fritz M, Herzschuh U, Wetterich S, Lantuit H, De Pascale GP, Pollard WH, Schirmermeister L (2012) Late glacial and Holocene sedimentation, vegetation, and climate history from easternmost Beringia (Northern Yukon Territory, Canada). *Quatern Res* 78(3):549–560
- Fritz SC, Baker PA, Seltzer GO, Ballantyne A, Tapia P, Cheng H, Edwards RL (2007) Quaternary glaciation and hydrologic variation in the south American tropics as reconstructed from the Lake Titicaca drilling project. *Quatern Res* 68(3):410–420
- Gagan M, Ayliffe L, Beck JW, Cole J, Druffel E, Dunbar RB, Schrag D (2000) New views of tropical paleoclimates from corals. *Quatern Sci Rev* 19(1–5):45–64
- Gale HS (1914) Overflow of Owens lake occurs when wetness exceeds 2.4 times the historical mean. *US Geol Sum Bull* 580:251
- Gasse F (2000) Hydrological changes in the African tropics since the last glacial maximum. *Quatern Sci Rev* 19(1–5):189–211
- Gasse F, Van Campo E (2001) Late quaternary environmental changes from a pollen and diatom record in the southern tropics (Lake Tritrivakely, Madagascar). *Palaeogeogr Palaeoclimatol Palaeoecol* 167(3–4):287–308
- Gates WL (1976) The numerical simulation of ice-age climate with a global general circulation model. *J Atmos Sci* 33(10):1844–1873
- Genty D, Blamart D, Ouahdi R, Gilmour M, Baker A, Jouzel J, Van-Exter S (2003) Precise dating of Dansgaard–Oeschger climate oscillations in western Europe from stalagmite data. *Nature* 421(6925):833–837
- Glaser R, Riemann D, Schönbein J, Barriendos M, Brázdil R, Bertolin C, Camuffo D, Deutsch M, Dobrovolný P, van Engelen A et al (2010) The variability of European floods since AD 1500. *Clim Change* 101(1–2):235–256
- Gošlar T, Arnold M, Pazdur MF (1995) The Younger Dryas cold event—was it synchronous over the north Atlantic region? *Radiocarbon* 37(1):63–70
- Graham NE, Ammann C, Fleitmann D, Cobb K, Luterbacher J (2011) Support for global climate reorganization during the “Medieval climate anomaly.” *Clim Dyn* 37(5):1217–1245
- Graumlich LJ (1993) A 1000-year record of temperature and precipitation in the Sierra Nevada. *Quatern Res* 39(2):249–255
- Greenop R, Foster GL, Wilson PA, Lear CH (2014) Middle Miocene climate instability associated with high-amplitude CO₂ variability. *Paleoceanography* 29(9):845–853
- Grein M, Oehm C, Konrad W, Utescher T, Kunzmann L, Roth-Nebelsick A (2013) Atmospheric CO₂ from the late Oligocene to early Miocene based on photosynthesis data and fossil leaf characteristics. *Palaeogeogr Palaeoclimatol Palaeoecol* 374:41–51
- Greve P, Orlowsky B, Mueller B, Sheffield J, Reichstein M, Seneviratne SI (2014) Global assessment of trends in wetting and drying over land. *Nat Geosci* 7(10):716–721
- Grimm EC, Watts WA, Jacobson GL Jr, Hansen BC, Almquist HR, DieffenbacherKrall AC (2006) Evidence for warm wet heinrich events in florida. *Quatern Sci Rev* 25(17–18):2197–2211
- Guiot J (1992) The combination of historical documents and biological data in the reconstruction of climate variations in space and time. In: *European climate reconstructed from documentary data: methods and results*, pp 93–104
- Gupta AK, Anderson DM, Overpeck JT (2003) Abrupt changes in the Asian southwest monsoon during the Holocene and their links to the north Atlantic ocean. *Nature* 421(6921):354–357
- Haq BU (1973) Transgressions, climatic change and the diversity of calcareous nannoplankton. *Mar Geol* 15(2):M25–M30
- Harris EB, Kohn MJ, Strömberg CA (2020) Stable isotope compositions of herbivore teeth indicate climatic stability leading into the Mid-Miocene climatic optimum, in Idaho, USA. *Palaeogeogr Palaeoclimatol Palaeoecol* 546:109610
- Harzhauser M, Latal C, Piller WE (2007) The stable isotope archive of Lake Pannon as a mirror of late Miocene climate change. *Palaeogeogr Palaeoclimatol Palaeoecol* 249(3–4):335–350
- Haug GH, Hughen KA, Sigman DM, Peterson LC, Röhl U (2001) Southward migration of the intertropical convergence zone through the Holocene. *Science* 293(5533):1304–1308
- Hayes A, Kucera M, Kallel N, Sbaifi L, Rohling EJ (2005) Glacial Mediterranean sea surface temperatures based on planktonic foraminiferal assemblages. *Quatern Sci Rev* 24(7–9):999–1016
- Heikkilä M, Seppä H (2010) Holocene climate dynamics in Latvia, Eastern Baltic region: a pollen-based summer temperature reconstruction and regional comparison. *Boreas* 39(4):705–719
- Heinrich H (1988) Origin and consequences of cyclic ice rafting in the northeast Atlantic Ocean during the past 130,000 years. *Quatern Res* 29(2):142–152
- Heiri O, Brooks SJ, Renssen H, Bedford A, Hazekamp M, Ilyashuk B, Jeffers ES, Lang B, Kirilova E, Kuiper S et al (2014) Validation of climate model-inferred regional temperature change for late-glacial Europe. *Nat Commun* 5(1):1–7
- Held IM, Soden BJ (2006) Robust responses of the hydrological cycle to global warming. *J Clim* 19(21):5686–5699
- Hendy IL, Kennett JP (2000) Dansgaard–Oeschger cycles and the California current system: planktonic foraminiferal response to rapid climate change in Santa Barbara basin, ocean drilling program hole 893a. *Paleoceanography* 15(1):30–42
- Henrot A-J, François L, Favre E, Butzin M, Ouberdous M, Munhoven G (2010) Effects of CO₂, continental distribution, topography and vegetation changes on the climate at the Middle Miocene: a model study. *Clim past* 6(5):675
- Herold N, Huber M, Müller R (2011) Modeling the Miocene climatic optimum. Part I: land and atmosphere. *J Clim* 24(24):6353–6372
- Hodell DA, Anselmetti FS, Ariztegui D, Brenner M, Curtis JH, Gilli A, Grzesik DA, Guilderson TJ, Müller AD, Bush MB et al (2008) An 85-ka record of climate change in lowland central America. *Quatern Sci Rev* 27(11–12):1152–1165
- Holbourn A, Kuhnt W, Lyle M, Schneider L, Romero O, Andersen N (2014) Middle Miocene climate cooling linked to intensification of eastern equatorial Pacific upwelling. *Geology* 42(1):19–22
- Hou Z, Li J, Song C, Zhang J, Hui Z, Chen S, Xian F (2014) Understanding Miocene climate evolution in northeastern Tibet: stable carbon and oxygen isotope records from the western Tianshui Basin, China. *J Earth Sci* 25(2):357–365
- Hughen KA, Overpeck JT, Peterson LC, Trumbore S (1996) Rapid climate changes in the tropical Atlantic region during the last deglaciation. *Nature* 380(6569):51–54
- Hughen KA, Southon JR, Lehman SJ, Overpeck JT (2000) Synchronous radiocarbon and climate shifts during the last deglaciation. *Science* 290(5498):1951–1954
- Hughes MK, Diaz HF (1994) Was there a ‘Medieval warm period’, and if so, where and when? *Clim Change* 26(2–3):109–142

- Huntington TG (2006) Evidence for intensification of the global water cycle: review and synthesis. *J Hydrol* 319(1–4):83–95
- Huntington TG (2010) Climate warming-induced intensification of the hydrologic cycle: an assessment of the published record and potential impacts on agriculture. In: *Advances in agronomy*, vol 109. Elsevier, pp 1–53
- Isarin RF, Bohncke SJ (1999) Mean July temperatures during the Younger Dryas in northwestern and central Europe as inferred from climate indicator plant species. *Quatern Res* 51(2):158–173
- Ivanochko TS, Ganeshram RS, Brummer G-JA, Ganssen G, Jung SJ, Moreton SG, Kroon D (2005) Variations in tropical convection as an amplifier of global climate change at the millennial scale. *Earth Planet Sci Lett* 235(1–2):302–314
- Jiang H, Ding Z (2010) Eolian grain-size signature of the Sikouzi lacustrine sediments (Chinese Loess Plateau): implications for Neogene evolution of the East Asian winter monsoon. *Bulletin* 122(5–6):843–854
- Johnsen S, Dansgaard W, White J (1989) The origin of arctic precipitation under present and glacial conditions. *Tellus B Chem Phys Meteorol* 41(4):452–468
- Johnsen SJ, Dahl-Jensen D, Dansgaard W, Gundestrup N (1995) Greenland palaeotemperatures derived from grip bore hole temperature and ice core isotope profiles. *Tellus B Chem Phys Meteorol* 47(5):624–629
- Johnsen SJ, Dahl-Jensen D, Gundestrup N, Steffensen JP, Clausen HB, Miller H, Masson-Delmotte V, Sveinbjörnsdóttir AE, White J (2001) Oxygen isotope and palaeotemperature records from six Greenland ice-core stations: camp century, dye-3, grip2, renland and northgrip. *J Quatern Sci Publ Quatern Res Assoc* 16(4):299–307
- Johnston V, Borsato A, Frisia S, Spötl C, Dublyansky Y, Töchterle P, Hellstrom J, Bajo P, Edwards R, Cheng H (2018) Evidence of thermophilisation and elevation-dependent warming during the last interglacial in the Italian Alps. *Sci Rep* 8(1):1–11
- Jones PD, Mann ME (2004) Climate over past millennia. *Rev Geophys* 42(2)
- Jouzel J, Lorius C, Petit J-R, Genthon C, Barkov NI, Kotlyakov VM, Petrov VM (1987) Vostok ice core: a continuous isotope temperature record over the last climatic cycle (160,000 years). *Nature* 329(6138):403–408
- Justino F, Timmermann A, Merkel U, Souza EP (2005) Synoptic reorganization of atmospheric flow during the last glacial maximum. *J Clim* 18(15):2826–2846
- Kaiser K, Clausen I (2005) Palaeopedology and stratigraphy of the late Palaeolithic Alt Duvenstedt Site, Schleswig-Holstein (Northwest Germany). *Archäologisches Korrespondenzblatt* 35(4):447–466
- Karpuz NK, Jansen E (1992) A high-resolution diatom record of the last deglaciation from the SE Norwegian Sea: documentation of rapid climatic changes. *Paleoceanography* 7(4):499–520
- Kathayat G, Cheng H, Sinha A, Spötl C, Edwards RL, Zhang H, Li X, Yi L, Ning Y, Cai Y et al (2016) Indian monsoon variability on millennial-orbital timescales. *Sci Rep* 6:24374
- Kennett J (1994) The Middle Miocene climatic transition: East Antarctic ice sheet development, deep ocean circulation and global carbon cycling. *Palaeogeogr Palaeoclimatol Palaeoecol* 108:537–555
- Kim S-J, Lü JM, Yi S, Choi T, Kim B-M, Lee BY, Woo S-H, Kim Y (2010) Climate response over asia/arctic to change in orbital parameters for the last interglacial maximum. *Geosci J* 14(2):173–190
- Klitgaard-Kristensen D, Sejrup HP, Hafliðason H, Johnsen S, Spurk M (1998) A regional 8200 cal. yr bp cooling event in northwest Europe, induced by final stages of the laurentide ice-sheet deglaciation? *J Quatern Sci Publ Quatern Res Assoc* 13(2):165–169
- Knox JC, Wright H (1983) Responses of river systems to Holocene climates. *Late Quatern Environ US* 2:26–41
- Kotthoff U, Koutsodendrís A, Pross J, Schmiedl G, Bornemann A, Kaul C, Marino G, Peyron O, Schiebel R (2011) Impact of lateglacial cold events on the northern Aegean region reconstructed from marine and terrestrial proxy data. *J Quatern Sci* 26(1):86–96
- Kreutz KJ, Mayewski PA, Meeker LD, Twickler MS, Whitlow SI, Pittalwala II (1997) Bipolar changes in atmospheric circulation during the little ice age. *Science* 277(5330):1294–1296
- Kucera M, Weinelt M, Kiefer T, Pflaumann U, Hayes A, Weinelt M, Chen M-T, Mix AC, Barrows TT, Cortijo E et al (2005) Reconstruction of sea-surface temperatures from assemblages of planktonic foraminifera: multi-technique approach based on geographically constrained calibration data sets and its application to Glacial Atlantic and Pacific Oceans. *Quatern Sci Rev* 24(7–9):951–998
- Kuhlemann J, Kempf O (2002) Post-eocene evolution of the north alpine foreland basin and its response to alpine tectonics. *Sed Geol* 152(1–2):45–78
- Kuhlemann J, Rohling EJ, Krumrei I, Kubik P, Ivy-Ochs S, Kucera M (2008) Regional synthesis of mediterranean atmospheric circulation during the last glacial maximum. *Science* 321(5894):1338–1340
- Kwiecien O, Arz HW, Lamy F, Plessen B, Bahr A, Haug GH (2009) North Atlantic control on precipitation pattern in the Eastern Mediterranean/Black Sea region during the last glacial. *Quatern Res* 71(3):375–384
- Ladd M, Viau A, Way R, Gajewski K, Sawada M (2018) Variations in precipitation in North America during the past 2000 years. *The Holocene* 28(4):667–675
- Lamb HH (1965) The early Medieval warm epoch and its sequel. *Palaeogeogr Palaeoclimatol Palaeoecol* 1:13–37
- Lamb HH (2013) *Climate: present, past and future (Routledge revivals): volume 2: climatic history and the future*, vol 2. Routledge, London
- Lan J, Xu H, Lang Y, Yu K, Zhou P, Kang S, Zhou K, Wang X, Wang T, Cheng P et al (2020) Dramatic weakening of the east Asian summer monsoon in northern China during the transition from the Medieval warm period to the Little Ice Age. *Geology* 48(4):307–312
- Lang C, Leuenberger M, Schwander J, Johnsen S (1999) 16 °C rapid temperature variation in central Greenland 70,000 years ago. *Science* 286(5441):934–937
- Leduc G, Vidal L, Tachikawa K, Rostek F, Sonzogni C, Beaufort L, Bard E (2007) Moisture transport across Central America as a positive feedback on abrupt climatic changes. *Nature* 445(7130):908–911
- Lee K, Slowey N, Herbert T (2001) Glacial SSTs in the subtropical North Pacific: a comparison of UK0 37 $\delta^{18}O$ and foraminiferal assemblage temperature estimates. *Paleoceanography* 16:268–279
- Leopold E, Denton M (1987) Comparative age of grassland and steppe east and west of the northern rocky mountain. *Ann Mo Bot Gard* 74:841–867
- Leuschner DC, Sirocko F (2000) The low-latitude monsoon climate during Dansgaard–Oeschger cycles and heinrich events. *Quatern Sci Rev* 19(1–5):243–254
- Levin NE, Cerling TE, Passey BH, Harris JM, Ehleringer JR (2006) A stable isotope aridity index for terrestrial environments. *Proc Natl Acad Sci* 103(30):11201–11205
- Li C, Born A (2019) Coupled atmosphere-ice-ocean dynamics in Dansgaard–Oeschger events. *Quatern Sci Rev* 203:1–20
- Li Y, Zhang Y (2020) Synergy of the westerly winds and monsoons in the lake evolution of global closed basins since the last glacial maximum and implications for hydrological change in Central Asia. *Clim past* 16(6):2239–2254
- Li Y-X, Törnqvist TE, Nevitt JM, Kohl B (2012) Synchronizing a sea-level jump, final lake Agassiz drainage, and abrupt cooling 8200 years ago. *Earth Planet Sci Lett* 315:41–50
- Li Z, Quan X, Duzheng Y, Congbin F, Jiping C, Yoshino M (1987) The climatic changes of drought–wet in ancient Chang-an region of China during the last 1604 years
- Liu L, Eronen JT, Fortelius M (2009) Significant mid-latitude aridity in the Middle Miocene of East Asia. *Palaeogeogr Palaeoclimatol Palaeoecol* 279(3–4):201–206
- Liu W, Xie S-P, Liu Z, Zhu J (2017) Overlooked possibility of a collapsed Atlantic meridional overturning circulation in warming climate. *Sci Adv* 3(1):e1601666
- Ljungqvist FC, Krusic PJ, Sundqvist HS, Zorita E, Brattström G, Frank D (2016) Northern hemisphere hydroclimate variability over the past twelve centuries. *Nature* 532(7597):94–98
- Luckman BH (2000) The Little Ice Age in the canadian rockies. *Geomorphology* 32(3–4):357–384
- Luetscher M, Boch R, Sodemann H, Spötl C, Cheng H, Edwards RL, Frisia S, Hof F, Müller W (2015) North Atlantic storm track changes during the last glacial maximum recorded by alpine speleothems. *Nat Commun* 6(1):1–6
- Lukas S, Bradwell T (2010) Reconstruction of a lateglacial (Younger Dryas) mountain ice field in Sutherland, Northwestern Scotland, and its palaeoclimatic implications. *J Quatern Sci Publ Quatern Res Assoc* 25(4):567–580

- Luoto TP, Nevalainen L (2018) Temperature-precipitation relationship of the common era in Northern Europe. *Theor Appl Climatol* 132(3–4):933–938
- Mackay AW, Swann GE, Fagel N, Fietz S, Leng MJ, Morley D, Rioual P, Tarasov P (2013) Hydrological instability during the last interglacial in central Asia: a new diatom oxygen isotope record from lake Baikal. *Quatern Sci Rev* 66:45–54
- Magny M (1992) Holocene lake-level fluctuations in Jura and the northern Subalpine ranges, France: regional pattern and climatic implications. *Boreas* 21(4):319–334
- Magny M (2001) Palaeohydrological changes as reflected by lake-level fluctuations in the Swiss plateau, the Jura mountains and the northern french pre-alps during the last Glacial–Holocene transition: a regional synthesis. *Glob Planet Change* 30(1–2):85–101
- Magny M, Bègeot C (2004) Hydrological changes in the European mid-latitudes associated with freshwater outbursts from lake Agassiz during the Younger Dryas event and the early Holocene. *Quatern Res* 61(2):181–192
- Magny M, Bègeot C, Guiot J, Marguet A, Billaud Y (2003) Reconstruction and palaeoclimatic interpretation of Mid-Holocene vegetation and lake-level changes at Saint-Jorioz, Lake Annecy, French pre-alps. *The Holocene* 13(2):265–275
- Maher BA (2008) Holocene variability of the East Asian summer monsoon from Chinese cave records: a re-assessment. *The Holocene* 18(6):861–866
- Mangerud J, Løvlie R, Gulliksen S, Hufthammer A-K, Larsen E, Valen V (2003) Paleomagnetic correlations between Scandinavian ice-sheet fluctuations and Greenland Dansgaard–Oeschger events, 45000–25000 yr bp. *Quatern Res* 59(2):213–222
- Mann ME, Bradley RS, Hughes MK (1998) Global-scale temperature patterns and climate forcing over the past six centuries. *Nature* 392(6678):779–787
- Mann ME, Steinman BA, Brouillette DJ, Miller SK (2021) Multidecadal climate oscillations during the past millennium driven by volcanic forcing. *Science* 371(6533):1014–1019
- Mann ME, Zhang Z, Rutherford S, Bradley RS, Hughes MK, Shindell D, Ammann C, Faluvegi G, Ni F (2009) Global signatures and dynamical origins of the Little Ice Age and Medieval climate anomaly. *Science* 326(5957):1256–1260
- Marengo JA (2004) Interdecadal variability and trends of rainfall across the Amazon basin. *Theor Appl Climatol* 78(1–3):79–96
- Markonis Y, Hanel M, Mácá P, Kyselý J, Cook E (2018) Persistent multi-scale fluctuations shift European hydroclimate to its millennial boundaries. *Nat Commun* 9(1):1767
- Markonis Y, Papalexiou S, Martinkova M, Hanel M (2019) Assessment of water cycle intensification over land using a multisource global gridded precipitation dataset. *J Geophys Res Atmos* 124(21):11175–11187
- Martrat B, Grimalt JO, Lopez-Martinez C, Cacho I, Sierro FJ, Flores JA, Zahn R, Canals M, Curtis JH, Hodell DA (2004) Abrupt temperature changes in the western Mediterranean over the past 250,000 years. *Science* 306(5702):1762–1765
- Maslin MA, Burns SJ (2000) Reconstruction of the Amazon basin effective moisture availability over the past 14,000 years. *Science* 290(5500):2285–2287
- Matthews JA, Briffa KR (2005) The 'Little Ice Age': re-evaluation of an evolving concept. *Geogr Ann Ser B* 87(1):17–36
- Mauquoy D, Blaauw M, van Geel B, Borromei A, Quattrocchio M, Chambers FM, Possnert G (2004) Late Holocene climatic changes in Tierra Del Fuego based on multiproxy analyses of peat deposits. *Quatern Res* 61(2):148–158
- Mayewski PA, Bender M (1995) The gisp2 ice core record—paleoclimate highlights. *Rev Geophys* 33(52):1287–1296
- Mayewski PA, Meeker LD, Whitlow S, Twickler MS, Morrison MC, Alley RB, Bloomfield P, Taylor K (1993) The atmosphere during the Younger Dryas. *Science* 261(5118):195–197
- McGowan H, Campbell M, Callow JN, Lowry A, Wong H (2020) Evidence of wetdry cycles and mega-droughts in the Eemian climate of Southeast Australia. *Sci Rep* 10(1):1–10
- Meehl GA, Stocker TF, Collins WD, Friedlingstein P, Gaye T, Gregory JM, Kitoh A, Knutti R, Murphy JM, Noda A et al (2007) Global climate projections
- Meko D (1992) Dendroclimatic evidence from the great plains of the United States. In: Bradley RS, Jones PD (eds) *Climate since AD 1500*
- Members C-LIP (2006) Last interglacial Arctic warmth confirms polar amplification of climate change. *Quatern Sci Rev* 25(13–14):1383–1400
- Metcalfe S (1999) Diatoms from the Pretoria saltpan—a record of lake evolution and environmental change. Tswaing, investigations into the origin, age and palaeoenvironments of the Pretoria Saltpan. *Counc Geosci (geol Surv S Afr)* 172:192
- Methner K, Campani M, Fiebig J, Löffler N, Kempf O, Mulch A (2020) Middle Miocene long-term continental temperature change in and out of pace with marine climate records. *Sci Rep* 10(1):1–10
- Miller GH, Brigham-Grette J, Alley R, Anderson L, Bauch HA, Douglas M, Edwards M, Elias S, Finney B, Fitzpatrick JJ et al (2010) Temperature and precipitation history of the Arctic. *Quatern Sci Rev* 29(15–16):1679–1715
- Miller GH, Geirsdóttir A, Zhong Y, Larsen DJ, Otto-Bliesner BL, Holland MM, Bailey DA, Refsnider KA, Lehman SJ, Southon JR et al (2012) Abrupt onset of the little ice age triggered by volcanism and sustained by sea-ice/ocean feedbacks. *Geophys Res Lett* 39(2)
- Miller KG, Wright JD, Fairbanks RG (1991) Unlocking the ice house: Oligocene-miocene oxygen isotopes, eustasy, and margin erosion. *J Geophys Res Solid Earth* 96(B4):6829–6848
- Mohtadi M, Prange M, Oppo DW, De Pol-Holz R, Merkel U, Zhang X, Steinke S, Lückge A (2014) North Atlantic forcing of tropical indian ocean climate. *Nature* 509(7498):76–80
- Montoya M, von Storch H, Crowley TJ (2000) Climate simulation for 125 kyr bp with a coupled ocean–atmosphere general circulation model. *J Clim* 13(6):1057–1072
- Morales-García NM, Salla LK, Janis CM et al (2020) The Neogene Savannas of North America: a retrospective analysis on artiodactyl faunas. *Front Earth Sci* 8:191
- Moreno A, Pérez A, Frigola J, Nieto-Moreno V, Rodrigo-Gámiz M, Martrat B, González-Sampériz P, Morellón M, Martín-Puertas C, Corella JP et al (2012) The Medieval climate anomaly in the Iberian Peninsula reconstructed from marine and lake records. *Quatern Sci Rev* 43:16–32
- Nebout NC, Turon J, Zahn R, Capotondi L, Londeix L, Pahnke K (2002) Enhanced aridity and atmospheric high-pressure stability over the western Mediterranean during the north Atlantic cold events of the past 50 ky. *Geology* 30(10):863–866
- Nehme C, Verheyden S, Noble S, Farrant A, Sahy D, Hellstrom J, Delannoy J, Claeys P (2015) Reconstruction of mis 5 climate in the central levant using a stalagmite from Kanaan Cave, Lebanon. *Clim past* 11(12):1785–1799
- Nesje A, Dahl SO, Thun T, Nordli Ø (2008) The 'little Ice Age' glacial expansion in western Scandinavia: summer temperature or winter precipitation? *Clim Dyn* 30(78):789–801
- Nikolova I, Yin Q, Berger A, Singh U, Karami M (2013) The last interglacial (Eemian) climate simulated by LOVECLIM and CCSM3. *Clim past* 9:1789–1806
- Norris J, Chen G, Neelin JD (2019) Thermodynamic versus dynamic controls on extreme precipitation in a warming climate from the community earth system model large ensemble. *J Clim* 32(4):1025–1045
- O'Brien SR, Mayewski PA, Meeker LD, Meese DA, Twickler MS, Whitlow S (1995) Complexity of Holocene climate as reconstructed from a Greenland ice core. *Science* 270(5244):1962–1964
- On ZB, Akçer-Ön S, Özeren MS, Eriş KK, Greaves AM, Çağatay MN (2018) Climate proxies for the last 17.3 ka from lake hazar (eastern anatolia), extracted by independent component analysis of μ -xrf data. *Quatern Int* 486:17–28
- Orland JJ, He F, Bar-Matthews M, Chen G, Ayalon A, Kutzbach JE (2019) Resolving seasonal rainfall changes in the Middle East during the last interglacial period. *Proc Natl Acad Sci* 116(50):24985–24990
- Osipov EY, Khlystov OM (2010) Glaciers and meltwater flux to Lake Baikal during the last glacial maximum. *Palaeogeogr Palaeoclimatol Palaeoecol* 294(1–2):4–15
- Oster JL, Montañez IP, Mertz-Kraus R, Sharp WD, Stock GM, Spero HJ, Tinsley J, Zachos JC (2014) Millennial-scale variations in western Sierra Nevada precipitation during the last glacial cycle MIS 4/3 transition. *Quatern Res* 82(1):236–248
- Otto-Bliesner BL, Brady EC, Clauzet G, Tomas R, Levis S, Kothavala Z (2006) Last glacial maximum and Holocene climate in CCSM3. *J Clim* 19(11):2526–2544

- Otto-Bliesner BL, Rosenbloom N, Stone EJ, McKay NP, Lunt DJ, Brady EC, Overpeck JT (2013) How warm was the last interglacial? new model–data comparisons. *Philos Trans R Soc A Math Phys Eng Sci* 371(2001):20130097
- O’Gorman PA (2012) Sensitivity of tropical precipitation extremes to climate change. *Nat Geosci* 5(10):697–700
- Parish MC, Calder WJ, Shuman BN (2020) Millennial-scale increase in winter precipitation in the southern rocky mountains during the common era. *Quatern Res* 94:1–13
- Pascual R, Jaureguizar EO (1990) Evolving climates and mammal faunas in Cenozoic South America. In: *The plattyrhine fossil record*. Elsevier, pp 23–60
- Paterne M, Kallel N, Labeyrie L, Vautravers M, Duplessy J-C, Rossignol-Strick M, Cortijo E, Arnold M, Fontugne M (1999) Hydrological relationship between the North Atlantic Ocean and the Mediterranean Sea during the past 15–75 kyr. *Paleoceanography* 14(5):626–638
- Patridge T, Demenocal P, Lorentz S, Paiker M, Vogel J (1997) Orbital forcing of climate over South Africa: a 200,000-year rainfall record from the Pretoria saltpan. *Quatern Sci Rev* 16:1125–1133
- Pauling A, Luterbacher J, Casty C, Wanner H (2006) Five hundred years of gridded high-resolution precipitation reconstructions over Europe and the connection to large-scale circulation. *Clim Dyn* 26(4):387–405
- Pausata FS, Gaetani M, Messori G, Berg A, de Souza DM, Sage RF, deMenocal PB (2020) The greening of the Sahara: past changes and future implications. *One Earth* 2(3):235–250
- Pawłowski D, Plóciennik M, Brooks SJ, Luoto TP, Milecka K, Nevalainen L, Peyron O, Self A, Zieliński T (2015) A multiproxy study of Younger Dryas and early Holocene climatic conditions from the Grabia River paleo-oxbow lake (Central Poland). *Palaeogeogr Palaeoclimatol Palaeoecol* 438:34–50
- Pearson PN, Palmer MR (2000) Atmospheric carbon dioxide concentrations over the past 60 million years. *Nature* 406(6797):695–699
- Pedersen RA, Langen PL, Vinther BM (2017) The last interglacial climate: comparing direct and indirect impacts of insolation changes. *Clim Dyn* 48(9):3391–3407
- Peterson LC, Haug GH (2006) Variability in the mean latitude of the Atlantic intertropical convergence zone as recorded by riverine input of sediments to the Cariaco Basin (Venezuela). *Palaeogeogr Palaeoclimatol Palaeoecol* 234(1):97–113
- Peterson LC, Haug GH, Hughen KA, Röhl U (2000) Rapid changes in the hydrologic cycle of the tropical atlantic during the last glacial. *Science* 290(5498):1947–1951
- Petit-Maire N, Carbonel P, Reyss J-L, Sanlaville P, Abed A, Bourrouilh R, Fontugne M, Yasin S (2010) A vast Eemian Palaeolake in Southern Jordan (29 n). *Glob Planet Change* 72(4):368–373
- Polissar P, Abbott M, Wolfe A, Bezada M, Rull V, Bradley R (2006) Solar modulation of Little Ice Age climate in the tropical andes. *Proc Natl Acad Sci* 103(24):8937–8942
- Polyak VJ, Rasmussen JB, Asmerom Y (2004) Prolonged wet period in the southwestern United States through the Younger Dryas. *Geology* 32(1):5–8
- Pound MJ, Haywood AM, Salzmann U, Riding JB (2012) Global vegetation dynamics and latitudinal temperature gradients during the mid to late Miocene (15.97–5.33 ma). *EarthScience Rev* 112(1–2):1–22
- Praetorius SK, Condon A, Mix AC, Walczak MH, McKay JL, Du J (2020) The role of northeast Pacific meltwater events in deglacial climate change. *Sci Adv* 6(9):eaay2915
- Prell WL, Kutzbach JE (1987) Monsoon variability over the past 150,000 years. *J Geophys Res Atmos* 92(D7):8411–8425
- Prentice IC, Guiot J, Harrison SP (1992) Mediterranean vegetation, lake levels and palaeoclimate at the last glacial maximum. *Nature* 360(6405):658–660
- Prentice IC, Jolly D, Participants B (2000) Mid-Holocene and glacial-maximum vegetation geography of the northern continents and Africa. *J Biogeogr* 27(3):507–519
- Proctor C, Baker A, Barnes W, Gilmour M (2000) A thousand year speleothem proxy record of North Atlantic climate from Scotland. *Clim Dyn* 16(10–11):815–820
- Putnam AE, Broecker WS (2017) Human-induced changes in the distribution of rainfall. *Sci Adv* 3(5):e1600871
- Rach O, Brauer A, Wilkes H, Sachse D (2014) Delayed hydrological response to Greenland cooling at the onset of the Younger Dryas in Western Europe. *Nat Geosci* 7(2):109–112
- Rao Z, Li Y, Zhang J, Jia G, Chen F (2016) Investigating the long-term palaeoclimatic controls on the δd and $\delta 18o$ of precipitation during the Holocene in the Indian and East Asian monsoonal regions. *Earth Sci Rev* 159:292–305
- Rasmussen TL, Thomsen E, Moros M (2016) North Atlantic warming during Dansgaard–Oeschger events synchronous with Antarctic warming and out-of-phase with Greenland climate. *Sci Rep* 6(1):1–12
- Rein B, Lückge A, Sirocko F (2004) A major Holocene ENSO anomaly during the Medieval period. *Geophys Res Lett* 31(17)
- Ren G (1998) Pollen evidence for increased summer rainfall in the Medieval warm period at Maili, Northeast China. *Geophys Res Lett* 25(11):1931–1934
- Renssen H (2020) Comparison of climate model simulations of the Younger Dryas cold event. *Quaternary* 3(4):29
- Renssen H, Goosse H, Fichefet T, Campin J-M (2001) The 8.2 kyr BP event simulated by a global atmosphere–sea-ice–ocean model. *Geophys Res Lett* 28(8):1567–1570
- Renssen H, Goosse H, Roche DM, Seppä H (2018) The global hydroclimate response during the Younger Dryas event. *Quatern Sci Rev* 193:84–97
- Retallack GJ (1992) Middle Miocene fossil plants from Fort Ternan (Kenya) and evolution of African grasslands. *Paleobiology* 18:383–400
- Retallack GJ (2007) Cenozoic paleoclimate on land in North America. *J Geol* 115(3):271–294
- Reuter J, Stott L, Khider D, Sinha A, Cheng H, Edwards RL (2009) A new perspective on the hydroclimate variability in Northern South America during the Little Ice Age. *Geophys Res Lett* 36(21)
- Rhodes R, Bertler N, Baker J, Steen-Larsen HC, Sneed S, Morgenstern U, Johnsen SJ (2012) Little Ice Age climate and oceanic conditions of the Ross Sea, Antarctica from a coastal ice core record. *Clim Past* 8(4):1223–1238
- Rogers JC (1983) Spatial variability of Antarctic temperature anomalies and their association with the southern hemisphere atmospheric circulation. *Ann Assoc Am Geogr* 73(4):502–518
- Rohling E, Hayes A, De Rijk S, Kroon D, Zachariasse W, Eisma D (1998) Abrupt cold spells in the northwest Mediterranean. *Paleoceanography* 13(4):316–322
- Rojas M, Moreno P, Kageyama M, Crucifix M, Hewitt C, Abe-Ouchi A, Ohgaito R, Brady EC, Hope P (2009) The Southern Westerlies during the last glacial maximum in PMIP2 simulations. *Clim Dyn* 32(4):525–548
- Rosell-Melé A, Bard E, Emeis KC, Grieger B, Hewitt C, Müller PJ, Schneider RR (2004) Sea surface temperature anomalies in the oceans at the LGM estimated from the alkenone- $u37k^0$ index: comparison with GCMs. *Geophys Res Lett* 31(3)
- Rosenberg TM, Preusser F, Risberg J, Pliikk A, Kadi KA, Matter A, Fleitmann D (2013) Middle and Late Pleistocene humid periods recorded in palaeolake deposits of the Nafud Desert, Saudi Arabia. *Quatern Sci Rev* 70:109–123
- Rotnicki K (1991) Retrodiction of palaeodischarges of meandering and sinuous alluvial rivers and its palaeohydroclimatic implications. In: *Temperate palaeohydrology. Fluvial processes in the temperate zone during the last 15 000 years*, pp 431–471
- Samartin S, Heiri O, Lotter AF, Tinner W (2012) Climate warming and vegetation response after heinrich event 1 (16 700–16 000 cal yr BP) in Europe south of the alps. *Clim Past* 8(6):1913–1927
- Santos TP, Ballalai JM, Franco DR, Oliveira RR, Lessa DO, Venancio IM, Chiessi CM, Kuhnert H, Johnstone H, Albuquerque ALS (2020) Asymmetric response of the subtropical western South Atlantic thermocline to the Dansgaard–Oeschger events of marine isotope stages 5 and 3. *Quatern Sci Rev* 237:106307
- Schlunegger F, Burbank D, Matter A, Engesser B, Mödden C (1996) Magnetostratigraphic calibration of the Oligocene to Middle Miocene (30–15 ma) mammal biozones and depositional sequences of the Swiss Molasse Basin. *Ecoloe Geol Helv* 89(2):753–788
- Schmittner A, Urban NM, Shakun JD, Mahowald NM, Clark PU, Bartlein PJ, Mix AC, Rosell-Melé A (2011) Climate sensitivity estimated from temperature reconstructions of the last glacial maximum. *Science* 334(6061):1385–1388

- Schneider L, Cooke CA, Stansell ND, Haberle SG (2020) Effects of climate variability on mercury deposition during the older dryas and Younger Dryas in the Venezuelan andes. *J Paleolimnol* 63(3):211–224
- Schneider L, Smerdon JE, Büntgen U, Wilson RJ, Myglan VS, Kirilyanov AV, Esper J (2015) Revising midlatitude summer temperatures back to AD 600 based on a wood density network. *Geophys Res Lett* 42(11):4556–4562
- Scholz SR, Petersen SV, Escobar J, Jaramillo C, Hendy AJ, Allmon WD, Curtis JH, Anderson BM, Hoyos N, Restrepo JC et al (2020) Isotope sclero-chronology indicates enhanced seasonal precipitation in Northern South America (Colombia) during the Mid-Miocene climatic optimum. *Geology* 48:668–672
- Scussolini P, Bakker P, Guo C, Stepanek C, Zhang Q, Braconnot P, Cao J, Guarino M-V, Coumou D, Prange M et al (2019) Agreement between reconstructed and modeled boreal precipitation of the last interglacial. *Sci Adv* 5(11):eaax7047
- Seager R, Graham N, Herweijer C, Gordon AL, Kushnir Y, Cook E (2007) Blueprints for Medieval hydroclimate. *Quatern Sci Rev* 26(19–21):2322–2336
- Seftigen K, Goosse H, Klein F, Chen D (2017) Hydroclimate variability in Scandinavia over the last millennium—insights from a climate model-proxy data comparison. *Clim past* 13:1831
- Seierstad IK, Johnsen SJ, Vinther BM, Olsen J (2005) The duration of the Bølling–Allerød period (Greenland interstadial 1) in the grip ice core. *Ann Glaciol* 42:337–344
- Seppä H, MacDonald GM, Birks HJB, Gervais BR, Snyder JA (2008) Latequaternary summer temperature changes in the northern-European tree-line region. *Quatern Res* 69(3):404–412
- Serebryanny L, Andreev A, Malysova E, Tarasov P, Romanenko F (1998) Late-glacial and early-Holocene environments of Novaya Zemlya and the Kara Sea region of the Russian Arctic. *The Holocene* 8(3):323–330
- Shackleton NJ, Hall MA, Vincent E (2000) Phase relationships between millennial-scale events 64000–24000 years ago. *Paleoceanography* 15(6):565–569
- Sifeddine A, Martin I, Turcq B, Volkmer-Ribeiro C, Soubières F, Cordeiro RC, Suguio K (2001) Variations of the amazonian rainforest environment: a sedimentological record covering 30,000 years. *Palaeogeogr Palaeoclimatol Palaeoecol* 168(3–4):221–235
- Simon MH, Ziegler M, Bosmans J, Barker S, Reason CJ, Hall IR (2015) Eastern south african hydroclimate over the past 270,000 years. *Sci Rep* 5(1):1–10
- Sinha A, Cannariato KG, Stott LD, Li H-C, You C-F, Cheng H, Edwards RL, Singh IB (2005) Variability of southwest indian summer monsoon precipitation during the Bølling–Allerød. *Geology* 33(10):813–816
- Sirocko F, Seelos K, Schaber K, Rein B, Dreher F, Diehl M, Lehne R, Jäger K, Krbetschek M, Degering D (2005) A late eemian aridity pulse in Central Europe during the last glacial inception. *Nature* 436(7052):833–836
- Smith JA, Rodbell DT (2010) Cross-cutting moraines reveal evidence for North Atlantic influence on glaciers in the tropical andes. *J Quatern Sci Publ Quatern Res Assoc* 25(3):243–248
- Snowball I, Zillén L, Gaillard M-J (2002) Rapid early-Holocene environmental changes in northern Sweden based on studies of two varved lake-sediment sequences. *The Holocene* 12(1):7–16
- Snyder CW (2016) Evolution of global temperature over the past two million years. *Nature* 538(7624):226–228
- Solomon S, Manning M, Marquis M, Qin D et al (2007) Climate change 2007—the physical science basis: Working group I contribution to the fourth assessment report of the IPCC, vol 4. Cambridge University Press
- Song Y, Wang Q, An Z, Qiang X, Dong J, Chang H, Zhang M, Guo X (2018) Mid-Miocene climatic optimum: clay mineral evidence from the red clay succession, Longzhong Basin, Northern China. *Palaeogeogr Palaeoclimatol Palaeoecol* 512:46–55
- Stager JC, Ryves D, Cumming BF, Meeker LD, Beer J (2005) Solar variability and the levels of Lake Victoria, East Africa, during the last millenium. *J Paleolimnol* 33(2):243–251
- Stansell ND, Abbott MB, Rull V, Rodbell DT, Bezada M, Montoya E (2010) Abrupt Younger Dryas cooling in the northern tropics recorded in lake sediments from the Venezuelan andes. *Earth Planet Sci Lett* 293(1–2):154–163
- Stansell ND, Steinman BA, Abbott MB, Rubinov M, Roman-Lacayo M (2013) Lacustrine stable isotope record of precipitation changes in Nicaragua during the Little Ice Age and Medieval climate anomaly. *Geology* 41(2):151–154
- Starkel L (1991) Environmental changes at the Younger Dryas-preboreal transition and during the early Holocene: some distinctive aspects in Central Europe. *The Holocene* 1(3):234–242
- Steffensen JP (1997) The size distribution of microparticles from selected segments of the Greenland ice core project ice core representing different climatic periods. *J Geophys Res Oceans* 102(C12):26755–26763
- Stein R, Robert C (1985) Siliciclastic sediments at sites 588, 590, and 591: Neogene and paleogene evolution in the southwest pacific and Australian climate. *Initial Rep DSDP* 90:1437–1455
- Steininger FF (1999) Chronostratigraphy, geochronology and biochronology of the Miocene “European land mammal mega-zones” (ELMMZ) and the Miocene “mammal-zones (mn-zones)”. *Miocene Land Mamm Eur* 9–24
- Steinhorsdottir M, Jardine P, Rember W (2020) Near-future pco2 during the hot Mid Miocene climatic optimum. *Paleoceanogr Paleoclimatol e2020PA003900*.
- Stine S (1994) Extreme and persistent drought in California and Patagonia during Mediaeval time. *Nature* 369(6481):546–549
- Strandberg G, Brandefelt J, Kjellström E, Smith B (2011) High-resolution regional simulation of last glacial maximum climate in Europe. *Tellus A Dyn Meteorol Oceanogr* 63(1):107–125
- Street-Perrott FA, Perrott RA (1990) Abrupt climate fluctuations in the tropics: the influence of Atlantic Ocean circulation. *Nature* 343(6259):607–612
- Stuiver M, Grootes PM, Braziunas TF (1995) The GISP2 $\delta^{18}O$ climate record of the past 16,500 years and the role of the sun, ocean, and volcanoes. *Quatern Res* 44(3):341–354
- Suh YJ, Diefendorf AF, Freimuth EJ, Hyun S (2020) Last interglacial (mis 5e) and Holocene paleohydrology and paleovegetation of midcontinental North America from Gulf of Mexico sediments. *Quatern Sci Rev* 227:106066
- Sun J, Ma C, Cao X, Zhao Y, Deng Y, Zhao L, Zhu C (2019) Quantitative precipitation reconstruction in the east-central monsoonal China since the late glacial period. *Quatern Int* 521:175–184
- Sun J, Zhang Z (2008) Palynological evidence for the Mid-Miocene climatic optimum recorded in cenozoic sediments of the Tian Shan Range, Northwestern China. *Glob Planet Change* 64(1–2):53–68
- Thiagarajan N, Subhas AV, Southon JR, Eiler JM, Adkins JF (2014) Abrupt pre-Bølling–Allerød warming and circulation changes in the deep ocean. *Nature* 511(7507):75–78
- Thomas E, Booth L, Maslin M, Shackleton N (1995) Northeastern Atlantic benthic foraminifera during the last 45,000 years: changes in productivity seen from the bottom up. *Paleoceanography* 10(3):545–562
- Thomas ER, Wolff EW, Mulvaney R, Steffensen JP, Johnsen SJ, Arrowsmith C, White JW, Vaughn B, Popp T (2007) The 8.2 ka event from Greenland ice cores. *Quatern Sci Rev* 26(1–2):70–81
- Thompson LG (1991) Ice-core records with emphasis on the global record of the last 2000 years. *Glob Changes past* 2:201–224
- Thompson LG, Mosley-Thompson E, Davis M, Zagorodnov V, Howat I, Mikhailenko V, Lin P-N (2013) Annually resolved ice core records of tropical climate variability over the past 1800 years. *Science* 340(6135):945–950
- Thompson LG, Mosley-Thompson E, Davis ME, Lin P-N, Henderson KA, Cole-Dai J, Bolzan JF, Liu K-B (1995) Late glacial stage and Holocene tropical ice core records from Huascarán, Peru. *Science* 269(5220):46–50
- Tierney JE, deMenocal PB (2013) Abrupt shifts in horn of Africa hydroclimate since the last glacial maximum. *Science* 342(6160):843–846
- Till C, Guiot J et al (1990) Reconstruction of precipitation in morocco since 1100 AD based on cedrus atlantica tree-ring widths. *Quatern Res* 33(3):337–351
- Tofalo O, Orgeira MJ, Compagnucci R, Alonso MS, Ramos A (2011) Characterization of a loess–paleosols section including a new record of the last interglacial stage in Pampean Plain, Argentina. *J S Am Earth Sci* 31(1):81–92
- Törnqvist TE, Bick SJ, González JL, van der Borg K, de Jong AF (2004) Tracking the sea-level signature of the 8.2 ka cooling event: new constraints from the Mississippi delta. *Geophys Res Lett* 31(23)
- Trachsel M, Kamenik C, Grosjean M, McCarroll D, Moberg A, Brázdil R, Büntgen U, Dobrovolný P, Esper J, Frank DC et al (2012) Multi-archive summer temperature reconstruction for the European alps, AD 1053–1996. *Quatern Sci Rev* 46:66–79
- Trenberth KE (1998) Atmospheric moisture residence times and cycling: implications for rainfall rates and climate change. *Clim Change* 39(4):667–694

- Trouet V, Esper J, Graham NE, Baker A, Scourse JD, Frank DC (2009) Persistent positive North Atlantic oscillation mode dominated the Medieval climate anomaly. *Science* 324(5923):78–80
- Turney CS, Jones RT (2010) Does the agulhas current amplify global temperatures during super-interglacials? *J Quatern Sci* 25(6):839–843
- Tzedakis P, Drysdale RN, Margari V, Skinner LC, Menviel L, Rhodes RH, Taschetto AS, Hodell DA, Crowhurst SJ, Hellstrom JC et al (2018) Enhanced climate instability in the North Atlantic and Southern Europe during the last interglacial. *Nat Commun* 9(1):1–14
- Vaks A, Bar-Matthews M, Ayalon A, Matthews A, Frumkin A, Dayan U, Halicz L, Almogi-Labin A, Schilman B (2006) Paleoclimate and location of the border between Mediterranean climate region and the Sahara–Arabian desert as revealed by speleothems from the northern Negev Desert, Israel. *Earth Planet Sci Lett* 249(3–4):384–399
- Van Geel B, Raspopov O, Renssen H, Van der Plicht J, Dergachev V, Meijer H (1999) The role of solar forcing upon climate change. *Quatern Sci Rev* 18(3):331–338
- Van Kreveld S, Sarnthein M, Erlenkeuser H, Grootes P, Jung S, Nadeau M, Pflaumann U, Voelker A (2000) Potential links between surging ice sheets, circulation changes, and the Dansgaard–Oeschger cycles in the irmeringer sea, 60–18 kyr. *Paleoceanography* 15(4):425–442
- Vargas Godoy MR, Markonis Y, Hanel M, Kyselý J, Papalexiou SM (2021) The global water cycle budget: a chronological review. *Surv Geophys* 42(5):1075–1107
- Velichko A, Catto N, Drenova A, Klimanov V, Kremenetski K, Nechaev V (2002) Climate changes in east Europe and Siberia at the late glacial–Holocene transition. *Quatern Int* 91(1):75–99
- Verschuren D, Laird KR, Cumming BF (2000) Rainfall and drought in equatorial East Africa during the past 1,100 years. *Nature* 403(6768):410–414
- Viau A, Ladd M, Gajewski K (2012) The climate of North America during the past 2000 years reconstructed from pollen data. *Glob Planet Change* 84:75–83
- Villalba R (1994) Tree-ring and glacial evidence for the medieval warm epoch and the Little Ice Age in southern South America. In: Hughes MK, Diaz HF (eds) *The Medieval warm period*. Springer, Dordrecht, pp 183–197
- Voelker SL, Stambaugh MC, Guyette RP, Feng X, Grimley DA, Leavitt SW, Panyushkina I, Grimm EC, Marsicek JP, Shuman B et al (2015) Deglacial hydroclimate of midcontinental North America. *Quatern Res* 83(2):336–344
- Von Grafenstein U, Erlenkeuser H, Müller J, Jouzel J, Johnsen S (1998) The cold event 8200 years ago documented in oxygen isotope records of precipitation in Europe and Greenland. *Clim Dyn* 14(2):73–81
- Waelbroeck C, Paul A, Kucera M, Rosell-Melé A, Weinelt M, Schneider R, Mix AC, Abelmann A, Armand L, Bard E et al (2009) Constraints on the magnitude and patterns of ocean cooling at the last glacial maximum. *Nat Geosci* 2:127–132
- Wagner JD, Cole JE, Beck JW, Patchett PJ, Henderson GM, Barnett HR (2010) Moisture variability in the southwestern United States linked to abrupt glacial climate change. *Nat Geosci* 3(2):110–113
- Wan S, Li A, Clift PD, Stuu J-BW (2007) Development of the East Asian monsoon: mineralogical and sedimentologic records in the northern south China sea since 20 Ma. *Palaeogeogr Palaeoclimatol Palaeoecol* 254(3–4):561–582
- Wang L, Jiang W, Jiang D, Zou Y, Liu Y, Zhang E, Hao Q, Zhang D, Zhang D, Peng Z et al (2018) Prolonged heavy snowfall during the Younger Dryas. *J Geophys Res Atmos* 123(24):13–748
- Wang L-C, Behling H, Lee T-Q, Li H-C, Huh C-A, Shiao L-J, Chen S-H, Wu J-T (2013) Increased precipitation during the Little Ice Age in northern Taiwan inferred from diatoms and geochemistry in a sediment core from a subalpine lake. *J Paleolimnol* 49(4):619–631
- Wang X, Auler AS, Edwards RL, Cheng H, Cristalli PS, Smart PL, Richards DA, Shen C-C (2004) Wet periods in northeastern Brazil over the past 210 kyr linked to distant climate anomalies. *Nature* 432(7018):740–743
- Wang Y, Cheng H, Edwards RL, Kong X, Shao X, Chen S, Wu J, Jiang X, Wang X, An Z (2008) Millennial-and orbital-scale changes in the east Asian monsoon over the past 224,000 years. *Nature* 451(7182):1090–1093
- Wang Y-J, Cheng H, Edwards RL, An Z, Wu J, Shen C-C, Dorale JA (2001) A high-resolution absolute-dated late Pleistocene monsoon record from Hulu Cave, China. *Science* 294(5550):2345–2348
- Wassenburg JA, Dietrich S, Fietzke J, Fohlmeister J, Jochum KP, Scholz D, Richter DK, Sabaoui A, Spötl C, Lohmann G et al (2016) Reorganization of the north Atlantic oscillation during Early Holocene deglaciation. *Nat Geosci* 9(8):602–605
- Watterson I, O'Farrell S, Dix M (1997) Energy and water transport in climates simulated by a general circulation model that includes dynamic sea ice. *J Geophys Res Atmos* 102(D10):11027–11037
- Weaver AJ, Hughes TM (1994) Rapid interglacial climate fluctuations driven by North Atlantic Ocean circulation. *Nature* 367(6462):447–450
- Weber M-J, Grimm SB, Baales M (2011) Between warm and cold: impact of the Younger Dryas on human behavior in Central Europe. *Quatern Int* 242(2):277–301
- Wentz FJ, Ricciardulli L, Hilburn K, Mears C (2007) How much more rain will global warming bring? *Science* 317(5835):233–235
- Wetherald RT, Manabe S (2002) Simulation of hydrologic changes associated with global warming. *J Geophys Res Atmos* 107(D19):ACL-17
- Williams CJ, Guarino M-V, Capron E, Malmierca-Vallet I, Singarayer JS, Sime LC, Lunt DJ, Valdes PJ (2020) CMP6/PMIP4 simulations of the mid-Holocene and last interglacial using HadGEM3: comparison to the pre-industrial era, previous model versions and proxy data. *Clim past* 16(4):1429–1450
- Wolfe JA (1985) Distribution of major vegetational types during the tertiary. *Carbon Cycle Atmos CO2 Nat Var Archean Present* 32:357–375
- Woodhouse CA, Meko DM, MacDonald GM, Stahle DW, Cook ER (2010) A 1,200-year perspective of 21st century drought in Southwestern North America. *Proc Natl Acad Sci* 107(50):21283–21288
- Wright JD, Miller KG, Fairbanks RG (1992) Early and Middle Miocene stable isotopes: implications for deepwater circulation and climate. *Paleoceanography* 7(3):357–389
- Wright JS, Fu R, Worden JR, Chakraborty S, Clinton NE, Risi C, Sun Y, Yin L (2017) Rainforest-initiated wet season onset over the southern amazon. *Proc Natl Acad Sci* 114(32):8481–8486
- Wu S-D, Zhang L-J, Lin L, Yu S-X, Chen Z-D, Wang W (2018) Insights into the historical assembly of global dryland floras: The diversification of zygo-phylloceae. *BMC Evol Biol* 18(1):166
- Yang B, Braeuning A, Johnson KR, Yafeng S (2002) General characteristics of temperature variation in China during the last two millennia. *Geophys Res Lett* 29(9):38–41
- Yang Q, Li X, Zhou X, Zhao K, Sun N (2016) Quantitative reconstruction of summer precipitation using a Mid-Holocene $\delta^{13}C$ common millet record from Guanzhong Basin, Northern China. *Clim past* 12(12):2229–2240
- Yehudai M, Lazar B, Bar N, Kiro Y, Agnon A, Shaked Y, Stein M (2017) U-th dating of calcite corals from the Gulf of Aqaba. *Geochim Cosmochim Acta* 198:285–298
- Yokoyama Y, Lambeck K, De Deckker P, Johnston P, Fifield LK (2000) Timing of the last glacial maximum from observed sea-level minima. *Nature* 406(6797):713–716
- You Y (2010) Climate-model evaluation of the contribution of sea-surface temperature and carbon dioxide to the Middle Miocene climate optimum as a possible analogue of future climate change. *Aust J Earth Sci* 57(2):207–219
- You Y, Huber M, Müller R, Poulsen C, Ribbe J (2009) Simulation of the Middle Miocene climate optimum. *Geophys Res Lett* 36(4)
- Yung YL, Lee T, Wang C-H, Shieh Y-T (1996) Dust: a diagnostic of the hydrologic cycle during the last glacial maximum. *Science* 271(5251):962–963
- Zachos J, Pagani M, Sloan L, Thomas E, Billups K (2001) Trends, rhythms, and aberrations in global climate 65 Ma to present. *Science* 292(5517):686–693
- Zachos JC, Dickens GR, Zeebe RE (2008) An early Cenozoic perspective on greenhouse warming and carbon-cycle dynamics. *Nature* 451(7176):279–283
- Zaleha MJ (1997) Siwalik paleosols (Miocene, Northern Pakistan); genesis and controls on their formation. *J Sediment Res* 67(5):821–839
- Zappa G, Shepherd TG (2017) Storylines of atmospheric circulation change for European regional climate impact assessment. *J Clim* 30(16):6561–6577
- Zech M, Tuthorn M, Zech R, Schlütz F, Zech W, Glaser B (2014) A 16-ka $\delta^{18}O$ record of lacustrine sugar biomarkers from the high Himalaya reflects Indian summer monsoon variability. *J Paleolimnol* 51(2):241–251
- Zhang M, Bu Z, Li H, Liu S, Chen J, Cui Y (2021a) Hydrological variation recorded in a subalpine peatland of Northeast Asia since the Little Ice Age and its possible driving mechanisms. *Sci Total Environ* 772:144923
- Zhang Q, Bertell E, Axelsson J, Chen J, Han Z, de Nooijer W, Lu Z, Li Q, Zhang Q, Wyser K et al (2021b) Simulating the Mid-Holocene, last interglacial

- and mid-Pliocene climate with EC-Earth3-LR. *Geosci Model Dev* 14(2):1147–1169
- Zhang R, Sutton R, Danabasoglu G, Kwon Y-O, Marsh R, Yeager SG, Amrhein DE, Little CM (2019) A review of the role of the Atlantic Meridional overturning circulation in Atlantic multidecadal variability and associated climate impacts. *Rev Geophys* 57(2):316–375
- Zhang YG, Pagani M, Liu Z, Bohaty SM, DeConto R (2013) A 40-million-year history of atmospheric CO₂. *Philos Trans R Soc A Math Phys Eng Sci* 371(2001):20130096
- Zhao J, Thomas EK, Yao Y, DeAraujo J, Huang Y (2018) Major increase in winter and spring precipitation during the Little Ice Age in the westerly dominated Northern Qinghai-Tibetan Plateau. *Quatern Sci Rev* 199:30–40
- Zhao J, Xia Q, Collerson KD (2001) Timing and duration of the last interglacial inferred from high resolution u-series chronology of stalagmite growth in southern hemisphere. *Earth Planet Sci Lett* 184(3–4):635–644
- Zheng J, Wang W-C, Ge Q, Man Z, Zhang P (2006) Precipitation variability and extreme events in eastern China during the past 1500 years. *TAO Terr Atmos Ocean Sci* 17(3):579
- Zhong Y, Miller G, Otto-Bliesner B, Holland M, Bailey D, Schneider D, Geirsdottir A (2011) Centennial-scale climate change from decadal-paced explosive volcanism: a coupled sea ice-ocean mechanism. *Clim Dyn* 37(11–12):2373–2387
- Zhou W, Head MJ, Deng L (2001) Climate changes in northern China since the late pleistocene and its response to global change. *Quatern Int* 83:285–292

Publisher's Note

Springer Nature remains neutral with regard to jurisdictional claims in published maps and institutional affiliations.

Submit your manuscript to a SpringerOpen[®] journal and benefit from:

- ▶ Convenient online submission
- ▶ Rigorous peer review
- ▶ Open access: articles freely available online
- ▶ High visibility within the field
- ▶ Retaining the copyright to your article

Submit your next manuscript at ▶ [springeropen.com](https://www.springeropen.com)
